WRI-07-R004R

MERCURY CEM CALIBRATION

"TOPICAL REPORT"

Reporting Period Start 2004
Reporting Period End 2007

John F. Schabron
Joseph F. Rovani, Jr.
Susan S. Sorini

March 2007

DE-FC26-98FT40323
Task 58

For
U.S. Department of Energy
National Energy Technology Laboratory
Morgantown West Virginia

And
Electric Power Research Institute
3420 Hillview Avenue
Palo Alto, California, 94304

By
Western Research Institute
365 North 9th Street
Laramie, Wyoming, 82072

Kamalendu Das, Task 58

ACKNOWLEDGMENTS

Funding for this study was provided by the U.S. Department of Energy under Cooperative Agreement DE-FC26-98FT40323, and by the Electric Power Research Institute. Instruments were provided on loan to this project by Mercury-Instruments, Nippon/Horiba, and Thermo Fisher.

DISCLAIMER

ABSTRACT

The Clean Air Mercury Rule (CAMR) which was published in the Federal Register on May 18, 2005, requires that calibration of mercury continuous emissions monitors (CEMs) be performed with NIST-traceable standards. Western Research Institute (WRI) is working closely with the Electric Power Research Institute (EPRI), the National Institute of Standards and Technology (NIST), and the Environmental Protection Agency (EPA) to facilitate the development of the experimental criteria for a NIST traceability protocol for dynamic elemental mercury vapor generators. The traceability protocol will be written by EPA. Traceability will be based on the actual analysis of the output of each calibration unit at several concentration levels ranging from about 2-40 ug/m^3, and this analysis will be directly traceable to analyses by NIST using isotope dilution inductively coupled plasma / mass spectrometry (ID ICP/MS) through a chain of analyses linking the calibration unit in the power plant to the NIST ID ICP/MS. Prior to this project, NIST did not provide a recommended mercury vapor pressure equation or list mercury vapor pressure in its vapor pressure database. The NIST Physical and Chemical Properties Division in Boulder, Colorado was subcontracted under this project to study the issue in detail and to recommend a mercury vapor pressure equation that the vendors of mercury vapor pressure calibration units can use to calculate the elemental mercury vapor concentration in an equilibrium chamber at a particular temperature. As part of this study, a preliminary evaluation of calibration units from five vendors was made. The work was performed by NIST in Gaithersburg, MD and Joe Rovani from WRI who traveled to NIST as a Visiting Scientist.

EXECUTIVE SUMMARY

Approximately 1,000 coal fired power plant stacks will need installation of mercury continuous emissions monitors (CEMs) during 2007. The power industry desires to begin a full year of monitoring before the formal monitoring and reporting requirement begins on January 1, 2009. It is important for the industry to have available reliable, turnkey equipment from CEM vendors. Western Research Institute (WRI) is working closely with the Electric Power Research Institute (EPRI), the National Institute of Standards and Technology (NIST), and the Environmental Protection Agency (EPA) to facilitate the development of the experimental criteria for a NIST traceability protocol for dynamic elemental mercury vapor generators. The generators are used to calibrate mercury CEMs at power plant sites. The Clean Air Mercury Rule (CAMR) which was published in the Federal Register on May 18, 2005, requires that calibration be performed with NIST-traceable standards. It also requires that the calibration standard value be accurate within 2%. The traceability protocol will be based on the actual analysis of the output of each calibration unit at several concentration levels ranging from about 2-40 ug/m^3, and this analysis will be directly traceable to analyses by NIST using isotope dilution inductively coupled plasma / mass spectrometry (ID ICP/MS) through a chain of analyses linking the calibration unit in the power plant to the NIST ID ICP/MS.

Prior to this project, NIST did not provide a recommended mercury vapor pressure equation or list mercury vapor pressure in its vapor pressure database. The NIST Physical and Chemical Properties Division in Boulder, Colorado was subcontracted under this project to study the issue in detail and to recommend a mercury vapor pressure equation that the vendors of mercury vapor pressure calibration units can use to calculate the elemental mercury vapor concentration in an equilibrium chamber at a particular temperature. A NIST recommended equation was developed and published in the peer-reviewed literature as a result of this work. This equation is used to calculate the vapor pressure of liquid elemental mercury from the triple point to the boiling point. The equation provides a vapor pressure that is consistent with the Clausius/Clapeyron thermodynamic equation. The new NIST equation is different from some other equations in use, and it provides a vapor pressure at 20 ºC about 7% higher than the mercury vapor pressure listed in the 1928 International Critical Tables. There continues to be disagreement among the vendors on the correct vapor pressure equation for use in the calibration units. Because of this, it was agreed in a special meeting held in Orlando, FL in March 16, 2006 that the NIST traceability of calibration units would be performance based. The issue of the correct vapor pressure equation is now a side issue, and this is no longer in the critical path for establishing a NIST traceability protocol.

As part of this study, a preliminary evaluation of calibration units from five vendors was made. The work was performed by NIST in Gaithersburg, MD under subcontract to this project, and by Joe Rovani from WRI who traveled to NIST as a Visiting Scientist under a separate EPRI contract to help move the process along. Additional work is currently being performed by NIST

to establish the experimental procedures for the NIST traceability protocol. This protocol will be written by EPA and it is expected to be finalized sometime in 2007. Concurrent with these other activities, a draft standard specification for dynamic elemental calibrator units was written and submitted to ASTM subcommittee D22.03 on Ambient Air Monitoring for initial subcommittee balloting. Since it later became apparent from experimental results at NIST as part of this project, that different generator/calibrator units that apparently use similar equations do not necessarily provide the same output concentrations, the ASTM standard development activities were put on indefinite hold. The main focus is now on developing an optimal and user friendly analytical chain for the traceability protocol. The vendors are free to use any empirical equation or algorithm that provides an accurate correlation between the unit setting and the actual concentration output, which is traceable to an analysis by NIST.

TABLE OF CONTENTS

Page

OBJECTIVES

A main objective of the current work is to develop criteria for NIST traceability for mercury vapor standards for continuous emission monitor (CEM) calibration. This work is providing a direct contribution to the enablement of continuous emissions monitoring at coal-fired power plants in conformance with the Clean Air Mercury Rule (CAMR). EPA Specification 12 states that mercury CEMs must be calibrated with NIST-traceable standards. Although this requirement has been known since 1997, when the draft Specification 12 was circulated for comment, a NIST traceable standard to perform elemental mercury CEM calibration was not yet available in 2006. Initially it was thought that the calibration and implementation of mercury CEMs would be relatively simple, and implementation would follow the implementation of the Clean Air Interstate Rule (CAIR) SO_2 and NO_X monitoring, and sulfur emissions cap and trade. However, mercury has proven to be significantly more difficult to accurately determine than was originally thought. The purpose of this project is to evaluate issues related to the use of dynamic elemental mercury calibrators that are based on mercury vapor headspace above elemental mercury at a particular temperature. Although this work has moved the effort of developing NJIST traceable mercury CEM calibration standards significantly along the development path, more needs to be accomplished in conjunction with NIST and EPA before the process is complete.

INTRODUCTION

WRI is in a unique position to facilitate the process of development of NIST traceable calibration standards for mercury CEMs. As a result of this project, several issues that have not been uniformly addressed in the past, have been identified and have been examined in detail. These include the vapor pressure of mercury, and the performance of dynamic elemental mercury vapor generators from all five vendors from which such units are currently available. We are working closely with NIST to facilitate the development of a technically sound, yet practical traceability procedure that EPA can write into a new traceability protocol. The WRI analytical group has unique specialized capabilities in analytical method development and validation that are being applied to this effort.

One goal of the project is to critically evaluate the use of dynamic mercury vapor pressure generator technology for CEM calibration. This project involved the participation of three CEM calibrator vendors to provide equipment on loan to WRI for evaluation of the technology (Mercury-Instruments, Nippon/Horiba, and Thermo). This equipment was combined with equipment from two other vendors (PSA, Tekran) already in place at NIST in Gaithersburg, MD for evaluation and development of experimental procedures to implement as the main element of a traceability protocol. The results and recommendations from the current phase of the effort were provided to EPA, and EPA will incorporate this information in the traceability protocol for elemental mercury

calibration using dynamic generators. Without our participation, this process would not have proceeded to the point where it is today, and equipment from the three participating vendors would not have been included in the NIST work, or considered in the development of the traceability protocol. It is not the intent of this study to rank units from various vendors or recommend units from one vendor over another. It is assumed that the vendors will continuously improve their platforms and products as this technology is implemented. The primary purpose of this study is to evaluate the technical potential of the technology in general, and assist EPA and NIST in providing the necessary protocols to allow its implementation for CEM calibration.

Mercury Continuous Emissions Monitor Calibration

Western Research Institute (WRI) is working with the Electric Power Research Institute (EPRI), the National Institute for Standards and Technology (NIST), the U.S. Environmental Protection Agency (EPA), and instrument vendors to establish a NIST traceable standard for calibrating CEMs for elemental mercury. A separate but related issue is that of oxidized mercury standards (Mercal, Hovacal, others), which also will need to be addressed in the near future.

In 1997 EPA issued a draft Performance Specification 12 which states that mercury CEMs must be calibrated with NIST-traceable standards. This requirement was officially established with the final CAMR that issued on May 18, 2005 (Federal Register 2005). Although this requirement has been known since 1997, when the draft Specification 12 was circulated for comment, a NIST traceable standard to perform elemental mercury CEM calibration was not yet available as of 2006. Initially it was thought that the calibration and implementation of mercury CEMs would be relatively simple, and implementation would follow the implementation of CAIR SO_2 and NO_X monitoring, and sulfur emissions cap and trade. However, mercury in a gaseous medium, especially in stack gases, has proven to be significantly more difficult to accurately determine than was originally thought. Mercury vapor in either reduced or oxidized form is easily lost on surfaces or in transport due to adsorption and reaction processes. The purpose of this project was to evaluate issues related to the use of dynamic mercury calibrators that are based on mercury vapor headspace above elemental mercury at a particular temperature.

Calibration techniques for CEMs that have been proposed include calibration gas cylinders, mercury vapor permeation tubes, mercury diffusion tubes, and vapor pressure generators. The latter technology is currently generating significant interest. Saturated headspace devices contain a small amount of liquid elemental mercury in a temperature-controlled vessel. This technology has the possibility of generating large quantities of calibration gas over extended periods of time for CEM calibration. By precisely and accurately controlling and or measuring the equilibrium chamber temperature, a controlled concentration of mercury in nitrogen or air can be generated. This is diluted

further to provide a vapor calibration stream of known concentration. Several vendors are offering calibration devices based on this principle. These include Mercury-Instruments, Nippon/Horiba, PSA, Tekran, and Thermo.

RESULTS AND DISCUSSION

The Vapor Pressure of Mercury

Until this issue was explored in detail in the current work, it was widely accepted that the use of a mercury vapor pressure equation based on the mercury vapor pressure table in the 1928 International Critical Tables (ICT 1928) was all that was required to know the concentration of mercury in headspace at a particular temperature. This study undertook a comprehensive and critical evaluation of the various vapor pressure equations in use, and the equations that vendors could use to calculate the concentration output for their dynamic mercury generator units.

Prior to this project, the National Institute of Standards and Technology (NIST) did not provide a recommended mercury vapor pressure equation or list mercury vapor pressure in its vapor pressure database. The NIST Physical and Chemical Properties Division in Boulder, Colorado was subcontracted under this project to study the issue in detail and to recommend a mercury vapor pressure equation that the vendors of mercury vapor pressure calibrators can use to calculate the elemental mercury vapor concentration in a chamber at a particular temperature. NIST conducted a thorough study of the various sources of vapor pressure data, going back into the 19th century. NIST found that the most commonly used mercury vapor pressure data set, which was published in the 1928 International Critical tables, provided results that were subsequently improved upon by later researchers (ICT 1928). The NIST Physical and Chemical Properties Division issued a preliminary draft report of its findings in July 2005. Following changes based on comments from reviewers, a second draft report was issued in September 2005. The final report was issued in early 2006, and it is provided in Appendix A. A new NIST equation for the vapor pressure of mercury was provided as a result of this work. This equation calculates the vapor pressure of liquid elemental mercury from the triple point to the boiling point. The equation is different from some other equations in use, and it provides a vapor pressure at 20 ºC that is about 7% higher than the mercury vapor pressure listed in the 1928 International Critical Tables (Appendix A, Huber et al. 2006a, 2006b).

The new NIST equation has stirred up an assortment of responses. Apparently, many approaches for calculating mercury headspace concentrations for static and dynamic calibration units in the past have been based on various empirical equations that correlate with the mercury vapor pressure table published in Lange's Handbook, and in earlier CRC Handbooks (1970-1980). The Lange's table is the same one that was published in the 1928 International Critical Tables from the U.S. National Research Council (Langes 1992). The 86th edition of the CRC Handbook (2005-2006) now uses a

newer data set that provides values near the 2006 NIST equation values, based on the data set of Vulalovich and Fokin (1972). The ICT data set is discussed in the NIST report, and NIST considers it to be inaccurate in the 0 – 100 ºC range (Appendix A, Huber et al. 2006a, 2006b). After careful research and review of the literature, NIST selected a data set that they consider less uncertain for their new equation, within 1% (Ernsberger 1955).

The equation used in ASTM D 6350 (mercury in natural gas by gold amalgam, calibrated by passive headspace and syringe injection) is expressed as: log (ng/mL) = (-3104/K) + 11.709. The ASTM method references an article by Dumary et al. (1985). That article discusses the nuances of and problems associated with using syringe/headspace calibration, but it does not cite the data set source of the mercury vapor pressure equation. The so-called Lindberg Equation has also been used: [Hgo] (mg/m^3) = (A/T) * 10 EXP – (-B + C/T) where A = 3216522.61, B = 8.134459741, C = 3240.871534. These equations both provide results about 7% lower than the new NIST equation at 20 ºC. Dr. Steve Lindberg, a retired Distinguished Scientist from Oak Ridge National Laboratory, was contacted during the course of this study, and he does not recall the particulars of how the equation attributed to him came to be established in the early 1990's, or what data set was used. The focus of the work of the group he was leading was not to determine the theoretical vapor pressure of mercury, but to measure mercury contamination of environmental concern by measuring ambient mercury concentration levels. This equation, which was developed during the course of the work to calibrate the analysis systems, is closely based on the 1928 ICT mercury vapor pressure data table.

There continues to be disagreement among the vendors on the correct vapor pressure equation for use in the calibration units. Because of this, a special meeting to address the issue was held on March 16, 2006 in Orlando, FL, at the conclusion of the Pittsburgh Conference on Analytical Chemistry. Meeting attendees included representatives from EPRI, WRI, NIST (Boulder and Gaithersburg), EPA, and the vendors. At that meeting, the issue of the correct mercury vapor pressure was not resolved. However, it was agreed that the NIST traceability of calibration units would be performance based, by analysis of the actual output of each unit, and therefore would no longer depend on any particular vapor pressure equation or data set. The discussions on the most correct theoretical equation thus became a side issue, and this is no longer in the critical path for establishing a NIST traceability protocol.

CEM Calibration Traceability Protocol for Dynamic Mercury Generators

In the latter part of 2003, EPA contracted with NIST in Gaithersburg, MD to analyze the mercury concentrations of eleven mercury calibration gas cylinders provided by Spectra Gases, Inc (Mitchell and Dorko 2004). NIST analyzed the cylinders against NIST mercury in coal standards and mercury in water standards using an absorption spectrometer with gold amalgam pre-concentration. Three of the cylinders were provided

to EPA; four were returned to Spectra Gases, Inc. to use to check against other cylinders in the future; and four remain at NIST for future analyses to determine stability over time. The precision of the cylinder concentration determined by NIST is plus or minus 6%, and this is due to the cumulative uncertainties of the standards, the weighing, the digestion, the measurement etc. that is required by NIST to take into account, then multiply by 2 for the "NIST expanded uncertainty" (Mitchell and Dorko 2004). This uncertainty is not tight enough to meet the 2% uncertainty required by CAMR for cap-and-trade purposes. In addition, the methods used in this preliminary study were not standardized as procedures for a traceability protocol. Secondary cylinders calibrated against these will have larger plus or minus values. Other issues related to cylinder use such as equilibration time for passivation of the regulator surfaces and the large volumes of gases required for calibration, and the cost, are relevant factors to be considered in using this approach for calibration.

EPA traceability protocols for calibration of SO_2 and NO_2 analyzers require that a device used to certify permeation tubes incorporate a temperature measurement device that is certified against NIST traceable standards annually (Wright and Messner 1997). The flow meter must be checked annually against a NIST traceable standard also. In this protocol there are no requirements for periodic re-certification of units that are used in the field, or of the permeation tubes themselves after initial certification.

NIST has proposed the use of isotope dilution inductively coupled plasma / mass spectrometry (ID ICP/MS) as the benchmark technique for providing accurate analysis of the output from cylinders and dynamic vapor pressure generators used for CEM calibration. Throughout this project, ongoing discussions have been held with NIST, EPA, EPRI and the vendors in order to identify the key issues that need to be addressed. These discussions with NIST also have provided insight into the meaning of the term "NIST Traceable". NIST has been conducting a series of internal meetings to discuss the various ways that this has been defined in different situations. There are many different groups at NIST working independently of each other. At end of 2006, there is nothing that NIST has done with mercury cylinders, mercury permeation tubes, or vapor generators that they consider traceable. It is not appropriate for any vendor to claim NIST traceability until the traceability protocols are issued by EPA and followed by the vendors. This can not be done until specific detailed analysis protocols are developed and documented by EPA, including protocols used by NIST and protocols used by the vendors in their manufacturing facilities to compare units with a NIST standard. The gas cylinders or the mercury vapor pressure generator analyzed by NIST in 2004 are not to be considered NIST traceable, since these procedures have not been defined or published, or approved by NIST or EPA.

NIST will not offer a mercury vapor standard reference material (SRM) for sale, however the procedures for certifying a generator/calibrator or standard gas cylinder for a manufacturer that the manufacturer would use in the factory to certify other units are

being evaluated. EPA is using this information from NIST to develop traceability standard protocols in 2007.

Several new documents must be developed by EPA with technical input and experimental procedures provided by NIST. These include a protocol for the mercury compressed gas cylinders, possibly to be based on the model of the 1997 Traceability Protocol (Wright and Messna 1997). Although EPA is in the process of updating the air pollution standard traceability protocols (NO_X, SO_2), it is generally acknowledged that the mercury generator technology is unique enough that it will require separate protocols. A mercury vapor pressure generator also can contain a pressure transducer to automatically convert concentrations to standard temperature and pressure conditions from standard gases generated at different temperatures and altitudes. The inherent uncertainties of the temperature and pressure transducers will need to be considered also. Possibly, two documents are needed for the generators, namely a mercury gas generator certification protocol, and a mercury gas generator audit protocol. The period between recertification must also be determined by performing long term stability studies.

New protocols must also be written in the near future to address procedures for the NIST traceability of oxidized mercury vapor standards. Current work at NIST involves introducing the output from an oxidized standard (i.e., Mercal, Hovacal, others) into an absorbent solution by sparging. The solution is then spiked with an isotope-diluted standard solution, with a known ratio of isotope to standard. NIST has experimentally determined that there is a loss near 10.5% in the reduction/sparging step, so this procedure is designed to compensate for this, so that the losses are the same for the standard and the material they are checking. It has been observed by NIST that the output concentration of an oxidized mercury vapor generator is lower by several percent that would be predicted based on the liquid mercury standard solution that is converted to oxidized mercury vapor. This is likely due to inherent losses resulting from the less than quantitative efficiency of converting a liquid mercury standard solution to a vapor stream. Because of this, the oxidized standards also will need to be certified against an ID ICP/MS analysis at NIST, as a performance-based standard. An EPA traceability protocol for this will need to be written also, and it will likely address a procedure that would be used to ensure that the oxidized standard units that are deployed at power plants would be experimentally linked to the NIST ID ICP/MS analysis.

Evaluation of Dynamic Mercury Vapor Pressure Calibration Technology

This project involved the participation of three CEM calibrator vendors that provided equipment on loan to WRI for evaluation of the technology (Mercury-Instruments, Nippon/Horiba, and Thermo). This equipment was combined with equipment from two other vendors at NIST in Gaithersburg, MD (PSA, Tekran) for evaluation and development of experimental procedures to implement as the main element of a traceability protocol. Data sheets for each of the five generator/calibrator

units are provided in Appendix B. The information in these sheets is subject to change by the vendors.

Under subcontract to this project, NIST was commissioned to evaluate the concentration output of the dynamic calibration units from all five vendors. A copy of the NIST report is provided in Appendix C. The purpose of this study was not to evaluate the relative merits of a generator from one vendor against the generators from other vendors. The main purpose of this study was to define the concentration output characteristics of the generators from 2-40 ug/m^3 elemental mercury, and to develop optimal experimental conditions under which the generator output would be measured by isotope dilution ICP/MS as part of a traceability protocol. It is important to note that NIST observed a conversion efficiency of 89.5% when a diluted NIST aqueous mercury standard solution was reduced and sparged to provide an elemental mercury vapor stream to compare against the output of mercury vapor pressure generators (Appendix C, Section 6). A correction was made using an internal standard to compensate for this loss. The report notes that the output for each of the five units evaluated was highly linear. This is an important observation since it suggests that the actual measured concentration output can be easily adjusted to the desired concentration that is set on each unit using linear equations with adjustable intercept and slope values.

In addition, and under a separate contract with EPRI, WRI provided to NIST the assistance of a Visiting Scientist, Joe Rovani, during August and September 2006 to work at NIST to provide work to develop procedures to evaluate the output from the five calibration units. The work with the data generated in that study was continued under the current project. A report of these activities is provided in Appendix D. The purpose of this phase of the work was to provide assistance to NIST to better understand how the mercury concentration output from the generators can be measures as part of a traceability protocol. At the conclusion of this phase, additional experimental work is currently being conducted by NIST, and all of the data to date are being compiled to define the procedures that EPA will include in the traceability protocol documents that are expected to be provided by EPA in 2007.

The work at NIST shows that analyzers can drift over a relatively short period of time (Appendix D). Because of this, the certification protocol will involve requiring using so-called “nesting” analysis, in which the analysis of the output from the generator to be sent to a power plant is bracketed by the analysis of the output from a generator that is traceable to NIST ID ICP/MS. NIST does not feel that it is in their purview to deal with analyzer drift issues in the current study. Their focused objective at this time is to provide a calibration standard within a known accuracy limit, the percent value of which is yet to be determined.

NIST notes that additional work is needed (Appendix C, Section 8). For example, the data generated for the devices are not necessarily representative of other devices from

the same vendor, and that variation between similar devices is to be expected. Also, it is expected that there will be improvements and next generation devices available as this technology emerges with designs specific for CEM calibration. The output from several devices from each manufacturer should be examined. Also measurements on the repeatability of the generator out puts over a defined time frame are needed. In the ID ICP/MS work in Appendix C, all of the units were tested using high purity nitrogen. Tests need to be conducted using dry air because the nature of the transport medium used may affect results. WRI will be conducting many of these experiments as part of a continuation of this project.

Uncertainty and Accuracy Issues

The inherent uncertainty and stability of the mercury concentration output from the vapor pressure calibration units is a combination of the uncertainty (accuracy) and variability of the temperature measurement, the variability of equilibrium chamber temperature control, and the accuracy and inherent variability of two mass flow controllers. This makes it theoretically difficult, because of a combination of mechanical factors, to accurately accurately maintain a specific concentration output within 2%, which is what CAMR is requiring for a NIST traceable standard. For example the typical uncertainty in a mass flow controller is 0.5%. A generator unit typically employs a minimum of two mass flow controllers. The uncertainty of a NIST traceable thermometer to measure the temperature of the equilibrium chamber is typically 0.1ºC. Maintaining the equilibrium chamber at a set temperature requires a heating or thermoelectric cooling element, which can cycle on and off. Once the calibration gas is generated, it can be numerically converted to standard temperature and pressure value (STP, 0 ºC, 760 mm Hg), which requires the accurate measurement of ambient temperature and atmospheric pressure. Both the pressure transducer and thermometer used to measure atmospheric conditions will have uncertainties of their own. In addition to these considerations, each manufacturer produces a device with features unique to the particular device which affect the overall uncertainty. This is evident in the results from studies at NIST in the reports provided in Appendixes C and D. Therefore, the practical accuracy and stability specifications of such calibration devices will need to be determined experimentally.

On August 22, 2006, an entry in the Federal Register requested comments on the feasibility of the 2% requirement in the current CAMR (Federal Register 2006). Dr. Bill Dorko at NIST provided a written comment to EPA in which he stated that the required accuracy would need to be determined by what was technically and experimentally feasible, using actual laboratory data. At the preparation of this report, the issue remains unresolved.

Draft ASTM Standard Specification for Dynamic Calibration Units

In early 2006, a draft ASTM standard was prepared and balloted within ASTM D 22.03 on Ambient Air Monitoring. At that time it was believed that by standardizing the requirement for construction of key elements of the dynamic calibration units and specifying the NIST mercury vapor pressure equation, the output from mercury vapor generator units from various vendors would provide the same concentration levels at the same settings. Concurrent with these other activities, a draft standard specification for dynamic elemental calibration units was written and submitted to ASTM subcommittee D22.03 on Ambient Air Monitoring for initial subcommittee balloting. This was done towards the goal of establishing uniform criteria that would assure that each calibration unit conforming to the standard would provide the same concentrations of mercury when the same settings were used. This draft standard specified the use of the 2006 NIST mercury vapor pressure equation. The draft received 28 affirmative votes, 6 negative votes, and 51 abstentions. The negative votes cited disagreements over the correct mercury vapor pressure equation. Also, it later became apparent from results of work at NIST as part of this project, that different generator/calibrator units that apparently use similar equations do not necessarily provide same output concentrations. That is, there are more variables that are unit-specific than can be overcome by the use of a uniform equation. Because of these developments, the ASTM standard activities were put on indefinite hold. The main focus is now on developing an optimal and user friendly analytical chain for the traceability protocol. The vendors are free to use any empirical equation or algorithm that provides an accurate correlation between the unit setting and the actual concentration output traceable to a NIST analysis.

On The Use of Liquid Standards to Determine Mercury Vapor Pressure Equations for Mercury Vapor Pressure Calibration

It is important to undertake a brief discussion of an issue that has arisen frequently during the course of this study. This issue also arose during the ASTM draft standard activities relative to the use of mercury vapor pressure equations for determining the output of generator units. The key question is whether or not it is technically appropriate to use a diluted ASTM or any other aqueous liquid standard solution to directly calibrate a system for gas analysis. The only way this would be a valid approach is if it can be demonstrated experimentally that the conversion of the species of interest from liquid solution to vapor solution is 100% efficient. References frequently cited in the discussions related to the use of a mercury vapor pressure equation deal with mercury analysis using gold amalgam systems, and calibration checks using static headspace above mercury in air in a closed vessel. There are two cases outlined below, and the experimental results to date could possibly be used to support either case, since no definitive experiments on the efficiency of the chemical reaction/sparging step have been published. Until recently, no one has challenged the assumption behind Case I.

Case I. There has been a basic assumption that the 1928 International Critical Tables (ICT) vapor pressure table for mercury in the range 20-40 ºC is correct. All interpretations of results are based on this assumption. The results from diluted NIST mercury in water standard analysis involving chemical reaction and sparging have been observed to be within a few percent of the results from the direct injection of headspace above mercury when the ICT data set is used. For the ICT vapor pressure to be correct, an assumption must be made that the water standard analysis involving chemical reaction and sparging analysis is essentially 100% efficient, and there are no significant losses anywhere in the dilution, reduction, sparging, or amalgamation steps of the process.

Case II. If, on the other hand, the 2006 NIST equation is correct, it can be concluded that the water standard analysis involving chemical reaction and sparging analysis results in a loss of a few percent of mercury. That is why the sparging results would appear to correlate well with the ICT vapor pressure data, which are lower than the NIST equation data by a few percent. It must not be overlooked that the NIST equation is consistent with the Clausius-Clapeyron thermodynamics equation (Appendix A, Huber et al. 2006a, 2006b). In addition, recent experiments by NIST in Gaithersburg, MD observed a loss of mercury near 10.5% in the reduction/sparging step from NIST aqueous mercury standard solutions (Appendix C, Section 6).

1. Dumarey et al. (1985a**)** wrote a short communication where he describes the special conditions that must be met for calibration by static headspace to correlate with calibration by oxidation followed by reduction/sparging of an aqueous standard. Some of his comments are listed below.

1.1 The use of aqueous mercury standard solutions shows some important limitations. At low concentrations (<1 ug/L), the solutions become unstable. This is caused partly by sorption of the mercury on the vessel walls and partly by volatilization.

1.2 For best accuracy using liquid solutions, it is recommended to determine the minimum aeration time required for each type of sample independently.

1.3 The temperature of the water bath for the saturated vapor pressure equilibrium chamber must always be kept below ambient temperature to prevent condensation of saturated mercury in the syringe.

1.4 Gas syringes used to transfer saturated mercury in air from the equilibrium chamber to the analyzer must be preconditioned with at least 3 strokes to prevent losses due to partial sorption of mercury on the syringe walls.

1.5 Transfer to the gold amalgam absorber should be as fast as possible to avoid losses by diffusion of mercury through the needle tip

1.6 After some time, the mercury in the calibrator equilibrium chamber becomes oxidized at the surface by atmospheric oxygen.

1.7 Following all of these precautions, Dumarey states that he observed differences within 3% (he doesn't mention whether the differences were high, low, or random) of the results from the measurement of 1-50 ng of mercury, from either aqueous standard solution or saturated headspace. The data are not provided.

1.8 Dumarey uses a mercury vapor pressure consistent with the 1928 International Critical Tables (ICT) value, which gives a vapor concentration of 13.17 ng at 20 ºC. The source of the vapor pressure data was not cited.

2. Dumarey et al (1985b) demonstrated the use of gold coated sand to collect mercury samples in an article comparing the efficiency of various sorbent trap compositions for elemental mercury and other mercury species,. He used a second gold trap for the analytical amalgamation/desorption step (dual trap method). Highlights of the work are provided below.

2.1 Permeation tubes were used to generate air standards for elemental mercury, mercuric chloride, and volatile alkyl- and alkylchloro-mercury compounds. Presumably these were fabricated in the laboratory, since no source of the tubes is given.

2.2 Gold coated sand quantitatively adsorbed all of the various mercury forms studied, including elemental mercury and mercuric chloride.

2.3 The gold coating on the sand must be very thin to prevent memory effects between analyses.

2.4 Dumarey refers to the 1985a reference in which he stated that he observed a difference within 3% of the results from the measurement of 1-50 ng of mercury, from either aqueous standard solution or saturated headspace. Data for this observation are not provided.

3. Fitzgerald and Gill (1979) describe a two-stage gold amalgam technique for measuring mercury in atmosphere. Highlights of the analytical technique are listed below.

3.1 A single gold coated glass bead column is used to introduce mercury into the detector, because different columns provide different response characteristics with respect to the release of mercury to the detector upon heating. In this manner the

results are consistent for different samples and standards. A calibration curve of area vs. ng Hg is unique for a specific analytical gold amalgam column.

3.2 Different gold coated glass bead columns can be used to collect samples. The column is heated and the mercury is released to the analytical gold amalgam column.

3.3 Calibration is with air saturated with mercury from a sealed chamber at 25 ºC. The concentration of mercury is assumed to be 19.93 mg/L. This is close, but not identical to the 1928 ICT vapor pressure value. The source of the vapor pressure data was not cited. Nine replicate injections of a 1 ng mercury spike gave a relative standard deviation of 2.5%.

3.4 Several replicates of weighed standards of mercuric chloride in acid solution were reduced and sparged to compare with results from replicates of the 25 ºC static vapor pressure based gas calibration. The aqueous solutions gave results that were on average 2% lower than the gas standards, with relative standard deviations for both sets of measurements of 1.6-1.7%.

4. Gill and Bruland (1990) describe a study on mercury in freshwater systems using dual gold trap atomic fluorescence spectroscopy. The paper does not dwell much on the methodology, however there are some key observations listed below.

4.1 The precision associated with replicate additions of a gas-phase elemental Hg spike was reported to be approximately 1% relative standard deviation.

4.2 The precision of replicate measurements of a single sample for the aqueous reduction ($SnCl_2$) and sparging method was 10% relative standard deviation for samples containing more than 0.25 ng.

4.3 The authors do not describe the vapor pressure data used, however they refer to Fitzgerald and Gill, so the vapor pressure used is probably similar to ICT. No comparison between the vapor pressure and aqueous calibrations are made.

5. Bloom and Fitzgerald (1988**)** described studies of volatile mercury species using gas chromatography with cold vapor atomic fluorescence detection for mercury.

5.1 Calibration for elemental mercury was by static saturated headspace in a 250 mL sealed container with 5 g mercury liquid. No further detail on the calibration is provided.

The overall results from the above studies and the data provided by some vendors indicate that the ICT vapor pressure data correlate within a few percent of the analysis of

water standards. These studies all assume that the ICT vapor pressure data are correct. There is no consideration of any other vapor pressure data and its possible implications. The key assumption that must be made to arrive at the conclusion that the ICT vapor pressure data are correct is that the efficiency of the analysis of water standards by reduction/sparging is 100%. This assumption has never been shown experimentally to be correct. Indeed, there are hints in the literature and recent experimental results from NIST that a quantitative chemical reaction and transfer might actually be difficult to achieve. For example, see 1.1, 1.2, and 4.2 above. If the NIST mercury vapor pressure equation is correct, the actual values for elemental mercury vapor pressure are 6% higher than ICT at 25 ºC, and 7% higher at 20 ºC. This would mean that there is a loss of the order of 6-7% in the aqueous chemical reaction and sparging sequence. None of the above publications address that issue, and the studies were not designed to address that issue. The studies were all based on the key assumption that the mercury vapor pressure that was used is beyond question.

If the NIST vapor pressure equation is correct, then this would mean that possibly air analysis conducted in the past using vapor pressure calibration based on ICT are 6-7% low. However, ASTM D 6350 (mercury in natural gas) states that the repeatability of replicate saturated mercury vapor calibration injections can vary by 10%, and that difference in the practical application of this methodology is actually greater than the difference between the ICT and NIST vapor pressure equations.

It is beyond the scope of the current study to further address or resolve this issue. It is important, however, to recognize that this issue exists, since it often is discussed in the context of CEM calibration.

REFERENCES

Bloom, N., 1988, "Determination of Volatile Mercury Species at the Picogram Level by Low-Temperature Gas Chromatography with Cold Vapour Atomic Fluorescence Detection", Analytica Chimica Acta. 208, 151-161.

CRC Handbook of Chemistry and Physics, 2005-2006, 86th Edition, Taylor and Francis, NY., p. 6-126.

Dumarey, R., E. Temmerman, R. Dams, and J. Hoste, 1985a, "The Accuracy of the Vapour-Injection Calibration Method for the Determination of Mercury by Amalgamation/Cold Vapour Atomic Absorption Spectrometry", 170, 337-340.

Dumarey, R., R. Dams, and J. Hoste, 1985b, "Comparison of the Collection and Desorption Efficiency of Activated Charcoal, Silver, and Gold for the Determination of Vapor-Phase Atmospheric Mercury", Analytical Chemistry, 57, 2638-2643.

Ernsberger, F.M., Pitman, H.W., 1955, "New Absolute Manometer for Vapor Pressures in the Micron Range", Rev. Sci. Instrumen., 26(6), 584-589.

Federal Register, May 18, 2005. EPA 40 CFR Parts 60, 72, and 75. Standards of performance for New and Existing Stationary Sources: Electric Utility Steam Generating Units; Final Rule.

Federal Register, August 22, 2006. EPA 40 CFR Parts 72 and 75. Revisions to the Continuous Emissions Monitoring Rule for the Acid Rain Program, NOx Budget Trading Program, the Clean Air Interstate Rule, and the Clean Air Mercury Rule; Proposed Rule.

Fitzgerald, W.F. and G.A. Gill, 1979, "Subnanogram Determination of Mercury by Two-Stage Gold Amalgamation and Gas Phase Detection Applied to Atmospheric Analysis", Analytical Chemistry, 51 (11), 1714-1720.

Gill, G.A. and K.W. Bruland, 1990, "Mercury Speciation in Surface Freshwater Systems in California and Other Areas", Environ. Sci. Technol. 24, 1392-1400.

Huber, M.L., A. Laesecke, and D.G. Friend, 2006a. The Vapor Pressure of Mercury, NISTIR 6643.

Huber, M.L., A. Laesecke, and D.G. Friend, 2006b. Correlation for the Vapor Pressure of Mercury, Ind. Eng. Chem. Res. 45, 7351-7361.

ICT, 1928. International Critical Tables of Numerical Data, Physics, Chemistry, and Technology, Volume III, National Research Council, p. 206.

Lange's Handbook of Chemistry, 1992, 14th Edition, McGraw-Hill, NY, p. 5.24.

Mitchell, G.D. and W. Dorko, 2004. Final Report for Mercury in Nirtogen Gas Research Gas Mixture, EPA DW13939860-01-0.

Vukalovich, M.P., and L.R. Fokin, 1972. Thermophysical Properties of Mercury, Standards Press (USSR).

Wright, R.S. and M.J. Messner, 1997. Final Report: EPA Traceabilty Protocol for Assay and Certification of Gaseous Calibration Standards, EPA/600/R-97/121, National Technical Information Service no. PB98115314.

APPENDIX A

NIST REPORT ON MERCURY VAPOR PRESSURE

NISTIR 6643

The Vapor Pressure of Mercury

Marcia L. Huber
Arno Laesecke
Daniel G. Friend

National Institute of Standards and Technology
Technology Administration, U.S. Department of Commerce

NISTIR 6643

The Vapor Pressure of Mercury

Marcia L. Huber
Arno Laesecke
Daniel G. Friend
Physical and Chemical Properties Division
Chemical Science and Technology Laboratory
National Institute of Standards and Technology
Boulder, CO 80305-3328

April 2006

U.S. DEPARTMENT OF COMMERCE
Carlos M. Gutierrez, Secretary
TECHNOLOGY ADMINISTRATION
Robert Cresanti, Under Secretary of Commerce for Technology
NATIONAL INSTITUTE OF STANDARDS AND TECHNOLOGY
William Jeffrey, Director

Table of Contents

The Vapor Pressure of Mercury

Marcia L. Huber, Arno Laesecke, and Daniel G. Friend
National Institute of Standards and Technology*
Boulder, CO 80303-3328

In this report, we review the available measurements of the vapor pressure of mercury and develop a new correlation that is valid from the triple point to the critical point. The equation is a Wagner-type form, where the terms of the equation are selected by use of a simulated annealing optimization algorithm. In order to improve the reliability of the equation at low temperatures, heat capacity data were used in addition to vapor pressure data. We present comparisons with available experimental data and existing correlations. In the region of interest for this project, over the temperature range 0 °C to 60 °C, the estimated uncertainty (estimated as a combined expanded uncertainty with coverage factor of 2, 2σ) of the correlation is 1 %.

Keywords: correlation, mercury, vapor pressure.

1. Introduction

Recent concerns about mercury as an industrial pollutant have lead to increased interest in the detection and regulation of mercury in the environment [1]. The development of standardized equations for the thermophysical properties of mercury can aid this task. A critical evaluation of density, thermal expansion coefficients, and compressibilities as a function of temperature and pressure was conducted by Holman and ten Seldam [2]. Bettin and Fehlauer [3] recently reviewed the density of mercury for metrological applications. Vukalovich and Fokin's book [4] and the Gmelin Handbook [5] are both thorough treatises on the thermophysical properties of mercury. Thermal properties such as thermal conductivity and heat capacity were reviewed by Sakonidou et al. [6], while Hensel and Warren [7] cover other properties including optical and magnetic characteristics. To assess risks of exposure, it is important to have an accurate representation of the vapor pressure of mercury. Numerous compilations and correlations of the vapor pressure of mercury have been published [8-25], but there is no consensus on which is the best one to use for a given purpose. In this work, we review the existing experimental data and correlations, and provide a new representation of the vapor

* Physical and Chemical Properties Division, Chemical Science and Technology Laboratory.

pressure of mercury that is valid from the triple point to the critical point. We also present comparisons with both experimental data and correlations, and estimate the uncertainty of the correlation.

2. Experimental Vapor Pressure Data

Experimental measurements of the vapor pressure of mercury have a long history. A single vapor pressure point of mercury, the boiling point, was first measured in 1801 by Dalton [26], who obtained a value corresponding to 622 K; shortly thereafter, in 1803, Crichton [27] mentioned that the normal boiling point is above a temperature corresponding to 619 K. More recently, the normal boiling point of mercury was determined by Beattie et al. [28] as (356.58 ± 0.0016) °C, on the 1927 International Temperature Scale. This measurement was selected as a secondary fixed point on the ITS-48 Temperature scale [29]. Converted to the ITS-90 temperature scale [30], this value is (629.7653 ± 0.0016) K. The value recommended by Marsh [31] is 629.81 K (IPTS-68); on the International Practical Temperature Scale [32] of 1968, this was a secondary fixed point. Converted to ITS-90, this recommendation is 629.7683 K for the normal boiling point.

Regnault [33] published observations of the vapor pressure of mercury over a range of temperatures in 1862. Several of the early publications are by researchers who became quite famous, including Avogadro [34], Dalton [26], Hertz [35], Ramsay [36], and Haber [37]. Indeed, much of the work on mercury was done in the early part of the 20th century. Figure 1 shows the distribution of the experimental data. Table 1 gives a detailed compilation of sources of vapor-pressure data from 1862 to the present, along with the temperature range of the measurements, the experimental method used, and an estimate of the uncertainty of these measurements. In general, determinations of the purity of the mercury were not available; however, methods for the purification of mercury have been known for a long time, and samples of high purity were prepared before it was possible to quantify the purity [18]. The estimates of uncertainty were obtained by considering the experimental method and conditions, the original author's estimates (when available), and agreement with preliminary correlations. These correspond to our estimate of a combined expanded uncertainty with a coverage factor of

two. In Appendix A, we tabulate all experimental data for the vapor pressure of mercury collected in this study.

The experimental techniques used to measure vapor pressure can be grouped into three main categories: the static, quasistatic, and kinetic techniques are discussed by Dykyj et al. [38] and Ditchburn and Gilmour [14]. One of the simplest methods to measure the vapor pressure is a static method that involves placing the sample in a closed container, then removing any air and impurities, keeping the vessel at constant temperature, and then measuring the temperature and pressure after equilibrium has been established. It is generally limited to pressures above 10 kPa. In principle, it is applicable to any pressure, but in practice the presence of nonvolatile impurities can cause large systematic errors. With very careful sample preparation, it may be possible to go to lower pressures with this technique. Another static instrument is the isoteniscope. This type of instrument was used by Smith and Menzies [39, 40] in their early work on the vapor pressure of mercury. In this type of apparatus, the sample is placed in a bulb that is connected to a U-tube that acts as a manometer (i.e., a pressure sensor). The device is placed in a thermostat, and the external pressure is adjusted until it equals that of the vapor above the sample. Isoteniscopes are limited by the sensitivity of the pressure sensor. A third type of static method involves the use of an inclined piston gauge. The sample is placed in a cylinder fitted with a movable piston so that the pressure of the sample balances the weight (gravitational force) of the piston. This method is generally applicable over the range 0.1 kPa to 1.5 kPa.

Among the instruments classified as quasistatic are ebulliometers and transpiration methods. In both of them, a steady rate of boiling is established, and it is assumed that the pressure at steady state is equivalent to the equilibrium vapor pressure. In an ebulliometer, the sample is boiled at a pressure set by an external pressurizing gas (often helium) with the vapor passing through a reflux condenser before returning to the boiler. The temperature measured is that of the vapor just above the boiling liquid. An advantage to this method is that volatile impurities do not condense and are removed at the top of the apparatus. This method may also be set up in a comparative mode with two separate ebulliometers, one containing a reference fluid and the other containing the sample fluid connected with a common pressure line, so that direct measurement of the pressure is unnecessary. It is possible to make very accurate measurements with this type

of device, at pressures greater than about 2 kPa. The very accurate measurements of the vapor pressure of mercury by Ambrose and Sprake [18] were made with an ebulliometric technique. The transpiration method (also called gas saturation) involves passing a steady stream of an inert gas over or through the sample, which is held at constant temperature. The pressure is not measured directly, but rather is calculated from converting the concentration of the mercury in the gas stream to a partial pressure that is the vapor pressure of the sample. This type of method has a larger uncertainty than some of the other methods, generally ranging from 0.5 to 5 % [38]. It is most useful over a pressure range of 0.1 to 5 kPa. For example, Burlingame [43] and Dauphinee [49,50] used the transpiration method in their measurements.

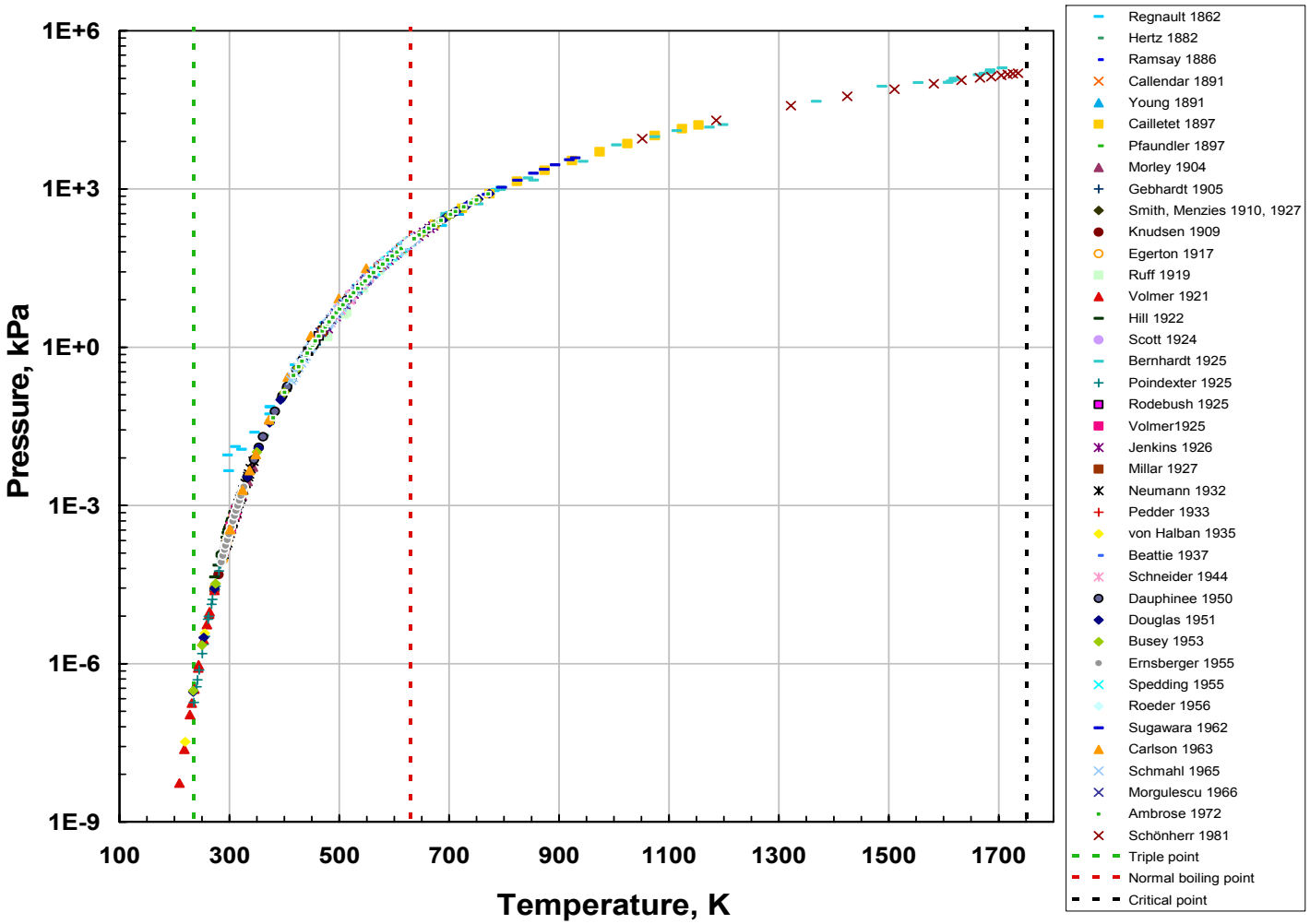

Figure 1 Experimental vapor pressure data for mercury.

Table 1 Summary of available data for the vapor pressure of mercury. References in boldface indicate primary data sets (see text).

First Author	Year	Method	No. pts.	*T* range, K	Estimated uncertainty, %
Ambrose [18]	1972	ebulliometer	113	417-771	less than 0.03, greatest at lowest *T*
Beattie [28]	1937	boiling tube	42	623-636	0.03
Bernhardt [41]	1925	3 static methods	27	694-1706	varies from 2 to >15
Bessel-Hagen [42]	1881	Töpler vacuum pump	2	273-293	>20
Burlingame [43]	1968	transpiration	38	344-409	4
Busey [44]	1953	derived from caloric properties	24	234-750	varies from 0.2 to 3.5 at lowest *T*
Cailletet [45]	1900	Bourdon manometer	11	673-1154	varies from 1 to 7
Callendar [46]	1891	Meyer tube	2	630	0.2
Cammenga [47]	1969	effusion	graphical results	273-325	
Carlson [48]	1963	effusion	9	299-549	varies from 3 to >20
Dauphinee [49, 50]	1950,1951	transpiration	18	305-455	5
Douglas [51]	1951	derived from caloric properties	30	234-773	varies from 0.03 (at normal boiling point) to 1.5 at lowest *T*
Durrans [52]	1920	gives table attributed to Smith and Menzies[39]	46	273-723	
Egerton [53]	1917	effusion	27	289-309	5
Ernsberger [54]	1955	piston manometer	18	285-327	1
Galchenko [55]	1978	static method	graphical results	523-723	3
Galchenko [56]	1984	atomic absorption	correlating equation only	723-873	3
Gebhardt [57]	1905	boiling tube	9	403-483	8
Haber [37]	1914	vibrating quartz filament	1	293	2
Hagen [58]	1882	differential pressure	5	273-473	>20

First Author	Year	Method	No. pts.	*T* range, K	Estimated uncertainty, %
Hensel [59]	1966	electrical resistance	graphical results	1073-critical	not available
Hertz [35]	1882	static absolute manometer	9	363-480	5
Heycock [60]	1913	not available	1	630	0.2
Hildenbrand [61]	1964	torsion-effusion	6	295-332	5
Hill [62]	1922	radiometer principle	19	272-308	30
Hubbard [63]	1982	static	graphical results	742-1271	not available
Jenkins [64]	1926	isoteniscope	21	479-671	0.1 to >20
Kahlbaum [65]	1894	ebulliometer	43	393-493	>10
Knudsen [66]	1909	effusion	10	273-324	varies from 5 to 10
Knudsen [67]	1910	radiometer principle	7	263-298	varies from 5 to 10

Table 1 Continued.

First Author	Year	Method	No. pts.	*T* range, K	Estimated uncertainty, %
Kordes [68]	1929	temperature scanning evaporation method	2	630-632	4
Mayer [69]	1930	effusion	82	261-298	5, except greater at $T<270$
McLeod [70]	1883	transpiration	1	293	>20
Menzies [39, 40]	1910,1927	isoteniscope	46	395-708	0.5
Millar [71]	1927	isoteniscope	6	468-614	2
Morley [72]	1904	transpiration	6	289-343	varies from 8 to >20
Murgulescu [73]	1966	quasi-static	9	301-549	3
Neumann [74]	1932	torsion balance	19	290-344	6
Pedder [75]	1933	transpiration	3	559-573	2

Pfaundler [76]	1897	gas saturation	3	288-372	12
Poindexter [77]	1925	ionization gage	17*	235-293	5-20, greatest at lowest *T*
Raabe [78]	2003	computer simulation	20	408-1575	varies from 0.5 to >20
Ramsay [36]	1886	isoteniscope	13	495-721	varies from 0.3 to 10 at highest *T*
Regnault [33]	1862	isoteniscope	29	297-785	~6 for *T*>400, much higher for lower *T*
Rodebush [79]	1925	quasi-static	7	444-476	1
Roeder [80]	1956	quartz spiral manometer	7	413-614	2
Ruff [81]	1919	temperature scanning evaporation method	12	478-630	>20
Schmahl [82]	1965	static method	43	412-640	1.5
Schneider [83]	1944	gas saturation	23	484-575	10
Schönherr [84]	1981	electrical conductivity	13	1052-1735	3
Scott [85]	1924	vibrating quartz filament	1	293	2
Shpil'rain [86]	1971	ebulliometer	50	554-883	0.6 to 0.8
Spedding [87]	1955	isoteniscope	13	534-630	0.03
Stock [88]*	1929	transpiration	3	253-283	20
Sugawara [9]	1962	static method	14	602-930	2
van der Plaats [89]	1886	transpiration	26	273-358	
Villiers [90]	1913	ebulliometer	12	333-373	6
Volmer [91]	1925	effusion	10	303-313	3
von Halban [92]	1935	resonance light absorption	1*	255	7
Young [93]	1891	static	11	457-718	2

- Excludes points below the triple point.

The Knudsen effusion method is a type of vapor pressure measurement classified as a dynamic method. In this type of experiment, a steady rate of evaporation through an orifice into a vacuum is established, and pressure is calculated from the flow rate through the orifice by use of kinetic theory. This method is applicable at very low pressures (below 0.1 kPa), but generally has high uncertainties.

As indicated in Table 1, many measurements have been made on the vapor pressure of mercury. However, only a limited number of these are comprehensive and have uncertainty levels of one percent or less. These sets have been identified as primary data sets in our work and are indicated by boldface type in Table 1. In general, the most accurate measurements were those made with ebulliometric methods. Ambrose and Sprake [18] used an ebulliometric technique for their measurements from 380 K to 771 K. These data have an uncertainty of about 0.03 % or lower, with the largest uncertainty at the lowest temperatures. Beattie et al. [28] very accurately determined the boiling point of mercury over the temperature range 623 K to 636 K. Spedding and Dye [87] used an isoteniscope to measure the vapor pressure over the range 534 K to 630 K, with uncertainties on the order of 0.03 % except at the lowest temperatures where they are larger. Menzies [40, 94] used an isoteniscope at temperatures from 395 K to 708 K, but these data show more scatter and have larger uncertainties than the sets mentioned above; however, the uncertainties are still less than 0.5 %. Shpil'rain and Nikanorov [86] used an ebulliometric method extending from 554 K to 883 K. Their data are more consistent with the measurements of Ambrose and Sprake [18] in their region of overlap than are other high temperature sets, such as those by Sugawara et al. [9] , Bernhardt [41] or Cailletet et al. [45], and thus were selected as the primary data for the high temperature region from about 700 K to 900 K. In addition, although the uncertainty is higher than 1 %, we have selected the data of Schönherr and Hensel [84] for the highest temperature region, 1052 K to 1735 K. This data set was obtained by observing changes in the electrical conductivity. At fixed pressures, the temperature was raised, and when a discontinuity was observed, this was taken as an indication of phase change.

All of the sets mentioned so far are for temperatures greater than 380 K. At lower temperatures, the measurements are much more uncertain and display significant scatter. In

the low temperature range, we considered the measurements of Ernsberger and Pitman [54] to be the most accurate. These measurements were made with an absolute manometer method, with uncertainties on the order of 1 %, and they cover the temperature range 285 K to 327 K. This data set has been adopted in the metrology community for use in precision manometry, and has been described as reliable and confirmed by heat capacity measurements [95]. The reliability and thermodynamic consistency of these data will be discussed in more detail in a later section of this document.

The end points of the vapor pressure curve for stable vapor-liquid equilibrium are the triple point and the critical point. Metastable points may be obtained at points below the triple point. In principle, the three phase-boundary curves that meet at the gas-liquid-solid triple point of a pure substance continue beyond this intersection so that the phase equilibria become metastable relative to the third phase, which is absolutely stable. Vapor-liquid equilibrium along the vapor pressure curve continued below the triple point becomes metastable relative to the solid phase, and vapor-solid equilibrium along the sublimation pressure curve continued above the triple point becomes metastable relative to the liquid phase. Although the former has been realized in experiments [96], metastable phase equilibria are one of the least investigated phenomena of the behavior of matter. Their existence in principle is mentioned here because three datasets in the present collection report mercury vapor pressure data at temperatures below the triple point: Poindexter [77], Stock and Zimmermann [88], and von Halban [92]. The farthest reaching data below the triple point temperature are the results of Poindexter, covering a range from 194 K to 293 K. However, in this work we restrict our study to points above the triple point, although all points are tabulated in Appendix A.

The triple point of mercury has been designated as a fixed point of the ITS-90 [30] temperature scale, with a value of 234.3156 K. The critical point has been measured by several investigators; these values are listed in Table 2, along with uncertainty estimates provided by the authors. One of the first measurements of the critical point was made by Koenigsberger [97] in 1912, who made visual observations in a quartz tube and reported the critical temperature of mercury to be near 1270 °C (1543 K). This measurement was later criticized by Menzies [94] who reported that the critical temperature was at least 1275 °C

(1548 K). Another early determination was that of Bernhardt [41] who extrapolated his vapor pressure observations, and used Bender's [98] value of 1650 °C (1923 K) for the critical temperature, while estimating the critical pressure to be in the range 294.2 to 343.2 MPa. Later, Birch [99] determined the critical point by observing the changes in electrical resistance as a function of temperature at constant pressure. The review paper of Mathews [100] adopted Birch's values for the critical point. Ambrose [101] and also Vargaftik et al. [8] instead selected the value obtained by Franck and Hensel [102], also obtained from studies of changes in electrical resistance. Kikoin and Senchenkov [103] used electrical conductivity experiments to locate the critical point, Neale and Cusack [104] observed changes in the Seebeck voltage, while Götzlaff [13] analyzed isochoric and isobaric PVT data extrapolated to the saturation boundary. Most recently Kozhevnikov et al. [105] observed changes in the speed of sound along isobars as a function of temperature to determine the critical point. The value by Bernhardt [41] is too high both in pressure and in temperature. The critical temperature of Franck and Hensel [102] agrees very well with that obtained by Kozhevnikov et al. [105], while the critical pressure of Götzlaff [13] agrees very well with that of Kozhevnikov et al. [105] In this work we adopted the critical point of Kozhevnikov et al. [105].

Table 2 The critical temperature and pressure of mercury.*

First Author	Year	T_c (K)	p_c (MPa)
Koenigsberger [97]	1912	~1543	
Menzies [94]	1913	>1548	
Bender [98]	1915	1923	
Meyer [106]	1921	1747	
Bernhardt [41]	1925	1923	294.2 - 343.2
Birch [99]	1932	1733 ± 20	161 ± 5
Franck [59, 102]	1966	1763.15 ± 15	151 ± 3
Kikoin [103]	1967	1753 ± 10	152 ± 1
Neale [104]	1979	1768 ± 8	167.5 ± 2.5
Hubbard [107]	1983	1750	172
Götzlaff [13]	1988	1751 ± 1	167.3 ± 0.2
Kozhevnikov [105]	1996	1764 ± 1	167 ± 3

*Uncertainties are expressed in kelvins and megapascals for the temperature and pressure, respectively.

3. Correlation Development

Numerous expressions have been used to represent the vapor pressure of a pure fluid; many are reviewed in Růžička and Majer [108]. Equations of the general form

$$ln(p/p_c) = (T_c/T)\sum_i a_i \tau^{i/2} \quad , \tag{1}$$

where $\tau = 1\text{-}T/T_c$, are attributed to Wagner [109-112] and have been used successfully to represent the vapor pressures of a wide variety of fluids. Lemmon and Goodwin [113] used the Wagner form with exponents (1, 1.5, 2.5, and 5) to represent the vapor pressures of normal alkanes up to C_{36}. This form, which we will call Wagner 2.5-5, is one of the most widely used forms along with the equation with exponents (1, 1.5, 3, and 6) [109, 110], which we call Wagner 3-6. The 2.5-5 form has emerged as the generally preferred form [114]. When the data set is extensive and of high quality, other forms with alternative sets of exponents with additional terms have been used. For example, a Wagner equation with exponents (1, 1.5, 2, 2.5, and 5.5) was used to represent the vapor pressure of acetonitrile [115], and another variant of the Wagner equation, with exponents (1, 1.89, 2, 3, and 3.6), was used to represent the vapor pressure of heavy water [116] from the triple point to the critical point to within the experimental scatter of the measurements. The International Association for the Properties of Water and Steam (IAPWS) formulation for the vapor pressure of water [117, 118] uses a six-term Wagner equation with exponents of (1, 1.5, 3, 3.5, 4, and 7.5).

Since there is a lack of high-quality experimental vapor-pressure data in the low temperature region (T < 285 K), liquid heat capacity measurements at low temperatures can be used to supplement the vapor-pressure data [108, 114, 119]. This permits the simultaneous regression of heat capacity and vapor-pressure data to determine the coefficients of a vapor pressure equation that is valid down to the triple point. An alternative method is to use an expression involving enthalpies of vaporization in addition to vapor-pressure data [120]. Both of these approaches can be used to ensure that the vapor pressure is thermodynamically consistent with other thermodynamic data.

King and Al-Najjar [119] related heat capacity and vapor pressure using

$$\frac{d}{dT}\left(T^2\frac{d\ln p_{sat}}{dT}\right)=\frac{C_p^0-C_p^L-G}{R} \quad , \tag{2}$$

where $C_p°$ and C_p^{L} are the heat capacities at constant pressure of the ideal gas and the saturated liquid, R is the molar gas constant [121] R=8.314 472 J/(mol·K), p_{sat} is the vapor pressure, and G represents vapor phase nonidealities and is given by

$$G=T\left(p_{sat}\frac{d^2B}{dT^2}+2\frac{dp_{sat}}{dT}\left(\frac{dB}{dT}-\frac{dV_L}{dT}\right)+\frac{d^2p_{sat}}{dT^2}\left(B-V_L\right)\right). \tag{3}$$

In this expression, B is the second virial coefficient and V_{L} is the molar volume of the liquid. We restrict the use of this equation to temperatures lower than 270 K, where vapor pressures are on the order of 10^{-5} kPa. In this region, we treat the gas phase as ideal so that the G term may be neglected. (For example, we applied equations in Douglas et al. [51] for the virial coefficients, liquid volumes, heat capacities, vapor pressures and their derivatives, and estimated that the magnitude of the term G at 270 K relative to the heat capacity difference in eq (2) is on the order 10^{-4} %.) Assuming that mercury can be considered as an ideal monatomic gas for these low pressures, the ideal gas heat capacity for mercury is $C_p° = 5R/2$ [122]. With these assumptions, after the derivatives of the vapor pressure in eq (2) are taken analytically incorporating the specific form of the vapor pressure correlation function of eq (1), one obtains the simple expression $(5R/2 - C_p^{\mathrm{L}})/R = (T/T_{\mathrm{c}})\Sigma a_i(i/2)(i/2 - 1)\square^{i/2-1}$.

Busey and Giauque [44] measured the heat capacity C_{p} of mercury from 15 to 330 K with estimated uncertainties of 0.1 %. Amitin et al. [123] also measured the heat capacity of mercury at temperatures from 5 K to 300 K, with an estimated uncertainty of 1 %. The smoothed data over the temperature range 234 K to 270 K from these two sources were identified as primary data for use in the regression, in addition to the primary vapor pressure data discussed above. The smoothed heat capacity data from these two sources are listed in Appendix B.

For our analysis of both p_{sat} and C_{p} experimental data, all temperatures were first converted to the ITS-90 scale. Data taken prior to 1927 were converted to ITS-90 assuming

that the older data were on the International Temperature Scale of 1927, although we realize this introduces additional uncertainties. Except for the data of Menzies [40], all primary data were measured after 1927. The temperatures of the data of Menzies were first converted to the 1948 temperature scale by use of the procedure given by Douglas et al. [51] and then were converted to ITS-90.

We regressed the primary data set to three different Wagner-type expressions: the 3-6, the 2.5-5, and a variable exponent expression where the exponents were selected from a bank of terms by use of a simulated annealing procedure [124, 125]. Simulated annealing is an optimization technique that can be used in complex problems where there may be multiple local minima. It is a combinatorial method that does not require derivatives and does not depend upon "traveling downhill"; it also is relatively easy to implement. An example program using the simulated annealing to solve the Traveling Salesman Problem is given in the book by Press et al. [125]. In this work, the search space contained a bank of terms where the bank contained exponents with powers of τ in increments of 0.5, with terms up to τ^{12}. We followed the recommendation of Harvey and Lemmon [116] and required the equation to contain terms of order 1, 1.89, and 2, based on theoretical considerations on the behavior near the critical point. The simulated annealing algorithm was used to determine the optimal terms from the bank of terms. We implemented a Lundy and Mees [126] annealing schedule, similar to that of earlier work [127]. During the regression, one can treat the critical pressure as a variable to be determined in the regression, or it can be fixed. Due to concerns about the quality and amount of experimental data in the temperature range 930 K to 1764 K, we adopted the critical point of Kozhevnikov et al. [105] rather than determining it by fitting experimental data. The minimization was done with orthogonal distance regression using the NIST statistical package ODRPACK [128]. For the regression, the data were weighted according to their estimated uncertainty (u) with weights of $1/u^2$. In addition, the vapor pressure data were given a relative weight factor of one, and the heat capacity data a relative weight factor of 0.02. Points that deviated by more than three standard deviations from preliminary fits were considered outliers and were not included in the statistics and final regression.

The 2.5-5 form of the Wagner equation provided a better fit of the primary data set than the 3.0-6 form; further improvement resulted from the use of the simulated annealing algorithm. Upon closer inspection, we noted that although one could reasonably reproduce the numerical value of the heat capacity, it was not possible to reproduce well the slope of the saturated liquid heat capacity near the triple point without degrading the fit in other regions. We note that the liquid heat capacity at saturation of mercury as a function of temperature displays an interesting behavior—a distinct minimum in the curve is observed below the normal boiling point, as shown in Figure 2. Douglas et al. [51] noted that other liquid metals such as sodium and potassium also exhibit this behavior. Among nonmetals, we observe that water displays this feature; however, it is not observed in simple hydrocarbons such as linear alkanes. In order to simultaneously fit the vapor pressure and liquid heat capacity data, and have the correct behavior of the slope of the heat capacity as a function of temperature along the saturation boundary, we increased the number of terms in the regression from 5 to 6 and used the simulated annealing algorithm to obtain our final equation,

$$ln(p/p_c) = (T_c/T)\left(a_1\tau + a_2\tau^{1.89} + a_3\tau^2 + a_4\tau^8 + a_5\tau^{8.5} + a_6\tau^9\right). \quad (4)$$

The regressed coefficients and their standard deviations are given in Table 3a, and fixed parameters for eq (4) are given in Table 3b. Table 4 gives sample values of the vapor pressure calculated from eq (4) over the temperature range 273.15 to 333.15 K. For validation of computer code, more digits than are statistically meaningful are given. For the calibration community, we also have included in Table 4 the density of saturated mercury vapor in moles per liter and nanograms per milliliter obtained assuming the ideal gas law applies, $\rho = p/(R \cdot T)$. We use the currently accepted values of the molar gas constant [121] R = 8.314 472 J/(mol·K) and the relative atomic mass [129] of mercury, 200.59 g/mol.

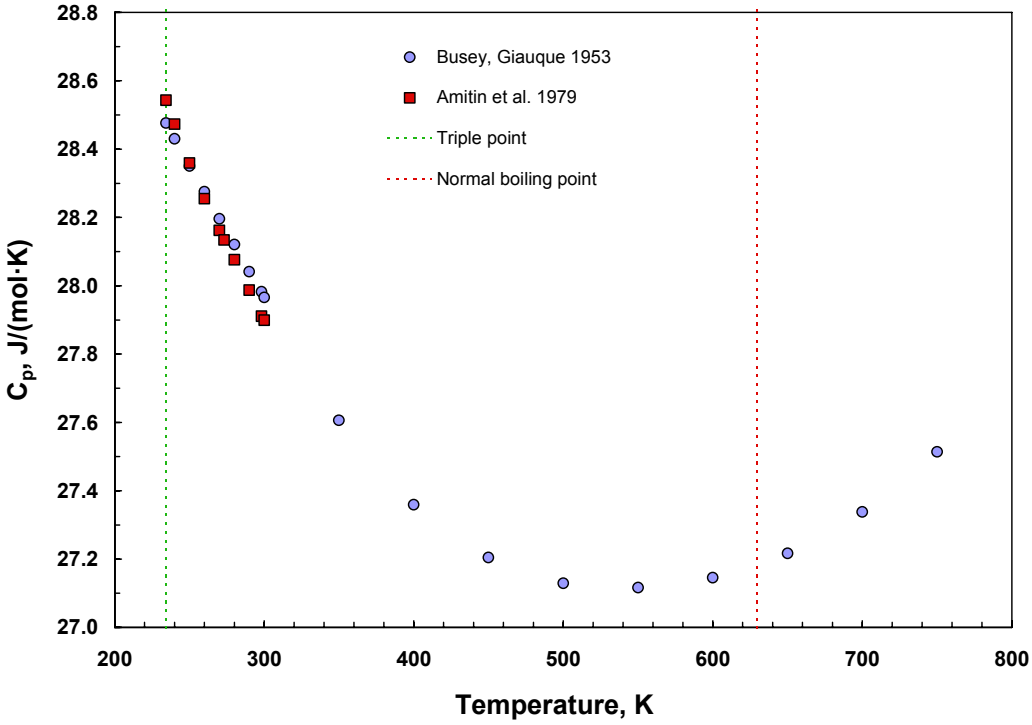

Figure 2 Temperature dependence of the heat capacity of saturated liquid mercury.

Table 3a Fitted values of the parameters in eq (4) and their standard deviations.

i	a_i	**Std. dev.**
1	- 4.576 183 68	0.0472
2	-1.407 262 77	0.8448
3	2.362 635 41	0.8204
4	-31.088 998 5	1.3439
5	58.018 395 9	2.4999
6	-27.630 454 6	1.1798

Table 3b Fixed parameters in eq (4).

T_c **(K)**	p_c **(MPa)**
1764	167

Table 4 Vapor pressure of mercury calculated with eq (4) from 273 K to 333 K.

T, K	*t*, °C	*p*, MPa	Ideal gas density,† mol/L	Ideal gas density,† ng/mL	*T*, K	*t*, °C	*p*, MPa	Ideal gas density,† mol/L	Ideal gas density,† ng/mL
273.15	0	$2.698829\cdot10^{-8}$	$1.188337\cdot10^{-8}$	2.383684	304.15	31	$4.259045\cdot10^{-7}$	$1.684185\cdot10^{-7}$	33.78306
274.15	1	$2.979392\cdot10^{-8}$	$1.307088\cdot10^{-8}$	2.621887	305.15	32	$4.611495\cdot10^{-7}$	$1.817581\cdot10^{-7}$	36.45885
275.15	2	$3.286720\cdot10^{-8}$	$1.436675\cdot10^{-8}$	2.881826	306.15	33	$4.990473\cdot10^{-7}$	$1.960527\cdot10^{-7}$	39.32620
276.15	3	$3.623129\cdot10^{-8}$	$1.577990\cdot10^{-8}$	3.165289	307.15	34	$5.397770\cdot10^{-7}$	$2.113631\cdot10^{-7}$	42.39732
277.15	4	$3.991118\cdot10^{-8}$	$1.731989\cdot10^{-8}$	3.474196	308.15	35	$5.835283\cdot10^{-7}$	$2.277535\cdot10^{-7}$	45.68508
278.15	5	$4.393376\cdot10^{-8}$	$1.899698\cdot10^{-8}$	3.810605	309.15	36	$6.305024\cdot10^{-7}$	$2.452917\cdot10^{-7}$	49.20305
279.15	6	$4.832795\cdot10^{-8}$	$2.082217\cdot10^{-8}$	4.176720	310.15	37	$6.809117\cdot10^{-7}$	$2.640489\cdot10^{-7}$	52.96556
280.15	7	$5.312487\cdot10^{-8}$	$2.280723\cdot10^{-8}$	4.574903	311.15	38	$7.349813\cdot10^{-7}$	$2.841004\cdot10^{-7}$	56.98770
281.15	8	$5.835798\cdot10^{-8}$	$2.496477\cdot10^{-8}$	5.007682	312.15	39	$7.929493\cdot10^{-7}$	$3.055255\cdot10^{-7}$	61.28535
282.15	9	$6.406319\cdot10^{-8}$	$2.730825\cdot10^{-8}$	5.477762	313.15	40	$8.550671\cdot10^{-7}$	$3.284075\cdot10^{-7}$	65.87527
283.15	10	$7.027907\cdot10^{-8}$	$2.985209\cdot10^{-8}$	5.988031	314.15	41	$9.216005\cdot10^{-7}$	$3.528344\cdot10^{-7}$	70.77506
284.15	11	$7.704698\cdot10^{-8}$	$3.261169\cdot10^{-8}$	6.541579	315.15	42	$9.928302\cdot10^{-7}$	$3.788986\cdot10^{-7}$	76.00327
285.15	12	$8.441128\cdot10^{-8}$	$3.560348\cdot10^{-8}$	7.141702	316.15	43	$1.069052\cdot10^{-6}$	$4.066972\cdot10^{-7}$	81.57939
286.15	13	$9.241950\cdot10^{-8}$	$3.884501\cdot10^{-8}$	7.791920	317.15	44	$1.150580\cdot10^{-6}$	$4.363324\cdot10^{-7}$	87.52391
287.15	14	$1.011225\cdot10^{-7}$	$4.235498\cdot10^{-8}$	8.495986	318.15	45	$1.237743\cdot10^{-6}$	$4.679116\cdot10^{-7}$	93.85838
288.15	15	$1.105749\cdot10^{-7}$	$4.615334\cdot10^{-8}$	9.257899	319.15	46	$1.330888\cdot10^{-6}$	$5.015475\cdot10^{-7}$	100.6054
289.15	16	$1.208348\cdot10^{-7}$	$5.026135\cdot10^{-8}$	10.08192	320.15	47	$1.430383\cdot10^{-6}$	$5.373585\cdot10^{-7}$	107.7888
290.15	17	$1.319646\cdot10^{-7}$	$5.470161\cdot10^{-8}$	10.97260	321.15	48	$1.536613\cdot10^{-6}$	$5.754690\cdot10^{-7}$	115.4333
291.15	18	$1.440308\cdot10^{-7}$	$5.949822\cdot10^{-8}$	11.93475	322.15	49	$1.649985\cdot10^{-6}$	$6.160093\cdot10^{-7}$	123.5653
292.15	19	$1.571046\cdot10^{-7}$	$6.467678\cdot10^{-8}$	12.97352	323.15	50	$1.770928\cdot10^{-6}$	$6.591162\cdot10^{-7}$	132.2121
293.15	20	$1.712619\cdot10^{-7}$	$7.026452\cdot10^{-8}$	14.09436	324.15	51	$1.899890\cdot10^{-6}$	$7.049329\cdot10^{-7}$	141.4025
294.15	21	$1.865835\cdot10^{-7}$	$7.629036\cdot10^{-8}$	15.30308	325.15	52	$2.037347\cdot10^{-6}$	$7.536097\cdot10^{-7}$	151.1666
295.15	22	$2.031558\cdot10^{-7}$	$8.278502\cdot10^{-8}$	16.60585	326.15	53	$2.183795\cdot10^{-6}$	$8.053040\cdot10^{-7}$	161.5359
296.15	23	$2.210708\cdot10^{-7}$	$8.978112\cdot10^{-8}$	18.00919	327.15	54	$2.339760\cdot10^{-6}$	$8.601806\cdot10^{-7}$	172.5436
297.15	24	$2.404265\cdot10^{-7}$	$9.731323\cdot10^{-8}$	19.52006	328.15	55	$2.505789\cdot10^{-6}$	$9.184118\cdot10^{-7}$	184.2242
298.15	25	$2.613271\cdot10^{-7}$	$1.054180\cdot10^{-7}$	21.14581	329.15	56	$2.682462\cdot10^{-6}$	$9.801783\cdot10^{-7}$	196.6140

299.15	26	$2.838837 \cdot 10^{-7}$	$1.141344 \cdot 10^{-7}$	22.89423	330.15	57	$2.870385 \cdot 10^{-6}$	$1.045669 \cdot 10^{-6}$	209.7507
300.15	27	$3.082141 \cdot 10^{-7}$	$1.235036 \cdot 10^{-7}$	24.77358	331.15	58	$3.070193 \cdot 10^{-6}$	$1.115081 \cdot 10^{-6}$	223.6740
301.15	28	$3.344440 \cdot 10^{-7}$	$1.335691 \cdot 10^{-7}$	26.79262	332.15	59	$3.282555 \cdot 10^{-6}$	$1.188620 \cdot 10^{-6}$	238.4253
302.15	29	$3.627066 \cdot 10^{-7}$	$1.443770 \cdot 10^{-7}$	28.96059	333.15	60	$3.508170 \cdot 10^{-6}$	$1.266503 \cdot 10^{-6}$	254.0478
303.15	30	$3.931433 \cdot 10^{-7}$	$1.559763 \cdot 10^{-7}$	31.28729					

† Assumes ideal gas law applies.

4. Comparison with Experimental Data

For the 294 vapor pressure points in the primary data set, the average absolute deviation is 0.14 %, the bias is –0.028 %, and the root mean square deviation is 0.35 % where we use the definitions AAD = $(100/n)\Sigma\text{abs}(p_i^{\text{calc}}/ p_i^{\text{expt}} - 1)$, BIAS = $(100/n)\ \Sigma(p_i^{\text{calc}}/ p_i^{\text{expt}} - 1)$, and $\text{RMS}^2 = (100/n)(\ \Sigma(p_i^{\text{calc}}/ p_i^{\text{expt}} - 1)^2 - ((100/n)\ \Sigma(p_i^{\text{calc}}/ p_i^{\text{expt}} - 1))^2$, where n is the number of points. The AAD and RMS for the primary data are given in Table 5. The normal boiling point calculated by this equation is 629.7705 K.

Figure 3 compares the primary data set with our correlation, eq (4). The data of Ernsberger and Pitman [54] display substantial scatter, but the results are within their estimated experimental uncertainty of 1 %. The data of Shpil'rain and Nikanorov [86] also display a fairly high scatter, but again it is within their uncertainty estimate (0.6 % to 0.8 %). The very accurate measurements of Beattie et al. [28] are in the vicinity of the normal boiling point, and the correlation, eq (4), indicates an uncertainty of 0.02 %, at a coverage factor of 2. The measurements of Spedding and Dye [87] and those of Ambrose and Sprake [18] also are represented well by our correlation, although the lowest temperature points display larger scatter than at higher temperatures. The measurements of Menzies [39, 40] are also represented to within their estimated uncertainty. The highest temperature data of Schönherr and Hensel [84] are represented with an AAD of 1 % and a standard deviation of 1.4 %; several points are outside of the range of the plot and are not shown. The correlation is valid to the critical point at 1764 K, but does not account for a metal-nonmetal transition [63] in mercury at approximately 1360 K that results in a change of slope in the vapor pressure curve.

Table 5 Summary of comparisons of the correlation with the primary data for the vapor pressure of mercury.

First author	No. pts.	*T* range, K	Estimated uncertainty, %	AAD %	RMS %
Ambrose [18]	113*	417-771	less than 0.03, greatest at lowest *T*	0.02	0.06
Beattie [28]	42	623-636	0.03	0.01	0.01
Ernsberger [54]	18	285-327	1	0.33	0.35
Menzies [39, 40]	46**	395-708	0.5	0.14	0.20
Schönherr [84]	13	1052-1735	3	1.06	1.42
Shpil'rain [86]	50	554-883	0.6-0.8	0.25	0.29
Spedding [87]	13	534-630	0.03	0.05	0.06

* Two outliers at 380 K and 400 K were not included in statistics.
** One outlier at 395 K was not included in statistics.

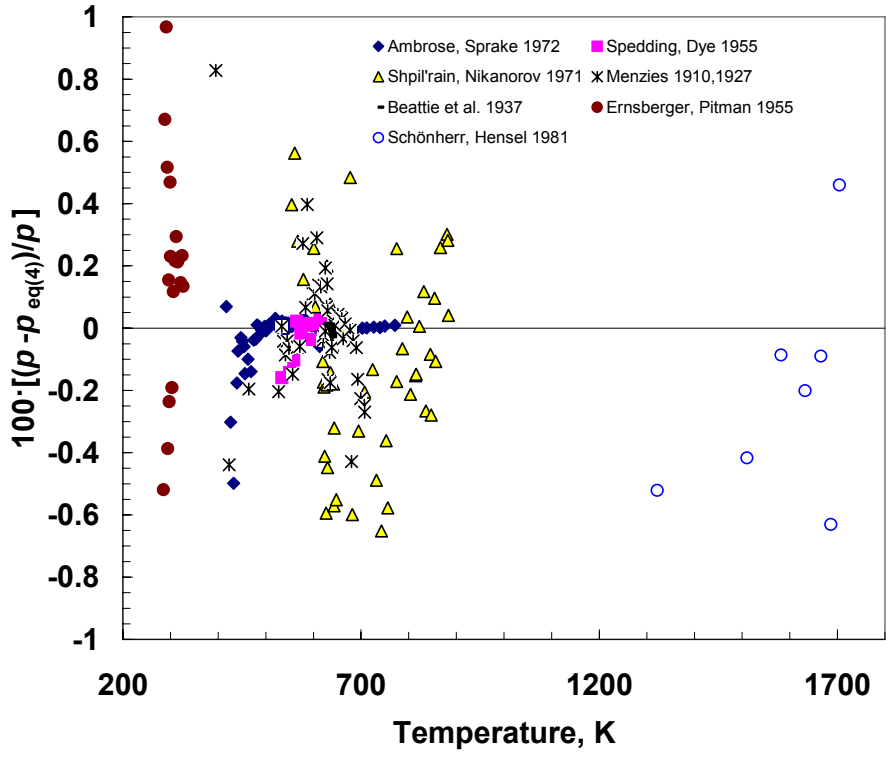

Figure 3 Deviations between the correlation given in eq (4) and the primary data set.

Figure 4 compares selected data not used in the regression (secondary data) with the correlation eq (4), and Table 6 summarizes comparisons with all secondary data. It is interesting to note that the behavior of the correlation at low temperatures falls in between the values of Douglas et al. [51] and those of Busey and Giauque [44]. Both of these sets were not obtained from direct vapor pressure measurements, but rather were calculated based upon caloric measurements combined with vapor pressure data at higher temperatures. The data of Schmahl et al. [82] cover a range of temperature from 412 to 640 K and are in good agreement with the correlation. The measurements of Burlingame [43] and of Dauphinee [49,50] were made by use of a transpiration technique with uncertainties on the order of 4 to 5 %, and the correlation represents them within this range of deviations. Figure 4 also displays considerably more scatter at both the high and low temperature ends of the plot.

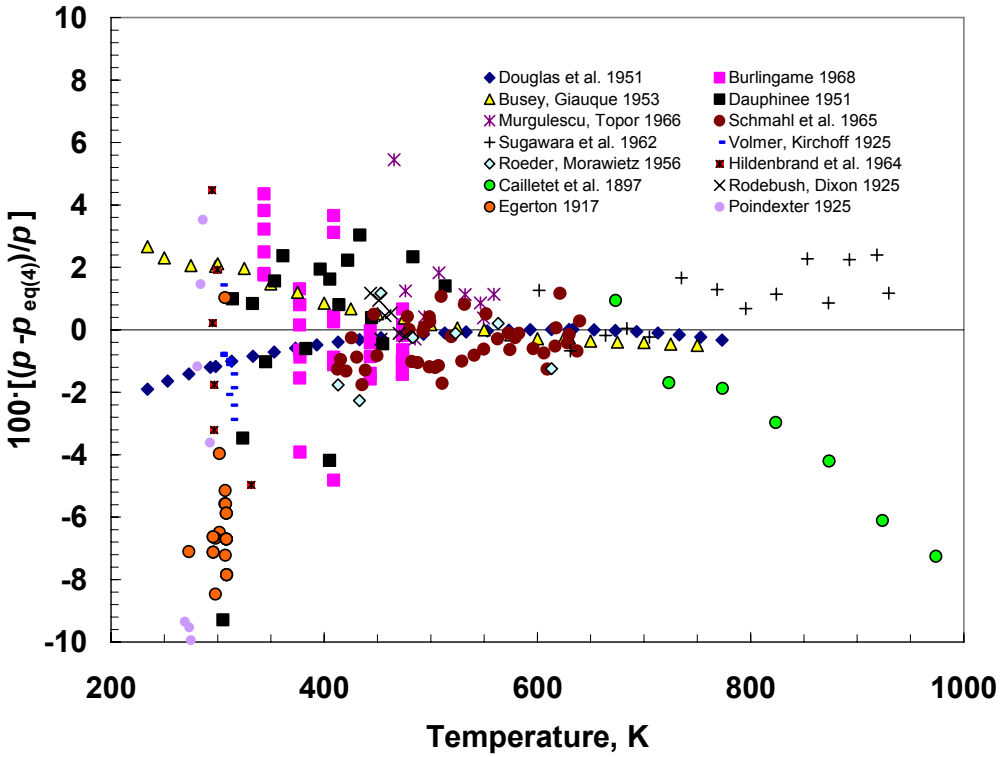

Figure 4 Deviations between the correlation given in eq (4) and selected secondary data.

Table 6 Summary of comparisons of the correlation given in eq (4) with secondary data for the vapor pressure of mercury.

First author	No. pts.	*T* range, K	Estimated uncertainty, %	AAD %	RMS %
Bernhardt [41]	27	694-1706	varies from 2 to >15	14.13	17.26
Bessel-Hagen [42]	2	273-293	>20	96.12	2.50
Burlingame [43]	38	344-409	4	1.44	1.92
Busey [44]	24	234-750	varies from 0.2 to 3.5 at lowest *T*	0.90	1.03
Cailletet [45]	11	673-1154	varies from 1 to7	3.97	2.26
Callendar [46]	2	630	0.2	0.17	0.14
Cammenga [47]	graphical results	273-325			
Carlson [48]	9	299-549	varies from 3 to >20	19.74	16.83
Dauphinee [49, 50]	18	305-455	5	2.14	2.94
Douglas [51]	30	234-773	var. from 0.03 (at normal boiling point) to 1.5 at lowest *T*	0.45	0.54
Durrans [52]	19	290-344		4.63	3.06
Egerton [53]	27*	289-309	5	6.99	2.34
Galchenko [55]	graphical results	523-723	3	na	na
Gebhardt [57]	9	403-483	8	3.34	4.03
Haber [37]	1	293	2	1.84	na
Hagen [58]	5	273-473	>20	51.02	57.44
Hensel [59]	graphical results	1073-critical	na	na	na
Hertz [35]	9	363-480	5	4.50	1.94
Heycock [60]	1	630	0.2	0.21	Na
Hildenbrand [61]	6	295-332	5	2.76	3.16
Hill [62]	19	272-308	30	29.40	4.38
Hubbard [63]	graphical results	742-1271	na	na	na
Jenkins [64]	21	479-671	varies from 0.1 to >20	5.08	5.67
Kahlbaum [65]	43	393-493	>10	8.89	9.47
Knudsen [66]	10	273-324	varies from 5 to 10	7.36	1.67
Knudsen [67]	7	263-298	varies from 5 to 10	7.12	7.64
Kordes [68]	2	630-632	4	2.59	1.84
Mayer [69]	82	261-298	5, except greater at *T*<270	6.72	8.86
McLeod [70]	1	293	>20	77.65	na
Millar [71]	6	468-614	2	1.27	1.84
Morley [72]	6	289-343	varies from 8 to >20	17.58	11.82
Murgulescu [73]	9	301-549	3	1.41	1.56

First author	No. pts.	*T* range, K	Estimated uncertainty, %	AAD %	RMS %
Neumann [74]	19	290-344	6	4.63	3.06
Pedder [75]	3	559-573	2	1.14	0.94
Pfaundler [76]	3	288-372	12	8.06	5.76
Poindexter [77]	17	235-293	>5-20; greatest at lowest *T*	28.23	29.19
Ramsay [36]	13	495-721	varies from 0.3 to 10 at highest *T*	3.23	3.02
Regnault [33]	29	297-785	~6 for *T*>400, much higher for lower *T*	24.74	34.03
Rodebush [79]	7	444-476	1	0.53	0.54

Table 6 Continued.

First author	No. pts.	*T* range, K	Estimated uncertainty, %	AAD %	RMS %
Roeder [80]	7	413-614	2	1.00	1.11
Ruff [81]	12	478-630	>20	22.49	25.78
Schmahl [82]	43	412-640	1.5	0.70	0.71
Schneider [83]	23	484-575	10	4.04	5.02
Scott [85]	1	293	2	1.11	na
Stock [88]	3	253-283	20	15.05	16.80
Sugawara [9]	14	602-930	2	1.15	0.95
van der Plaats [89]	26	273-358		86.65	23.03
Villiers [90]	12	333-373	6	4.76	3.24
Volmer [91]	10	303-313	3	1.57	1.13
von Halban [92]	2	220-255	7	8.15	2.21
Young [93]	11	457-718	2	1.40	1.30

* One outlier at 288.6 K was not included in statistics. na: not applicable

5. Comparisons with Correlations from the Literature

Figures 5a and 5b compare correlations and tables for the vapor pressure of mercury in different temperature regions obtained in the literature. In these figures we define percent deviation as $100\cdot(p_{eq4}-p_{corr})/p_{eq4}$, where p_{corr} is the vapor pressure from correlations in the literature and p_{eq4} is that obtained from eq (4). We also show the estimated uncertainty band of the new correlation, eq (4), by a heavy black line. The existing correlations in the literature agree well with each other and with the new correlation in the intermediate temperature region from about 400 K to the normal boiling point. In this region, there is a fair number of high quality experimental data. At low temperatures, the existing correlations differ from each other and some differ from the new correlation. As mentioned earlier, there is a paucity of high quality direct vapor-pressure measurements in this region, and we feel that simultaneously using low temperature heat capacity data allows our new correlation to display the proper behavior in the low temperature region. We also had access to newer data that some of the earlier correlations did not include. For example, the Lange's Handbook correlation [130] is based upon the International Critical Tables of 1928 [131], while the most recent CRC Handbook [132] values are based upon Vargaftik et al. [8], which itself is based upon the 1972 book of Vukalovich and Fokin [4]. Some earlier editions of the CRC Handbook (for example the 57th Ed., 1976-1977, p. D-182) used the values from the International Critical Tables of 1928 [131]. Few correlations are applicable for higher temperatures. The maximum temperature limit of the Korea Thermophysical Properties Databank correlation, KDB [133], is given as 654.15 K. The maximum of the PTB equation [22] is 930 K; these correlations should not be extrapolated outside of their given ranges. At the highest temperatures, there are considerable differences among the various correlations; however, there is also a lack of experimental measurements in this region. The de Kruif correlation [20, 21] does not specifically state the temperature limits of the correlation, but the very thorough literature survey in the thesis [20] indicates that the only high temperature data used in their work were those of Bernhardt [41] and Cailletet et al. [45], and they did not have access to the more recent measurements of Shpil'rain and Nikanorov [86], Sugawara et al. [9], or Schönherr and Hensel [84]. Lange's Handbook [130] includes a note in their table identifying 900 °C as the critical point; this model deviates substantially from the other correlations at high temperatures. The DIPPR [134] and Yaws [135] correlations appear

indistinguishable on the plot, and both have adopted a critical point of 1735 K and 160.8 MPa. Our correlation agrees very well with these correlations up to about 1500 K, where the differences are probably due to the critical point adopted in the correlations. Also, the correlation of Schmutzler (as presented in Götzlaff [13]) adopts a different critical point from the selection here; it uses T_c = 1751 K and p_c = 167.3 MPa. We note that the tabulated values in the book by Hensel and Warren [7] appear to have been generated from the Schmutzler [13] correlation.

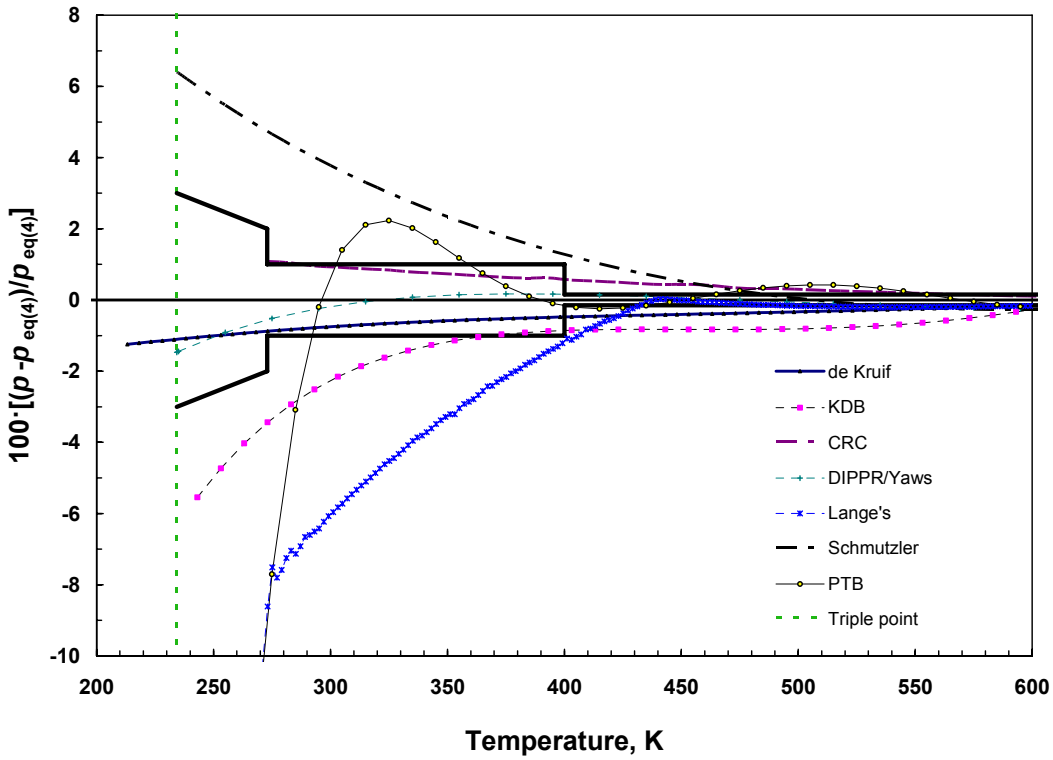

Figure 5a Comparison of the new correlation, eq (4), with previous compilations and correlations in the low temperature region up to 600 K. The uncertainty band for eq (4) is indicated by a heavy black solid line.

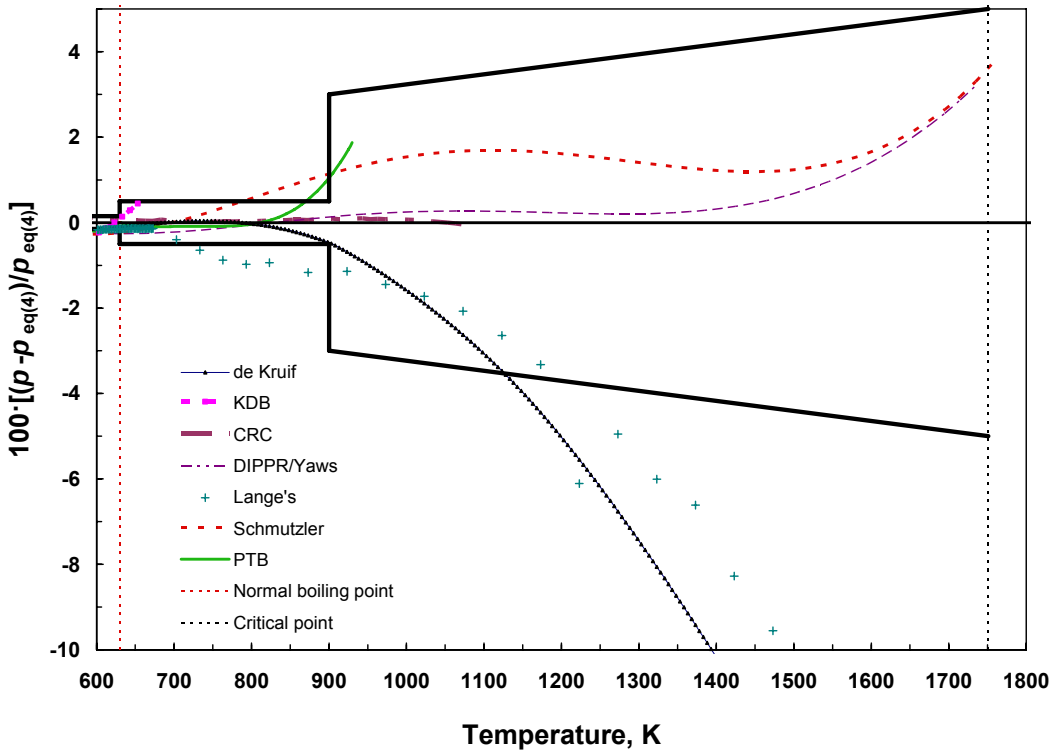

Figure 5 Comparison of the new correlation, eq (4), with previous compilations and correlations in the high temperature region from 600 K to the critical temperature. The uncertainty band for eq (4) is indicated by a heavy black solid line.

6. Detailed Comparisons for the Temperature Range 0 °C to 60 °C

The temperature range from 0 °C to 60 °C is of particular interest for this project. Unfortunately, in this region there are very few vapor pressure data of high accuracy. Our approach, as detailed above, was to identify the data sets of highest quality and supplement the vapor pressure data with low-temperature heat capacity data to improve the behavior of the correlation at low temperatures and to ensure thermodynamic consistency. The data of Ernsberger and Pitman [54] are the only direct vapor pressure measurements of low uncertainty (1 %) available in this region, and were the only low-temperature vapor pressure data used in the regression. Figure 6a shows the deviations of all data with estimated uncertainties of 3 % or less in this temperature range, while Figure 6b shows comparisons with all sets with estimated uncertainties of 6 % or less. The data of both Busey and Giauque [44] and Douglas, Ball and

Ginnings [51] were not direct measurements but rather were values obtained from their analysis of heat capacity data. Our correlation does not agree with these sets to within their estimated uncertainties; neither do the sets agree with each other to within these uncertainties. The single data point of Scott [85] at 293 K, determined with a quartz fiber manometer with an estimated uncertainty of 2 %, is represented by our correlation within this margin. The measurements of Volmer and Kirchoff [91] have a slightly higher (3 %) estimated uncertainty and are represented well by the correlation.

Figure 7 compares correlations in the literature with eq (4) for the temperature range 273 K to 333 K (0 °C to 60 °C). There are four correlations that agree with eq (4) to within our estimated uncertainty of 1 %: those by de Kruif [20, 21], DIPPR [134], Yaws [135], and Mukhachev et al. [16]. Yaws [135] does not state the uncertainty of his equation; however the DIPPR [134] equation reports an estimated uncertainty of less than 3 %, and the two correlations are almost indistinguishable from one another. The DIPPR correlation was developed by fitting vapor pressure data, with a primary data set consisting of 54 experimental points from Ambrose and Sprake [18] for temperatures from 426 K to 771 K, nine smoothed points from the correlation of Stull [11] for 399 K to 596 K, and 81 points from the tables in Vargaftik [136] for temperatures 273 K to 1073 K [137]. The correlation of de Kruif [20, 21] was developed by use of the method of Clark

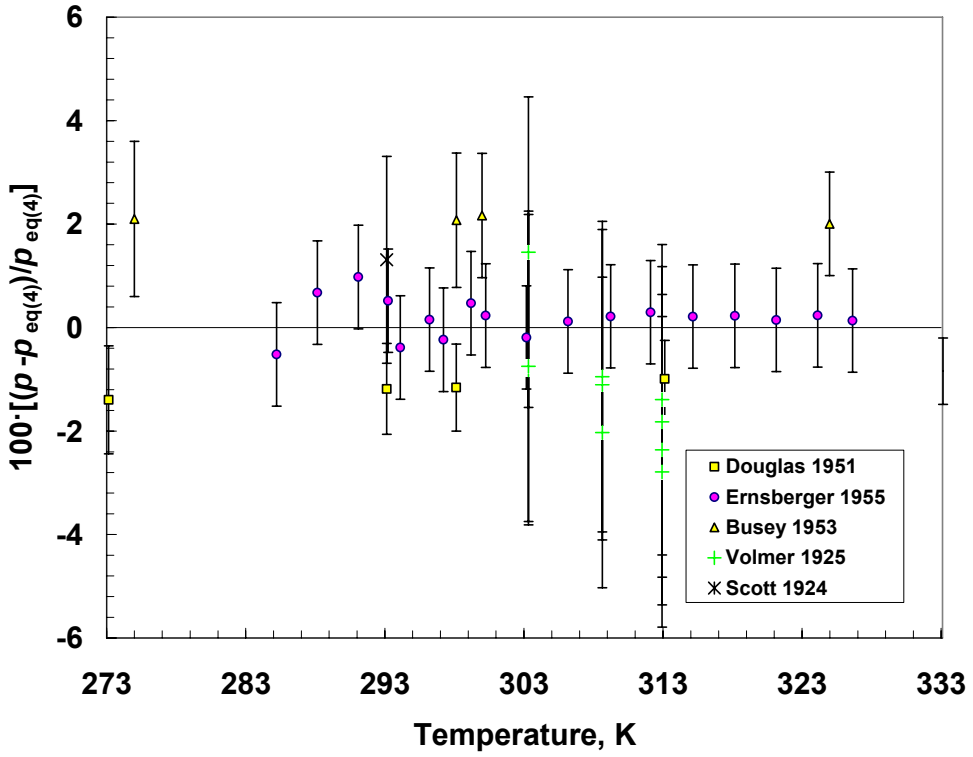

Figure 6a Comparison of the new correlation, eq (4), in the temperature range 273 K to 333 K, with experimental data with estimated uncertainties of 3 % or less.

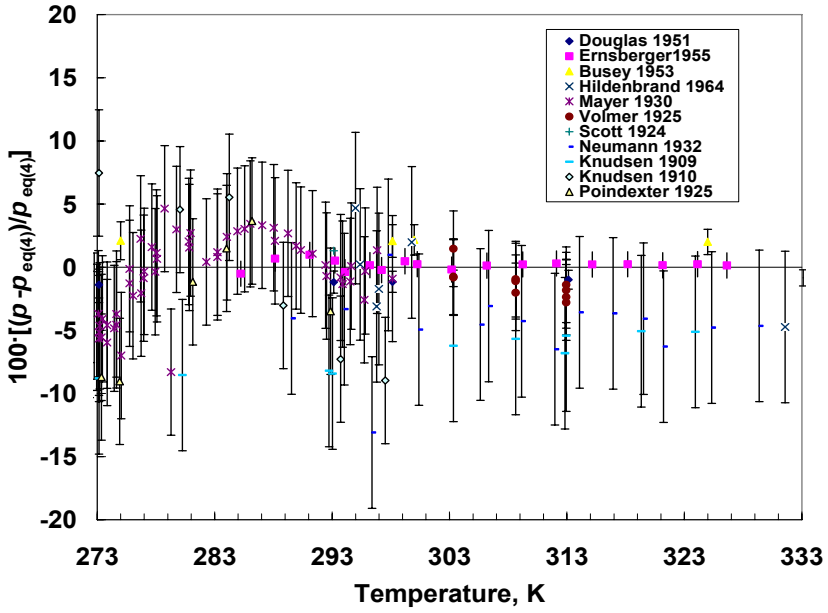

Figure 6b Comparison of the new correlation, eq (4), in the temperature range 273 K to 333 K, with experimental data with estimated uncertainties of 6 % or less.

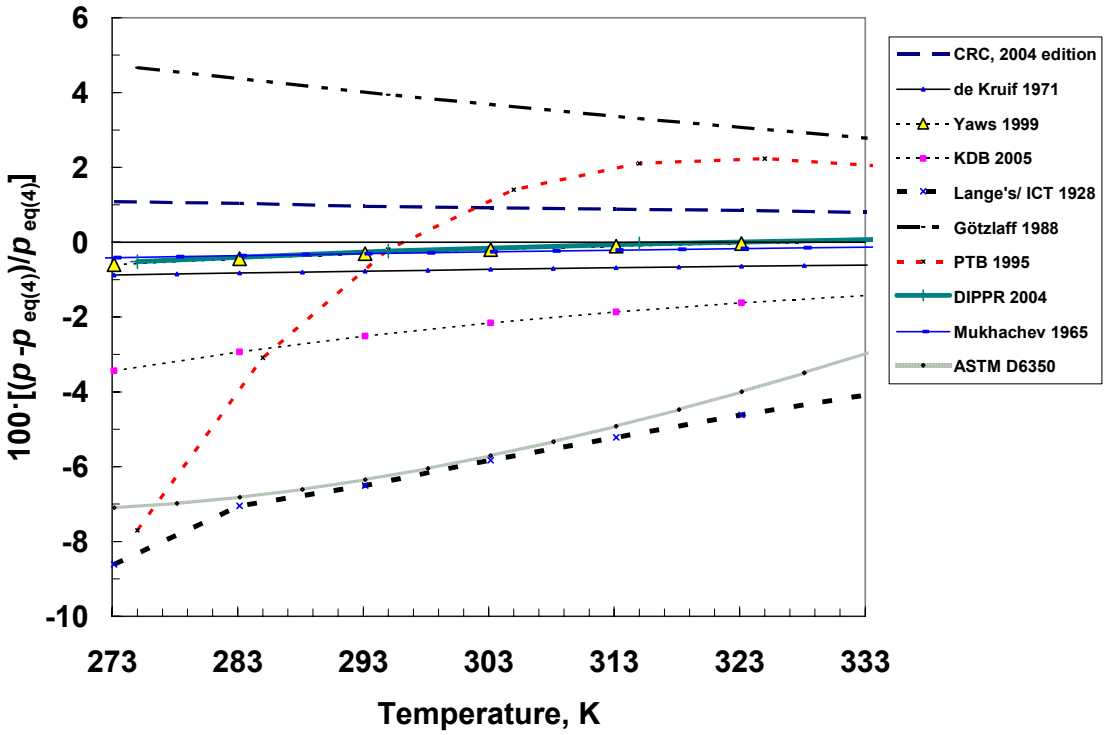

Figure 7 Comparison of the new correlation, eq (4), in the temperature range 273 K to 333 K, with correlations from the literature.

and Glew [138] that, in addition to vapor pressure data, used supplementary data such as heat capacities, Gibbs free energies of vaporization and enthalpies of vaporization to develop the correlation. The curve from the CRC Handbook, 85th Edition is based on that of Vargaftik et al. [8], which itself is based upon Vukalovich and Fokin [4]. The Vukalovich and Fokin [4] source lists the data used in the development of the equation, and apparently they were unaware of the data of Ernsberger and Pitman [54]. As mentioned earlier, Ernsberger and Pitman [54] give an estimated uncertainty of 1 % for their measurements, and they seem to be the most reliable vapor pressure measurements in the 0 °C to 60 °C range. The Mukhachev et al. [16] correlation was developed from caloric data such as heat of vaporization and heat capacities along with the normal boiling point of mercury. The KDB correlation [133] is presented only as a set of coefficients with a range of applicability, and we do not know the data used in its development; it is consistently lower than our correlation. The PTB curve [22], with a reported maximum uncertainty of 4 %, is very different in shape from all the others investigated. This analysis did not incorporate caloric data, and the experimental data in the 0 °C to 60 °C range that were used

in the regression were those of Poindexter [77] and Neumann and Völker [74]. The equation recommended in the ASTM Standard D6350 [139] is presented in terms of a concentration in nanograms per milliliter. We converted the expression to vapor pressure by applying the ideal gas law and using a relative molar mass [129] of 200.59 and gas constant [121] R = 8.314472 J/(mol·K). It agrees well with the values from Lange's Handbook [130]. The curve from Lange's Handbook [130] deviates the most from our correlation, approaching 10 % at 273 K, and gives vapor pressures that are lower than all the other correlations. The curve in Lange's Handbook [130] is based upon the 1928 International Critical Tables (ICT) [131] and was developed with only the limited data and computational methods available at that time.

Since it has been used extensively in handbooks and in industrial standards, further discussion of the 1928 International Critical Tables is warranted. A total of 28 references are given for the 1928 International Critical Tables, with the most recent dated 1926. In addition, some of these references are not original data but rather analysis of literature data [17, 140-143], and only 8 of the references [53, 66, 67, 72, 76, 77, 85, 90] contain data in the range 273 K to 333 K. Details are not given concerning how the data were weighted or the uncertainties of the numbers presented, and it is difficult to know the exact procedure used to obtain the values in the table. However, it was not uncommon, prior to the widespread use of computers, to employ graphical methods. For example, Stull [11] in 1947 states, "the analytical method...was based on semilogarithmic charts measuring 30 × 42 inches (where 1 mm. = 1° C) and colored map tacks representing the plotted points over which a taut thread was stretched." Comparisons with the data cited in the International Critical Tables (Figure 8) indicate that the values of the 1928 International Critical Tables (ICT) [131] in the range 0 °C to 60 °C are in closest agreement with the 1909 data of Knudsen [66]. Figure 8 shows the percent deviations from eq (4) for all of the data cited in the 1928 ICT, the ICT values [131], and the data of Ernsberger and Pitman [54]. The 1955 data of Ernsberger and Pitman [54] were not available to the authors of the ICT Table; however, it is the primary data source we used in the low temperature region. In addition, Ernsberger and Pitman [54] noted that although the ICT tables are given to four significant figures, the uncertainty is probably 5 to 10 % due to the uncertainties in the measurements upon which the ICT table for mercury is based. Further discussion on the Knudsen [66] data follows since it appears that the ICT tables agree most closely with this particular data set.

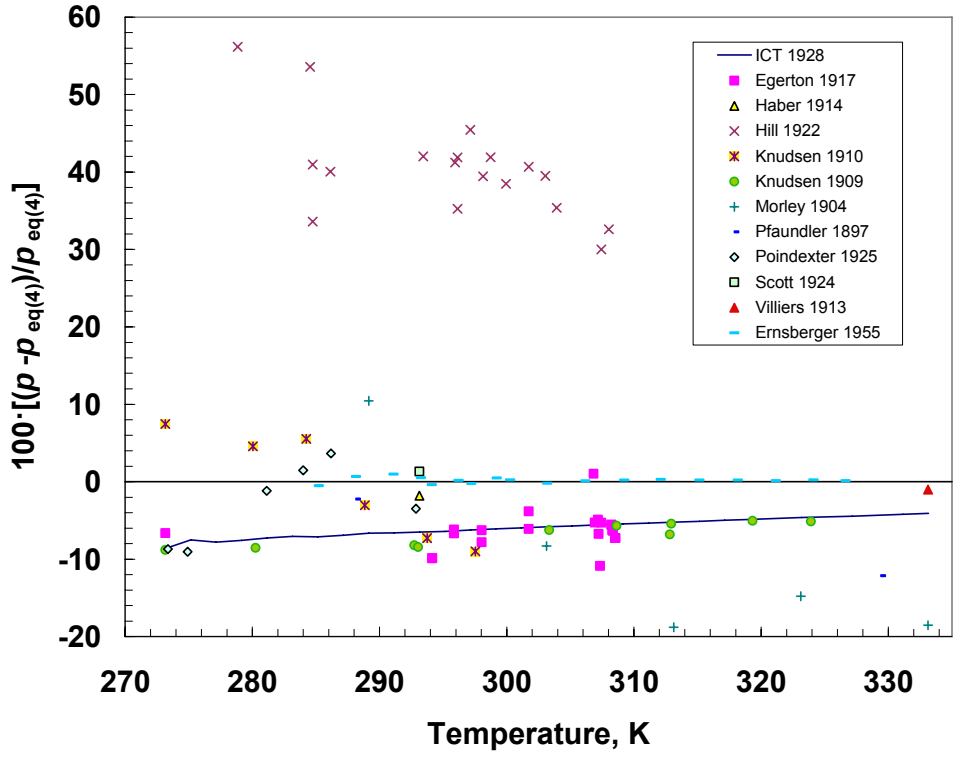

Figure 8 Comparison of the new correlation, eq (4), in the temperature range 273 K to 333 K, with data cited in the references for the 1928 International Critical Tables (ICT) [131], the values in the 1928 ICT, and the data of Ernsberger and Pitman [54].

The vapor pressure data of Knudsen [66] were obtained in 1909 using an effusion method. In fact, it was the very first measurement of this type, and the method is now often called "the Knudsen effusion method" or "the Knudsen method." Several variants of this method have been developed and have been in continuous use from 1909 until the present day. Cater [144] discussed the state of the art in of the effusion method in 1978; as recently as 2006, Zaitsau et al. [145] used the Knudsen method to measure the vapor pressure of ε-caprolactam. The basic method developed by Knudsen involves the flow of vapor from a space where it is in equilibrium with a solid or a liquid at a known temperature into a high vacuum through a fine hole or tube. With a known orifice size and geometry, one can measure the flow rate and calculate the vapor pressure with equations based on kinetic theory. The measurements that Knudsen made in 1909 were done very carefully. One measurement at 0 °C took 13 days to complete—his method of detection was to condense the effusing mercury vapor and measure its volume at room temperature in a capillary tube located below the condenser. However, even today, with state of

the art equipment, estimated uncertainties for mass-loss Knudsen effusion methods are about 5 % [146, 147] for pressures on the order of 10^{-1} Pa to 1 Pa. EPA guidelines [148] give an estimated repeatability of 10 % to 30 % for mass-loss effusion methods for the pressure range 10^{-3} Pa to 1 Pa. Measurements at such low pressures are difficult; some factors that can contribute to the uncertainty are temperature measurement and control, determination of the weight-loss, and knowledge of the orifice geometry. For finite orifice lengths, the geometry must be well known in order to compute the Clausing factor, which corrects for the fact that some molecules may strike the orifice wall and be returned to the cell [144]. In contrast, there is a 1 % uncertainty associated with the direct manometric method of Ernsberger and Pittman [54].

One can also demonstrate that the ICT Tables, apparently based on the data of Knudsen [66], are thermodynamically inconsistent with low temperature heat capacity data. Figure 9a shows comparisons of the calculated and experimental values of heat capacity, and Figure 9b compares the experimental and calculated values for the vapor pressure using the present vapor pressure equation eq (4). Sakonidou et al. [6] reviewed the availability of heat capacity data for mercury and identified three major sets of heat capacity data for the low temperature (below 60 °C) region: Busey and Giauque [44] (0.1 % uncertainty), Douglas et al. [51] (1 % uncertainty) and Amitin et al. [123](1 % uncertainty). These sets of heat capacity data are represented to within their experimental uncertainties, as are the vapor pressure data of Ernberger and Pitman [54] (1 % uncertainty). The Knudsen data [66] are represented to within 5 % to 10 %, a level consistent with the effusion technique, with the highest deviations at the lowest temperatures. Therefore, our equation represents all of these data sets to within their uncertainties, and the heat capacity data are thermodynamically consistent with the vapor pressure data. However, if one refits the vapor pressure equation, but instead of using the data of Ernsberger and Pitman [54] as primary data, one instead uses the data of Knudsen [66], and adjusts the weights so that the resulting vapor pressure equation represents the Knudsen data to within 2 %, it is no longer possible to represent the heat capacities to within their experimental uncertainty, as shown in Figure 10a. This indicates that the Knudsen data, at a 2 % uncertainty level, are thermodynamically inconsistent with the heat capacity measurements. Therefore the 1928 ICT Tables, that represent the Knudsen data to better than 2 %, are thermodynamically inconsistent with the heat capacity measurements of Busey and Giauque [44], Douglas et al. [51], and Amitin

et al. [123]. To summarize, the effusion data of Knudsen [66] can be assigned a temperature-dependent uncertainty of 5 % to 10 %; any attempt to ascribe a smaller uncertainty to this data set would be inconsistent with the more recent data of Ernsberger and Pitman [54], Busey and Giauque [44], Douglas et al. [51], and Amitin et al. [123].

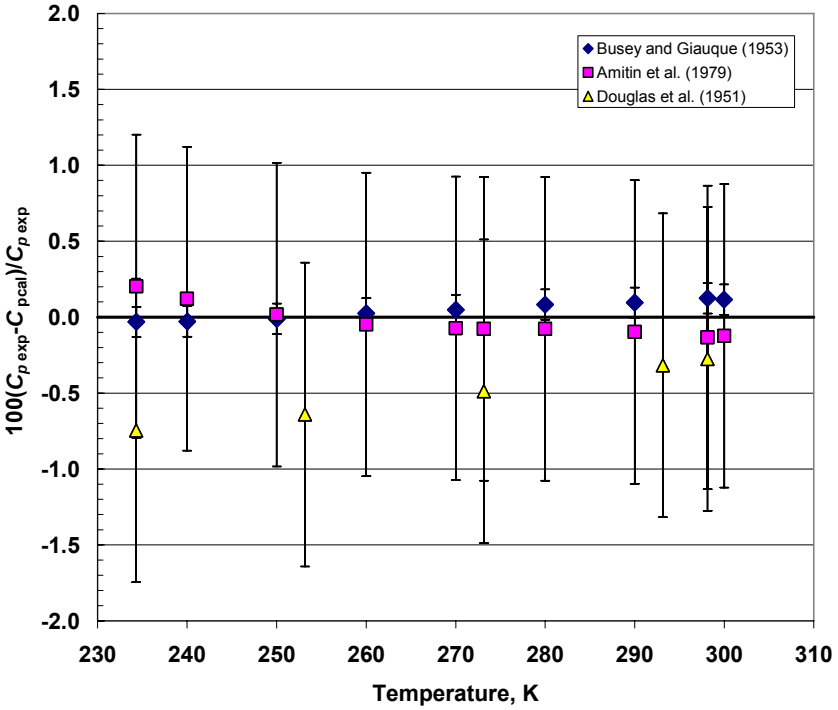

Figure 9a Comparison of heat capacities calculated with the present correlation, eq (4) and eq (2), with experimental heat capacity data.

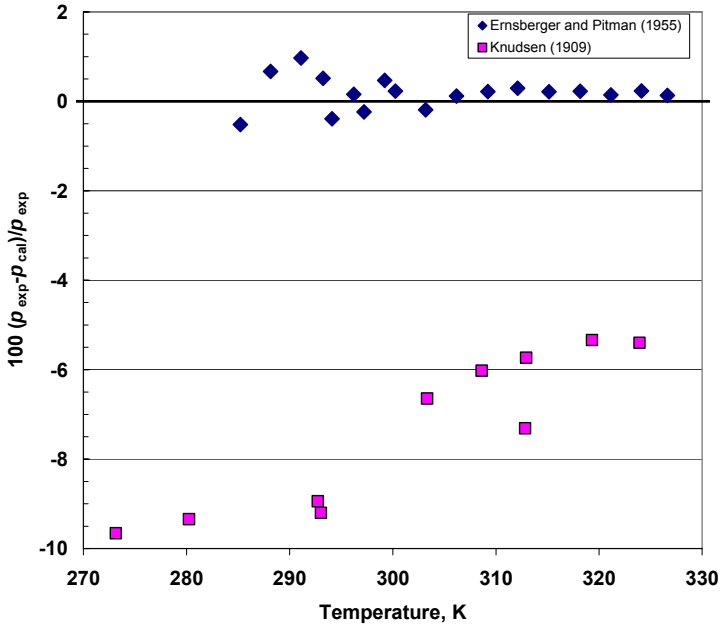

Figure 9b Comparison of vapor pressures calculated with the present correlation, eq (4), with experimental vapor pressure data.

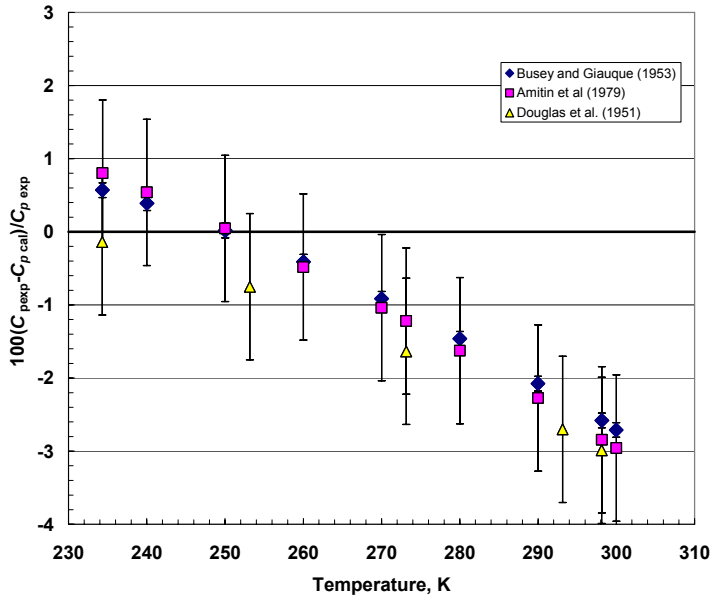

Figure 10a Comparison of heat capacities calculated with eq (1) and eq (2), subject to the constraint that the vapor pressure data of Knudsen be represented to within 2 %, with experimental heat capacity data.

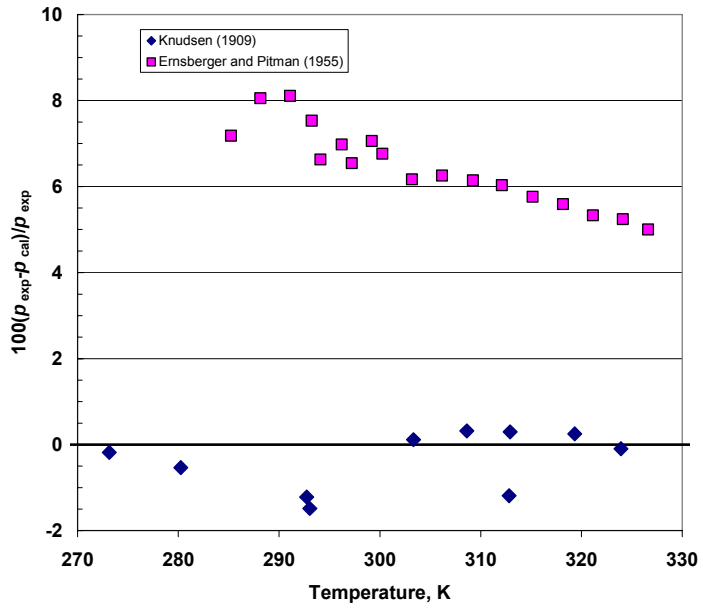

Figure 10b Comparison of vapor pressures calculated with eq (1) and eq (2), subject to the constraint that the vapor pressure data of Knudsen be represented to within 2 %, with experimental vapor pressure data.

7. Conclusions

We developed a new correlation for the vapor pressure of mercury that is valid from the triple point [30], 234.3156 K to the critical point [105], 1764 K using a Wagner-type equation. We have determined the uncertainties to be associated with the equation through our comparisons with the primary experimental data and consideration of the uncertainties of these data as discussed above. The estimated uncertainty at a coverage factor of two varies from 3 % near the triple point to 1 % for temperatures from 273 K to 400 K; 0.15 % for the intermediate temperature region from 400 K to the normal boiling point at 629.77 K; for temperatures above the normal boiling point but below about 900 K it is 0.5 %; and for temperatures between 900 K and the critical point we estimate the uncertainty is about 5 %. The new correlation gives a normal boiling point (101.325 kPa) of 629.77 K.

This project was supported in part by the Western Research Institute, and was prepared with the support of the U.S. Department of Energy, under Award No. DE-FC26-98FT40323. However, any opinions, findings, conclusions, or recommendations expressed herein are those of NIST and do not necessarily reflect the views of the DOE. We thank the staff of the Department of Commerce Boulder Laboratories Library for their dedication and cheerful assistance in obtaining the historic literature necessary for this project, and Dr. Harro Bauer (Physikalisch-Technische Bundesanstalt, Braunschweig, Germany) for providing us with a copy of ref. [22]. We thank NIST PREP student Justin Chichester for assistance with the preparation of this manuscript and NIST Guest Researcher Ilmudtin Abdulagatov for assistance with Russian literature. We also acknowledge helpful discussions with our NIST colleagues Mark McLinden, Allan Harvey, and Gerald Mitchell, and with Dr. John Schabron of the Western Research Institute.

9. References

[1] Selin, N.E. Mercury is rising: Is global action needed to protect human health and the environment? Environment. 47(1): 22-35; 2005.

[2] Holman, G.J.F.; ten Seldam, C.A. A critical evaluation of the thermophysical properties of mercury. J. Phys. Chem. Ref. Data. 23(5): 807-827; 1994.

[3] Bettin, H.; Fehlauer, H. Density of mercury—measurements and reference values. Metrologia. 41: S16-S23; 2004.

[4] Vukalovich, M.P.; Fokin, L.R. *Thermophysical Properties of Mercury*. Moscow: Standards Press; 1972.

[5] *Gmelin Handbuch der Anorganischen Chemie. Quecksilber. No. 34.* , Verlag Chemie: Weinheim/Bergstrasse; 1960.

[6] Sakonidou, E.P.; Assael, M.J.; Nieto de Castro, C.; Van den Berg, H.R.; Wakeham, W.A. A review of the experimental data for the thermal properties of liquid mercury, gallium and indium. in Thermal Conductivity 24: Thermal Expansion 12 Joint Conferences. Pittsburgh, PA; 1999.

[7] Hensel, F.; Warren, W.W., Jr. *Fluid Metals. The Liquid-Vapor Transition of Metals*. Princeton: Princeton University Press; 1999. Physical Chemistry: Science and Engineering, ed. Prausnitz, J.M.; Brewer, L. 244 p.

[8] Vargaftik, N.B.; Vinogradov, Y.K.; Yargin, V.S. *Handbook of Physical Properties of Liquids and Gases*. New York: Begell House; 1996. 3rd ed. 1359 p.

[9] Sugawara, S.; Sato, T.; Minamiyama, T. On the equation of state of mercury vapour. Bulletin of JSME. 5(20): 711-718; 1962.

[10] Hicks, W.T. Evaluation of vapor-pressure data for mercury, lithium, sodium, and potassium. J. Chem. Phys. 38(8): 1873-1880; 1963.

[11] Stull, D.R. Vapor pressure of pure substances. Inorganic compounds. Ind. Eng. Chem. 39(4): 540-550; 1947.
[12] Epstein, L.F.; Powers, M.D. The vapor pressure of liquid mercury from the triple point to the critical point. Atomic Energy Commision, AECU-1640. 1951.
[13] Götzlaff, W. Zustandsgleichung und elektrischer Transport am kritischen Punkt des fluiden Quecksilbers. Dr. rer. nat. Thesis, Philipps-Universität Marburg, Marburg, Germany, 1988.
[14] Ditchburn, R.W.; Gilmour, J.C. The vapor pressures of monatomic vapors. Rev. Mod. Phys. 13: 310-327; 1941.
[15] Honig, R.E.; Kramer, D.A. Vapor pressure data for the solid and liquid elements. RCA Review. 30(2): 285-288; 1969.
[16] Mukhachev, G.A.; Borodin, V.A.; Poskonon, Y.A. Temperature variation of the thermodynamic properties of mercury. Russ. J. Phys. Chem. 39(8): 1080-1083; 1965.
[17] Laby, T.H. A recalculation of the vapor pressure of mercury. Phil. Mag. 6(16): 789-796; 1908.
[18] Ambrose, D.; Sprake, C.H.S. The vapour pressure of mercury. J. Chem. Thermodyn. 4: 603-620; 1972.
[19] Kelley, K.K. Contributions to the data on theoretical metallurgy. III. The free energies of vaporization and vapor pressures of inorganic substances, U.S. Bureau of Mines, Bulletin 383: Washington D.C. 1935.
[20] de Kruif, C.G. The determination of enthalpies of sublimation by means of thermal conductivity manometers. PhD Thesis, Rijksuniversitlit Utrecht, Utrecht, The Netherlands, 1971.
[21] de Kruif, C.G.; van Ginkel, C.H.D.; Langenberg, A. Vapour pressure and thermodynamic function changes of mercury. Recl. Trav. Chim. Pays-Bas. 92: 599-600; 1973.
[22] PTB Physikalisch-Technische Bundesanstalt (PTB)-Stoffdatenblätter SDB 12. Mercury, PTB: Braunschweig and Berlin. 1995.
[23] Uchida, H. Mercury vapour tables and i-s diagram (in Japanese). Trans. JSME. 17(62): 70-77; 1951.
[24] Alcock, C.B.; Itkin, V.P.; Horrigan, M.K. Vapour pressure equations for the metallic elements: 298-2500 K. Can. Metall. Q. 23(3): 309-313; 1984.
[25] Nesmeyanov, A.N. *Vapor Pressure of the Elements (translated from the Russian by J.I. Carasso)*. New York: Academic Press; 1963. 469 p.
[26] Dalton, J. Experimental Essays. II. On the force of steam or vapour from water and various other liquids, both in a vacuum and in air. Mem. Proc. - Manchester Lit. Philos. Soc. 5(2): 550-574; 1801.
[27] Crichton, J. On the freezing point of tin, and the boiling point of mercury; with a description of a self-registering thermometer. Phil. Mag. (March): 147-148; 1803.
[28] Beattie, J.A.; Blaisdell, B.E.; Kaminsky, J. An experimental study of the absolute temperature scale. IV. Reproducibility of the mercury boiling point. The effect of pressure on the mercury boiling point. Proc. Am. Acad. Arts Sci. 71: 375-385; 1937.
[29] Hall, J.A.; Barber, C.R. The International Temperature Scale—1948 Revision. Br. J. Appl. Phys. 1(4): 81-85; 1950.
[30] Preston-Thomas, H. The international temperature scale of 1990 (ITS-90). Metrologia. 27: 3-10; 1990.

[31] Marsh, K.N. ed. Recommended Reference Materials for the Realization of Physicochemical Properties., Blackwell Scientific: Oxford, UK; 1987.
[32] Preston-Thomas, H. The international practical temperature scale of 1968 amended edition of 1975. Metrologia. 12: 7-17; 1976.
[33] Regnault, V. Forces élastiques des vapeurs. Mem. Acad. Sci. Inst. Fr. 26: 506-525; 1862.
[34] Avogadro, A. Ueber die Spannkraft des Quecksilberdampfs bei verschiedenen Temperaturen. Pogg. Ann. 27: 60-80; 1833.
[35] Hertz, H. On the pressure of saturated mercury (in German). Ann. Phys. Chem. 17: 193-200; 1882.
[36] Ramsay, W.; Young, S. On the vapour-pressures of mercury. J. Chem. Soc. (London). 49: 37-50; 1886.
[37] Haber, F.; Kerschbaum, F. Measurement of low pressures with a vibrating quartz filament. Determination of the vapor pressure of mercury and iodine. (in German). Z. Elektrochem. Ang. Phys. Chem. 20: 296-305; 1914.
[38] Dykyj, J.; Svoboda, J.; Wilhoit, R.C.; Frenkel, M.; Hall, K.R., Vapor pressure and Antoine constants for hydrocarbons, and sulfur, selenium, tellurium and halogen containing organic compounds., in *Vapor Pressure of Chemicals, subvolume A*, Hall, K.R., Editor. Landolt-Börnstein Numerical Data and Functional Relationships in Science and Technology, Group IV: Physical Chemistry, Volume 20, Springer; 1999.
[39] Smith, A.; Menzies, A.W.C. Studies in vapor pressure: IV. A redetermination of the vapor pressures of mercury from 250° to 435°. J. Am. Chem. Soc. 32: 1434-1447; 1910.
[40] Menzies, A.W.C. The vapour pressures of liquid mercury. Z. Phys. Chem. 130: 90-94; 1927.
[41] Bernhardt, F. Saturation pressure of mercury up to 2000 kg/cm^2 (in German). Phys. Z. 26(6): 265-275; 1925.
[42] Bessel-Hagen, E. Ueber eine neue Form der Töpler'schen Quecksilberluftpumpe und einige mit ihr angestellte Versuche. Ann. Phys. Chem. 12(2): 425-445; 1881.
[43] Burlingame, J.W. Dilute solutions of mercury in liquid binary alloys. PhD Thesis, University of Pennsylvania, Philadelphia, PA, 1968.
[44] Busey, R.H.; Giauque, W.F. The heat capacity of mercury from 15 to 330°K. Thermodynamic properties of solid, liquid and gas. Heat of fusion and vaporization. J. Am. Chem. Soc. 75: 806-809; 1953.
[45] Cailletet, L.; Colardeau, E.; Rivière, C. Recherches sur les tensions de le vapeur de mercure saturée. Compt. Rend. 130: 1585-1591; 1900.
[46] Callendar, H.L.; Griffiths, E.H. On the determination of the boiling-point of sulphur, and on a method of standardising platinum resistance thermometers by reference to it. Experiments made at the Cavendish Laboratory, Cambridge. Phil. Trans. R. Soc. Lond. A. 182: 119-157; 1891.
[47] Cammenga, H.K. The determination of high precision vapour pressure of mercury and its importance as reference pressure for studies on vapour pressure and rate of evaporation. in Proceedings of the 1st International Conference on Calorimetry and Thermodynamics. Warsaw, Poland. 1969.
[48] Carlson, K.D.; Gilles, P.W.; Thorn, R.J. Molecular and hydrodynamical effusion of mercury vapor from Knudsen cells. J. Chem. Phys. 38(11): 2725-2735; 1963.

[49] Dauphinee, T.M. The measurement of the vapour pressure of mercury in the intermediate pressure range. PhD Thesis, University of British Columbia, Vancouver, Canada, 1950.
[50] Dauphinee, T.M. The vapor pressure of mercury from 40°C to 240°C: (5 microns to 6 cm) Measured by the streaming method. J. Chem. Phys. 19: 389-390; 1951.
[51] Douglas, T.B.; Ball, A.F.; Ginnings, D.C. Heat capacity of liquid mercury between 0° and 450°C; calculation of certain thermodynamic properties of the saturated liquid and vapor. Nat. Bur. Stand. (U.S.) J. Res. NBS. 46(4): 334-348; 1951.
[52] Durrans, T.H. A treatise on distillation. Perfumery and Essential Oil Record. 11S: 154-198; 1920.
[53] Egerton, A.C. The vapour pressure of zinc, cadmium, and mercury. Phil. Mag. 33(193): 33-48; 1917.
[54] Ernsberger, F.M.; Pitman, H.W. New absolute manometer for vapor pressures in the micron range. Rev. Sci. Instrum. 26(6): 584-589; 1955.
[55] Galchenko, I.E.; Pelevin, O.V.; Sokolov, A.M. Determination of the partial vapor pressure of the volatile component by the static method. Industrial Laboratory. 44(12): 1699-1700; 1978.
[56] Galchenko, I.E.; Pelevin, O.V.; Sokolov, A.M. Determination of the vapor pressure of mercury over melts in the Hg-Cd-Te system. Inorganic Materials. 20(7): 952-955; 1984.
[57] Gebhardt, A. Über den Dampfdruck von Quecksilber und Natrium. Ber. Dtsch. Phys. Ges. 7: 184-185; 1905.
[58] Hagen, E.B. On the tensions of saturated mercury vapor at low temperatures (in German). Ann. Phys. Chem. 16: 610-618; 1882.
[59] Hensel, F.; Franck, E.U. Elektrische Leitfähigkeit und Dichte von überkritischem, gasförmigem Quecksilber unter hohen Drucken. Ber. Bunsenges. Phys. Chem. 70(9/10): 1154-1160; 1966.
[60] Heycock, C.T.; Lamplough, F.E.E. The boiling points of mercury, cadmium, zinc, potassium, and sodium. Proc. Chem. Soc. 28: 3-4; 1913.
[61] Hildenbrand, D.L.; Hall, W.F.; Ju, F.; Potter, N.D. Vapor pressures and vapor thermodynamic properties of some lithium and magnesium halides. J. Chem. Phys. 40(10): 2882-2890; 1964.
[62] Hill, C.F. Measurement of mercury vapor pressure by means of the Knudsen pressure gauge. Phys. Rev. 20: 259-266; 1922.
[63] Hubbard, S.R.; Ross, R.G. Slope anomaly in the vapour pressure curve of Hg. Nature. 295: 682-683; 1982.
[64] Jenkins, C.H.M. The determination of the vapour tensions of mercury, cadmium and zinc by a modified manometric method. Proc. R. Soc. London, A. 110(754): 456-463; 1926.
[65] Kahlbaum, G.W.A. Studies of vapor pressure measurements (in German). Z. Phys. Chem. 13: 14-55; 1894.
[66] Knudsen, M. Experimental determination of the pressure of saturated mercury vapors at 0°C and at higher temperatures. (in German). Ann. Phys. 29: 179-193; 1909.
[67] Knudsen, M. An absolute manometer (in German). Ann. Phys. 32(4): 890-842; 1910.
[68] Kordes, E.; Raaz, F. Aufnahme von Siedediagrammen binärer hochsiedender Flüssigkeitsgemische. Z. Anorg. Allg. Chem. 181: 225-236; 1929.

[69] Mayer, H. On a new method for measurements of the lowest vapor pressures: the vapor pressures of mercury and potassium. III. Communication (in German). Zeitschr. f. Physik. 67: 240-263; 1930.
[70] McLeod, F.R.S. On the pressure of the vapour of mercury at the ordinary temperature. Report of the Meeting of the British Association for the Advancement of Science. 443-444; 1883.
[71] Millar, R.W. The vapor pressures of potassium amalgams. J. Am. Chem. Soc. 49: 3003-3010; 1927.
[72] Morley, E.W. On the vapour-pressure of mercury at ordinary temperatures. Phil. Mag. 7: 662-667; 1904.
[73] Murgulescu, I.G.; Topor, L. Vapour pressure and molecular association of NaCl, NaBr vapours. Rev. Roum. Chim. 11: 1353-1360; 1966.
[74] Neumann, K.; Völker, E. A torsion balance method for measurements of lowest vapor pressures (in German). Z. Phys. Chem. 161: 33-45; 1932.
[75] Pedder, J.S.; Barratt, S. The determination of the vapour pressures of amalgams by a dynamic method. J. Chem. Soc. (London). 537-546; 1933.
[76] Pfaundler, L. On the tension of mercury vapor in the interval 0°C to 100°C (in German). Ann. Phys. Chem. 63(3): 36-43; 1897.
[77] Poindexter, F.E. Mercury vapor pressure at low temperatures. Phys. Rev. 26: 859-868; 1925.
[78] Raabe, G.; Sadus, R.J. Molecular simulation of the vapor-liquid coexistence of mercury. J. Chem. Phys. 119(13): 6691-6697; 2003.
[79] Rodebush, W.H.; Dixon, A.L. The vapor pressures of metals; a new experimental method. Phys. Rev. 26: 851-858; 1925.
[80] Roeder, A.; Morawietz, W. Investigations on the occurrence of compound molecules in the vapor of potassium-mercury melts (in German). Z. f. Elektrochemie. 60: 431-454; 1956.
[81] Ruff, O.; Bergdahl, B. Studies at high temperatures. XII The measurement of vapor tensions at very high temperatures and some observations of the solubility of carbon in metals (in German). Z. Anorg. Allg. Chem. 106: 76-94; 1919.
[82] Schmahl, N.G.; Barthel, J.; Kaloff, H. An apparatus for vapor pressure measurements at elevated temperatures with a static method. Three-term vapor pressure equation for mercury (in German). Z. Phys. Chem. 46(3-4): 183-189; 1965.
[83] Schneider, A.; Schupp, K. The vapor pressure of tellurium (in German). Z. Elektrochem. Ang. Phys. Chem. 50: 163-167; 1944.
[84] Schönherr, G.; Hensel, F. Unusual thermodynamic and electrical properties of metallic solutions near the critical point of the almost pure solvent. Ber. Bunsenges. Phys. Chem. 85: 361-367; 1981.
[85] Scott, D.H. A determination of the vapour pressures of cesium and rubidium, and a calculation of their chemical constants. Phil. Mag. 47: 32-50; 1924.
[86] Shpil'rain, E.E.; Nikanorov, E.V. Measurement of the vapor pressure of mercury by the boiling point method. High Temp. 9: 585-587; 1971.
[87] Spedding, F.H.; Dye, J.L. The vapor pressure of mercury at 250-360°. J. Phys. Chem. 59: 581-583; 1955.

[88] Stock, A.; Zimmermann, W. Vapor pressures of mercury and some mercury compounds at low temperatures (in German). Monatsh. Chem. 53-54: 786-790; 1929.
[89] van der Plaats, J.D. Sur le poids et la tension de la vapeur de mercure, saturée à la température ambiante. Recl. Trav. Chim. Pays-Bas. 5: 149-183; 1886.
[90] Villiers, M.A. Sur la vapeur emise par le mercure dans les gaz rarefies et sur les tensions maxima de vapeur du mercure. Ann. Chim. Phys. 30: 588-633; 1913.
[91] Volmer, M.; Kirchhoff, P. The vapor pressures of solid and liquid benzophenone between 0° und 48° (in German). Z. Phys. Chem. 115: 233-260; 1925.
[92] von Halban, H., H. Die Bestimmung von Quecksilberdampfdrucken aus der Resonanzlicht-absorption. Helv. Phys. Acta. 7: 856-875; 1935.
[93] Young, S. The vapour pressures of mercury. J. Chem. Soc. (London). 59: 629-634; 1891.
[94] Menzies, A.W.C. The critical temperature of mercury. J. Am. Chem. Soc. 35(9): 1065-1067; 1913.
[95] Guildner, L.A.; Terrien, J., Part 1: Mercury absolute manomoeters, in *Experimental Thermodynamics Volume II. Experimental Thermodynamics of Non-reacting Fluids.*, *Prepared under the sponsorship of the Internation Union of Pure and Applied Chemistry, Commission on Thermodynamics and Thermochemistry,* Le Neindre, B.; Vodar, B., Editors., Butterworths: London; 1975.
[96] Debenedetti, P.G. *Metastable Liquids. Concepts and Principles*. Princeton, NJ: Princeton University Press; 411 p.; 1996.
[97] Koenigsberger, J. Über die kritische Temperatur des Quecksilbers. Chem. Ztg. XXXVI(135): 1321; 1912.
[98] Bender, J. On the critical temperature of mercury (in German). Phys. Z. 16: 246-247; 1915.
[99] Birch, F. The electrical resistance and the critical point of mercury. Phys. Rev. 41: 641-648; 1932.
[100] Mathews, J.F. The critical constants of inorganic substances. Chem. Rev. 72(1): 71-100; 1972.
[101] Ambrose, D. Vapour-liquid critical properties, Natl. Phys. Lab., Div. Chem. Stand.: Teddington, U.K. p. 60. 1980.
[102] Franck, E.U.; Hensel, F. Metallic conductance of supercritical mercury gas at high pressures. Phys. Rev. 147(1): 109-110; 1966.
[103] Kikoin, I.K.; Senchenkov, A.P. Electrical conductivity and equation of state of mercury in the temperature range 0-2000°C and pressure range of 200-5000 Atm. Phys. Metals Metallog. 24(5): 74-89; 1967.
[104] Neale, F.E.; Cusack, N.E. Thermoelectric power near the critical point of expanded fluid mercury. J. Phys. F: Metal Phys. 9(1): 85-94; 1979.
[105] Kozhevnikov, V.; Arnold, D.; Grodzinskii, E.; Naurzakov, S. Phase transitions and critical phenomena in mercury fluid probed by sound. Fluid Phase Equilib. 125: 149-157; 1996.
[106] Meyer, G. Die kritische Temperatur des Quecksilber. Phys. Z. 22: 76-78; 1921.
[107] Hubbard, S.R.; Ross, R.G. Thermodynamic and electrical properties of fluid Hg up to the liquid-vapour critical point. J. Phys. C: Solid State Phys. 16: 6921-6931; 1983.
[108] Růžička, K.; Majer, V. Simple and controlled extrapolation of vapor pressures toward the triple point. AIChE J. 42(6): 1723-1740; 1996.

[109] Wagner, W. New vapour pressure measurements for argon and nitrogen and a new method for establishing rational vapour pressure equations. Cryogenics. 13(8): 470-482; 1973.
[110] Wagner, W. Corrigenda. New vapour pressure measurements for argon and nitrogen and a new method for establishing rational vapour pressure equations. Cryogenics. 14: 63; 1974.
[111] Wagner, W.; Ewers, J.; Pentermann, W. New vapour-pressure measurements and a new rational vapour-pressure equation for oxygen. J. Chem. Thermodyn. 8(11): 1049-1060; 1976.
[112] Wagner, W. *Eine mathematisch statistische Methode zum Aufstellen thermodynamischer Gleichungen - gezeigt am Beispiel der Dampfdruckkurve reiner fluider Stoffe*. Düsseldorf, FRG: VDI Verlag GmbH; Fortschritt-Berichte der VDI-Zeitschriften. Vol. Series 3, No. 39. 181 p.; 1974.
[113] Lemmon, E.W.; Goodwin, A.R.H. Critical properties and vapor pressure equation for alkanes C_nH_{2n+2}: normal alkanes with n<=36 and isomers for n=4 through n=9. J. Phys. Chem. Ref. Data. 29(1): 1-39; 2000.
[114] Poling, B.E.; Prausnitz, J.M.; O'Connell, J.P. *The properties of gases and liquids*. New York, NY: McGraw-Hill; 5th ed. 741 p.; 2001.
[115] Ewing, M.B.; Sanchez Ochoa, J.C. Vapor pressures of acetonitrile determined by comparative ebulliometry. J. Chem. Eng. Data. 49: 486-491; 2004.
[116] Harvey, A.H.; Lemmon, E.W. Correlation for the vapor pressure of heavy water from the triple point to the critical point. J. Phys. Chem. Ref. Data. 31(1): 173-181; 2002.
[117] Wagner, W.; Pruß, A. International equations for the saturation properties of ordinary water substance. Revised According to the International Temperature Scale of 1990. J. Phys. Chem. Ref. Data. 22: 783-787; 1993.
[118] Wagner, W.; Pruß, A. The IAPWS Formulation 1995 for the thermodynamic properties of ordinary water substance for general and scientific use. J. Phys. Chem. Ref. Data. 31(2): 387-535; 2002.
[119] King, M.B.; Al-Najjar, H. A method for correlating and extending vapour pressure data to lower temperatures using thermal data: vapour pressure equations for some n-alkanes at temperatures below the normal boiling point. Chem. Eng. Sci. 29(4): 1003-11; 1974.
[120] Tillner-Roth, R. A nonlinear regression analysis for estimating low-temperature vapor pressures and enthalpies of vaporization applied to refrigerants. Int. J. Thermophys. 17(6): 1365-1385; 1996.
[121] Mohr, P.J.; Taylor, B.N. CODATA recommended values of the fundamental physical constants: 2002. Rev. Mod. Phys. 77(1): 1-107; 2005.
[122] Chase, M.W., Jr. NIST-JANAF Thermochemical Tables. J. Phys. Chem. Ref. Data. Monograph No. 9, Fourth Edition; 1998.
[123] Amitin, E.B.; Lebedeva, E.G.; Paukov, I.E. The heat capacity of mercury in the range 5-300 K and the energy of formation and concentration of equilibrium vacancies in mercury. Russ. J. Phys. Chem. 53(10): 1528-1530; 1979.
[124] Kirkpatrick, S.; Gelatt, C.D.; Vecchi, M.P. Optimization by simulated annealing. Science. 220: 671-680; 1983.
[125] Press, W.H.; Flannery, B.P.; Teukolsky, S.A.; Vetterling, W.T. *Numerical Recipes. The Art of Scientific Computing*. Cambridge, U.K.: Cambridge University Press; 818 p.; 1986.

[126] Lundy, M.; Mees, A. Convergence of an annealing algorithm. Math. Prog. 34: 111-124; 1986.
[127] Huber, M.L. Structural optimization of vapor pressure correlations using simulated annealing and threshold accepting: application to R134a. Computers Chem. Engng. 18(10): 929-932; 1994.
[128] Boggs, P.T.; Byrd, R.H.; Rogers, J.E.; Schnabel, R.B. ODRPACK, Software for Orthogonal Distance Regression, NISTIR 4834, Natl. Inst. Stand. Technol; 1992.
[129] Loss, R.D. Atomic weights of the elements. Pure Appl. Chem. 75(8): 1107-1122; 2003.
[130] Lange, N.A. ed. Handbook of Chemistry. 10th ed., McGraw-Hill: New York; 1967.
[131] Washburn, E.W. ed. International Critical Tables of Numerical Data, Physics, Chemistry and Technology, Volume III., McGraw-Hill: New York; 1928.
[132] Lide, D.R. ed. CRC Handbook of Chemistry and Physics. 85th Edition ed., CRC Press: Boca Raton, FL.; 2004.
[133] KDB Korea Thermophysical Properties Databank (KDB), http://www.cheric.org/kdb/, Korea University. 2005.
[134] Rowley, J.R.; Wilding, W.V.; Oscarson, J.L.; Rowley, R.L. DIADEM, DIPPR Information and Data Evaluation Manager, v2.7.0, Brigham Young University: Provo, UT. 2004.
[135] Yaws, C.L. *Chemical Properties Handbook: Physical, Thermodynamics, Environmental Transport, Safety & Health Related Properties for Organic & Inorganic Chemicals*. McGraw-Hill Professional; 1999. 784 p.
[136] Vargaftik, N.B. *Tables on the Thermophysical Properties of Liquids and Gases*. New York: Halsted Press; 1975. 2nd ed.
[137] Rowley, R.L. personal communication to Huber, M.L.: Brigham Young University, Provo Utah 84602. 2006.
[138] Clarke, E.C.W.; Glew, D.N. Evaluation of thermodynamic functions from equlibrium constants. Trans. Farad. Soc. 62: 539-547; 1966.
[139] Standard Test Method for Mercury Sampling and Analysis in Natural Gas by Atomic Fluorescence Spectroscopy, D-6350-98, ASTM International; Reapproved 2003.
[140] Egerton, A.C. Note on the determination of chemical constants. Phil. Mag. 39: 1-20; 1920.
[141] Egerton, A.C. Note on vapour pressures of monatomic substances. Phil. Mag. 48: 1048-1054; 1924.
[142] Volmer, M.; Estermann, I. On the evaporation coefficients of solid and liquid mercury. (in German). Zeitschr. f. Physik. 7: 1-12; 1921.
[143] Jewitt, F.B. A new method of determining the vapour-density of metallic vapours, and an experimental application to the cases of sodium and mercury. Phil. Mag. 4: 546-554; 1902.
[144] Cater, E.D. The effusion method at 69: current state of the art. in Proceedings of the 10th Materials Research Symposium on Characterization of High Temperature Vapors and Gases. Nat. Bur. Stan. (U.S.), Special Publication 561. 1979.
[145] Zaitsau, D.H.; Paulechka, Y.U.; Kabo, G.J.; Kolpikau, A.N.; Emel'yanenko, V.N.; Heintz, A.; Verevkin, S.P. Thermodynamics of the sublimation and of the vaporization of ε-caprolactam. J. Chem. Eng. Data. 51: 130-135; 2006.

[146] Rohháč, V.; Růžička, K.; Růžička, V.; Zaitsau, D.H.; Kabo, G.J.; Diky, V.; Aim, K. Vapor pressure of diethyl phthalate. J. Chem. Thermodyn. 36: 929-937; 2004.
[147] Zaitsau, D.H.; Verevkin, S.P.; Paulechka, Y.U.; Kabo, G.J.; Sevruk, V.M. Comprehensive study of vapor pressures and enthalpies of vaporization of cyclohexyl esters. J. Chem. Eng. Data. 48: 1393-1400; 2003.
[148] Product Properties Test Guidelines, OPPTS 830.7950 Vapor Pressure, EPA Report 712-C-96-043, Office of Prevention, Pesticides and Toxic Substances (OPPTS), U.S. Environmental Protection Agency. 1996.

Appendix A. Detailed Listing of Experimental Data for the Vapor Pressure of Mercury

All temperatures have been converted to ITS-90. Data are arranged alphabetically by first author.

Data from Ambrose and Sprake [18]

T, K	p, kPa	T, K	p, kPa	T, K	p, kPa
379.934	0.046	681.168	237.992	635.136	111.503
400.340	0.139	685.426	253.933	636.491	114.202
417.095	0.293	702.724	327.808	621.615	87.311
426.204	0.424	711.623	371.975	623.249	89.986
432.281	0.538	726.554	456.609	624.850	92.662
439.292	0.706	739.690	543.039	626.410	95.342
441.719	0.774	749.788	617.883	627.956	98.055
447.681	0.964	771.124	802.526	629.467	100.770
451.381	1.101	481.650	3.023	630.924	103.440
454.121	1.213	488.128	3.689	632.343	106.101
456.320	1.309	494.925	4.522	633.750	108.792
462.634	1.627	500.619	5.339	635.136	111.504
469.182	2.024	506.657	6.342	636.492	114.202
474.565	2.414	513.690	7.708	621.622	87.323
479.040	2.784	520.258	9.205	623.266	90.010
485.150	3.369	526.171	10.753	624.853	92.671
491.856	4.128	533.782	13.074	626.418	95.353
497.530	4.882	541.589	15.879	627.958	98.060
533.454	12.965	546.934	18.080	629.466	100.764
541.345	15.780	555.219	21.998	630.924	103.441
549.473	19.193	562.504	26.013	632.343	106.101
554.721	21.742	572.032	32.173	633.750	108.794
562.759	26.162	579.202	37.584	635.130	111.489
572.231	32.313	587.994	45.215	636.492	114.202
579.977	38.203	596.471	53.760	621.625	87.331
589.082	46.244	605.005	63.675	623.267	90.014
597.320	54.686	612.930	74.144	624.855	92.672
605.650	64.484	621.863	87.728	626.413	95.348
611.991	72.866	628.996	99.929	627.951	98.043
621.147	86.564	629.758	101.311	629.465	100.764
627.808	97.795	630.156	102.037	630.923	103.440
628.883	99.711	621.619	87.316	632.342	106.098
629.949	101.643	623.258	90.004	633.747	108.789
638.367	118.032	624.850	92.667	635.135	111.501
629.365	100.600	626.421	95.363	636.488	114.195
639.863	121.141	627.960	98.061		
645.494	133.558	629.464	100.768		
654.707	155.987	630.923	103.440		
663.194	179.295	632.340	106.099		
671.779	205.659	633.748	108.792		

Data from Beattie, Blaisdell, and Kaminsky [28]

T, K	p, kPa	T, K	p, kPa	T, K	p, kPa
		635.647			
629.7632	101.325	6	112.492	631.1879	103.940
		635.458			
629.7648	101.325	9	112.121	632.6278	106.646
		634.150			
629.7666	101.325	9	109.565	633.9426	109.160
		632.801			
629.7676	101.325	4	106.976	634.9149	111.047
		631.404			
629.7632	101.325	4	104.344	633.6486	108.587
		629.963			
629.7663	101.325	3	101.688	632.2578	105.943
		628.422			
622.9608	89.5232	6	98.8973	630.6593	102.963
		626.852			
624.5575	92.1883	7	96.1257	629.1704	100.244
		625.393			
626.0545	94.7394	6	93.6046	627.6159	97.4703
		623.292			
627.6855	97.5908	7	90.0733	626.0489	94.7299
		623.079			
629.0765	100.075	7	89.7188	624.5171	92.1186
		624.988			
630.5802	102.819	4	92.9141	622.9920	89.5730
		626.762			
632.0069	105.472	4	95.9670		
		628.226			
633.4298	108.168	8	98.5483		
		629.756			
634.7126	110.655	2	101.312		

Data from Bernhardt [41]

T, K	p, kPa	T, K	p, kPa	T, K	p, kPa
693	343.2	1074	9807	1619	125500
693	313.8	1114	12750	1663	146100
743	568.8	1174	14910	1674	155900
753	519.8	1199	16670	1685	164400
794	980.7	1368	46090	1685	173600
794	1079	1488	88260	1685	181400
844	1618	1553	104000	1706	198100
854	1471	1608	105400		
944	3334	1614	111800		
1004	6865	1619	118700		

Data from Bessel-Hagen [42]

T, K	p, kPa
273	0.00197
293	0.00268

Data from Burlingame [43]

T, K	p, kPa	T, K	p, kPa	T, K	p, kPa
377.2	$4.560 \cdot 10^{-2}$	408.9	$2.045 \cdot 10^{-1}$	473.6	2.318
377.1	$4.613 \cdot 10^{-2}$	443.2	$8.126 \cdot 10^{-1}$	473.6	2.321
377.1	$4.546 \cdot 10^{-2}$	443.2	$8.069 \cdot 10^{-1}$	343.6	$7.186 \cdot 10^{-3}$
377.0	$4.613 \cdot 10^{-2}$	443.2	$8.083 \cdot 10^{-1}$	343.6	$6.999 \cdot 10^{-3}$
377.0	$4.560 \cdot 10^{-2}$	443.2	$8.162 \cdot 10^{-1}$	343.7	$7.146 \cdot 10^{-3}$
377.1	$4.506 \cdot 10^{-2}$	443.2	$8.194 \cdot 10^{-1}$	343.6	$7.146 \cdot 10^{-3}$
377.2	$4.426 \cdot 10^{-2}$	473.5	2.297	343.7	$7.039 \cdot 10^{-3}$
377.1	$4.613 \cdot 10^{-2}$	473.5	2.306	343.7	$7.093 \cdot 10^{-3}$
408.9	$2.074 \cdot 10^{-1}$	473.6	2.314		
408.9	$2.070 \cdot 10^{-1}$	473.6	2.353		
408.8	$2.122 \cdot 10^{-1}$	473.6	2.333		
408.8	$2.134 \cdot 10^{-1}$	473.6	2.337		
408.9	$1.971 \cdot 10^{-1}$	473.6	2.341		
408.8	$2.038 \cdot 10^{-1}$	473.6	2.316		
408.9	$2.042 \cdot 10^{-1}$	473.6	2.322		

Data from Busey and Giauque [44]

T, K	p, kPa	T, K	p, kPa
234.32	$3.07\cdot10^{-7}$	500.01	5.256
250.02	$2.24\cdot10^{-6}$	525.02	$1.044\cdot10^{1}$
275.00	$3.31\cdot10^{-5}$	550.03	$1.947\cdot10^{1}$
298.15	$2.67\cdot10^{-4}$	575.03	$3.429\cdot10^{1}$
299.98	$3.11\cdot10^{-4}$	600.04	$5.757\cdot10^{1}$
324.98	$2.05\cdot10^{-3}$	625.04	$9.274\cdot10^{1}$
349.97	$1.03\cdot10^{-2}$	629.92	$1.013\cdot10^{2}$
374.97	$4.144\cdot10^{-2}$	650.03	$1.437\cdot10^{2}$
399.98	$1.397\cdot10^{-1}$	675.03	$2.156\cdot10^{2}$
424.99	$4.077\cdot10^{-1}$	700.02	$3.140\cdot10^{2}$
449.99	1.054	725.01	$4.452\cdot10^{2}$
475.00	2.458	750.00	$6.165\cdot10^{2}$

Data from Cailletet , Colardeau, and Rivìere [45]

T, K	p, kPa	T, K	p, kPa	T, K	p, kPa
673	$2.13\cdot10^{2}$	924	$3.45\cdot10^{3}$	1154	$1.64\cdot10^{4}$
723	$4.31\cdot10^{2}$	974	$5.07\cdot10^{3}$		
774	$8.11\cdot10^{2}$	1024	$7.30\cdot10^{3}$		
824	$1.40\cdot10^{3}$	1074	$1.03\cdot10^{4}$		
874	$2.26\cdot10^{3}$	1124	$1.393\cdot10^{4}$		

Data from Callendar and Griffiths [46]

T,K	p, kPa
629.79	101.325
629.95	101.325

Data from Carlson, Gilles and Thorn [48]

T, K	p, kPa	T, K	p, kPa
301.38	$3.5064\cdot10^{-4}$	406.28	$2.718\cdot10^{-1}$
324.08	$1.947\cdot10^{-3}$	448.29	1.652
336.97	$4.626\cdot10^{-3}$	499.21	8.371
348.27	$9.306\cdot10^{-3}$	548.83	$3.145\cdot10^{1}$
372.17	$4.226\cdot10^{-2}$		

Data from Dauphinee [49, 50]

T, K	p, kPa	T, K	p, kPa
454.88	1.2407	345.08	$7.44739 \cdot 10^{-3}$
444.55	$8.6353 \cdot 10^{-1}$	353.45	$1.26496 \cdot 10^{-2}$
382.91	$6.0968 \cdot 10^{-2}$	361.31	$2.00317 \cdot 10^{-2}$
396.41	$1.1984 \cdot 10^{-1}$	405.29	$1.7885 \cdot 10^{-1}$
405.17	$1.6799 \cdot 10^{-1}$	483.27	3.2547
413.90	$2.5794 \cdot 10^{-1}$	513.53	7.7820
421.97	$3.6650 \cdot 10^{-1}$	332.82	$3.4624 \cdot 10^{-3}$
433.36	$5.8142 \cdot 10^{-1}$	314.02	$9.2179 \cdot 10^{-4}$
323.72	$1.78119 \cdot 10^{-3}$	305.00	$4.1703 \cdot 10^{-4}$

Data from Douglas, Ball, and Ginnings [51]

T, K	p, kPa	T, K	p, kPa	T, K	p, kPa
234.30	$2.921 \cdot 10^{-7}$	413.13	$2.4663 \cdot 10^{-1}$	$6.1319 \cdot 10^{2}$	$7.4557 \cdot 10^{1}$
253.17	$3.114 \cdot 10^{-6}$	433.14	$5.5722 \cdot 10^{-1}$	$6.2977 \cdot 10^{2}$	$1.0133 \cdot 10^{2}$
273.15	$2.661 \cdot 10^{-5}$	453.15	1.1697	$6.3318 \cdot 10^{2}$	$1.0772 \cdot 10^{2}$
293.14	$1.691 \cdot 10^{-4}$	473.15	2.3029	$6.5318 \cdot 10^{2}$	$1.52074 \cdot 10^{2}$
298.14	$2.580 \cdot 10^{-4}$	493.16	4.2859	$6.7318 \cdot 10^{2}$	$2.10201 \cdot 10^{2}$
313.13	$8.453 \cdot 10^{-4}$	513.17	7.5902	$6.9317 \cdot 10^{2}$	$2.85011 \cdot 10^{2}$
333.12	$3.4728 \cdot 10^{-3}$	533.17	$1.2863 \cdot 10^{1}$	$7.1317 \cdot 10^{2}$	$3.79714 \cdot 10^{2}$
353.12	$1.2126 \cdot 10^{-2}$	553.18	$2.0963 \cdot 10^{1}$	$7.3316 \cdot 10^{2}$	$4.9780 \cdot 10^{2}$
373.12	$3.6944 \cdot 10^{-2}$	573.18	$3.2986 \cdot 10^{1}$	$7.5315 \cdot 10^{2}$	$6.4300 \cdot 10^{2}$
393.13	$1.0028 \cdot 10^{-1}$	593.19	$5.0299 \cdot 10^{1}$	$7.7315 \cdot 10^{2}$	$8.1932 \cdot 10^{2}$

Data from Egerton [53]

T, K	*p*, kPa	*T*, K	*p*, kPa	*T*, K	*p*, kPa
306.83	$5.320 \cdot 10^{-4}$	298.04	$2.426 \cdot 10^{-4}$	308.53	$5.573 \cdot 10^{-4}$
306.93	$5.026 \cdot 10^{-4}$	295.86	$2.023 \cdot 10^{-4}$	294.14	$1.680 \cdot 10^{-4}$
307.43	$5.226 \cdot 10^{-4}$	295.86	$2.023 \cdot 10^{-4}$	307.23	$5.066 \cdot 10^{-4}$
307.18	$5.146 \cdot 10^{-4}$	308.23	$5.546 \cdot 10^{-4}$	308.33	$5.546 \cdot 10^{-4}$
288.64	$8.613 \cdot 10^{-5}$	308.53	$5.573 \cdot 10^{-4}$	308.33	$5.546 \cdot 10^{-4}$
307.33	$4.880 \cdot 10^{-4}$	308.53	$5.573 \cdot 10^{-4}$	308.33	$5.546 \cdot 10^{-4}$
273.15	$2.520 \cdot 10^{-5}$	294.14	$1.680 \cdot 10^{-4}$	308.33	$5.546 \cdot 10^{-4}$
301.73	$3.373 \cdot 10^{-4}$	295.86	$2.013 \cdot 10^{-4}$	308.53	$5.573 \cdot 10^{-4}$
298.04	$2.386 \cdot 10^{-4}$	295.86	$2.013 \cdot 10^{-4}$		
301.73	$3.293 \cdot 10^{-4}$	308.23	$5.546 \cdot 10^{-4}$		

Data from Ernsberger and Pitman [54]

T, K	*p*, kPa	*T*, K	*p*, kPa
285.22	$8.453 \cdot 10^{-5}$	315.15	$9.949 \cdot 10^{-4}$
288.15	$1.113 \cdot 10^{-4}$	318.17	$1.242 \cdot 10^{-3}$
291.10	$1.448 \cdot 10^{-4}$	321.15	$1.539 \cdot 10^{-3}$
294.11	$1.852 \cdot 10^{-4}$	324.12	$1.900 \cdot 10^{-3}$
297.22	$2.412 \cdot 10^{-4}$	326.63	$2.260 \cdot 10^{-3}$
300.25	$3.116 \cdot 10^{-4}$	293.24	$1.735 \cdot 10^{-4}$
303.18	$3.934 \cdot 10^{-4}$	296.22	$2.226 \cdot 10^{-4}$
306.17	$5.005 \cdot 10^{-4}$	299.20	$2.865 \cdot 10^{-4}$
309.23	$6.358 \cdot 10^{-4}$		
312.11	$7.929 \cdot 10^{-4}$		

Data from Gebhardt [57]

T, K	p, kPa	T, K	p, kPa
403.13	$1.47 \cdot 10^{-1}$	453.15	1.23
413.13	$2.40 \cdot 10^{-1}$	463.15	1.73
423.13	$3.73 \cdot 10^{-1}$	473.15	2.36
433.14	$5.73 \cdot 10^{-1}$	483.16	3.20
443.14	$8.40 \cdot 10^{-1}$		

Data from Haber and Kerschbaum [37]

T, K	p, kPa
293.142	$1.680 \cdot 10^{-4}$

Data from Hagen [58]

T, K	p, kPa
273.15	$2.00 \cdot 10^{-3}$
323.13	$5.60 \cdot 10^{-3}$
373.12	$2.80 \cdot 10^{-2}$
423.13	$2.56 \cdot 10^{-1}$
473.15	2.126

Data from Hertz [35]

T, K	p, kPa	T, K	p, kPa
362.52	$2.13 \cdot 10^{-2}$	457.85	1.472
390.13	$9.47 \cdot 10^{-2}$	463.55	1.719
427.34	$4.65 \cdot 10^{-1}$	476.15	2.713
438.94	$7.36 \cdot 10^{-1}$	480.06	3.010
450.54	1.09		

Data from Heycock and Lamplough [60]

T, K	p, kPa
628.89	101.325

Data from Hildenbrand, Hall, Ju and Potter [61]

T, K	p, kPa	T, K	p, kPa
295.4	$2.08 \cdot 10^{-4}$	295.0	$2.10 \cdot 10^{-4}$
296.8	$2.26 \cdot 10^{-4}$	299.8	$3.05 \cdot 10^{-4}$
297.0	$2.33 \cdot 10^{-4}$	331.6	$3.01 \cdot 10^{-3}$

Data from Hill [62]

T, K	p, kPa	T, K	p, kPa
272.45	$4.40 \cdot 10^{-5}$	297.14	$3.49 \cdot 10^{-4}$
278.85	$7.33 \cdot 10^{-5}$	298.14	$3.64 \cdot 10^{-4}$
284.54	$1.23 \cdot 10^{-4}$	298.73	$3.89 \cdot 10^{-4}$
284.74	$1.15 \cdot 10^{-4}$	299.93	$4.19 \cdot 10^{-4}$
284.74	$1.09 \cdot 10^{-4}$	301.73	$4.93 \cdot 10^{-4}$
286.14	$1.29 \cdot 10^{-4}$	303.03	$5.43 \cdot 10^{-4}$
293.44	$2.49 \cdot 10^{-4}$	303.93	$5.67 \cdot 10^{-4}$
295.94	$3.07 \cdot 10^{-4}$	307.43	$7.17 \cdot 10^{-4}$
296.14	$2.99 \cdot 10^{-4}$	308.03	$7.67 \cdot 10^{-4}$
296.14	$3.13 \cdot 10^{-4}$		

Data from Jenkins [64]

T, K	p, kPa	T, K	p, kPa
479.16	2.27	600.19	$5.56 \cdot 10^{1}$
493.66	3.80	604.19	$6.07 \cdot 10^{1}$
511.17	6.47	615.19	$7.76 \cdot 10^{1}$
520.67	8.27	623.19	$8.85 \cdot 10^{1}$
526.17	$1.01 \cdot 10^{1}$	631.19	$1.03 \cdot 10^{2}$
532.67	$1.21 \cdot 10^{1}$	637.71	$1.16 \cdot 10^{2}$
549.68	$1.85 \cdot 10^{1}$	643.74	$1.27 \cdot 10^{2}$
561.68	$2.513 \cdot 10^{1}$	653.77	$1.508 \cdot 10^{2}$
576.68	$3.56 \cdot 10^{1}$	664.31	$1.789 \cdot 10^{2}$
581.68	$3.79 \cdot 10^{1}$	670.83	$1.987 \cdot 10^{2}$
589.69	$4.47 \cdot 10^{1}$		

Data from Kahlbaum [65]

T, K	p, kPa	T, K	p, kPa	T, K	p, kPa
392.53	$1.16 \cdot 10^{-1}$	427.34	$4.64 \cdot 10^{-1}$	459.05	1.527
397.83	$1.83 \cdot 10^{-1}$	432.24	$5.64 \cdot 10^{-1}$	464.25	1.797
399.03	$1.68 \cdot 10^{-1}$	434.24	$5.85 \cdot 10^{-1}$	466.25	1.867
404.23	$2.81 \cdot 10^{-1}$	435.74	$6.17 \cdot 10^{-1}$	469.85	2.212
407.23	$2.21 \cdot 10^{-1}$	438.24	$6.83 \cdot 10^{-1}$	472.55	2.332
408.13	$2.43 \cdot 10^{-1}$	441.84	$8.03 \cdot 10^{-1}$	474.95	2.549
411.73	$2.93 \cdot 10^{-1}$	446.24	1.01	477.95	2.805
413.33	$3.53 \cdot 10^{-1}$	448.34	1.04	479.06	2.864
414.83	$3.13 \cdot 10^{-1}$	449.44	1.05	482.06	3.097
417.43	$2.67 \cdot 10^{-1}$	449.94	1.09	483.76	3.357
418.33	$3.81 \cdot 10^{-1}$	450.04	1.05	487.46	3.836
420.23	$3.69 \cdot 10^{-1}$	452.75	1.17	489.76	4.117
421.33	$3.96 \cdot 10^{-1}$	454.05	1.26	492.96	4.573
422.13	$4.25 \cdot 10^{-1}$	454.75	1.25		
424.64	$4.37 \cdot 10^{-1}$	456.15	1.409		

Data from Knudsen [67]

T, K	p, kPa	T, K	p, kPa
263.16	$1.10 \cdot 10^{-5}$	288.84	$1.14 \cdot 10^{-4}$
273.15	$2.90 \cdot 10^{-5}$	293.74	$1.67 \cdot 10^{-4}$
280.05	$5.50 \cdot 10^{-5}$	297.54	$2.26 \cdot 10^{-4}$
284.24	$8.20 \cdot 10^{-5}$		

Data from Knudsen [66]

T, K	p, kPa	T, K	p, kPa
273.15	$2.461 \cdot 10^{-5}$	308.63	$5.713 \cdot 10^{-4}$
280.25	$4.902 \cdot 10^{-5}$	312.93	$7.954 \cdot 10^{-4}$
292.74	$1.517 \cdot 10^{-4}$	319.33	$1.280 \cdot 10^{-3}$
293.04	$1.553 \cdot 10^{-4}$	312.83	$7.778 \cdot 10^{-4}$
303.33	$3.741 \cdot 10^{-4}$	323.93	$1.775 \cdot 10^{-3}$

Data from Kordes and Raaz [68]

T, K	p, kPa
630.19	101.325
632.19	101.325

Data from Mayer [69]

T, K	p, kPa	T, K	p, kPa	T, K	p, kPa
262.16	$6.27\cdot10^{-6}$	272.45	$2.45\cdot10^{-5}$	295.84	$2.15\cdot10^{-4}$
263.26	$7.73\cdot10^{-6}$	272.75	$2.49\cdot10^{-5}$	296.84	$2.37\cdot10^{-4}$
264.66	$9.20\cdot10^{-6}$	273.45	$2.67\cdot10^{-5}$	298.14	$2.59\cdot10^{-4}$
265.66	$1.04\cdot10^{-5}$	273.85	$2.76\cdot10^{-5}$	261.46	$6.13\cdot10^{-6}$
266.65	$1.15\cdot10^{-5}$	274.65	$2.99\cdot10^{-5}$	262.16	$6.80\cdot10^{-6}$
267.65	$1.29\cdot10^{-5}$	275.75	$3.48\cdot10^{-5}$	262.76	$7.47\cdot10^{-6}$
268.55	$1.48\cdot10^{-5}$	276.70	$3.91\cdot10^{-5}$	263.16	$8.13\cdot10^{-6}$
268.95	$1.53\cdot10^{-5}$	277.65	$4.25\cdot10^{-5}$	264.46	$9.47\cdot10^{-6}$
269.60	$1.65\cdot10^{-5}$	278.75	$4.87\cdot10^{-5}$	264.86	$1.01\cdot10^{-5}$
270.45	$1.85\cdot10^{-5}$	279.75	$5.27\cdot10^{-5}$	265.46	$1.11\cdot10^{-5}$
271.40	$2.09\cdot10^{-5}$	280.94	$5.88\cdot10^{-5}$	265.66	$1.12\cdot10^{-5}$
272.25	$2.32\cdot10^{-5}$	282.29	$6.52\cdot10^{-5}$	266.56	$1.29\cdot10^{-5}$
273.10	$2.59\cdot10^{-5}$	283.24	$7.15\cdot10^{-5}$	267.55	$1.51\cdot10^{-5}$
273.20	$2.59\cdot10^{-5}$	284.04	$7.81\cdot10^{-5}$	267.75	$1.47\cdot10^{-5}$
274.65	$3.01\cdot10^{-5}$	284.94	$8.52\cdot10^{-5}$	269.75	$1.81\cdot10^{-5}$
276.05	$3.51\cdot10^{-5}$	286.04	$9.47\cdot10^{-5}$	272.35	$2.36\cdot10^{-5}$
277.00	$3.92\cdot10^{-5}$	287.04	$1.03\cdot10^{-4}$	272.95	$2.52\cdot10^{-5}$
278.10	$4.40\cdot10^{-5}$	288.14	$1.13\cdot10^{-4}$	273.15	$2.55\cdot10^{-5}$
278.05	$4.40\cdot10^{-5}$	289.24	$1.25\cdot10^{-4}$	273.15	$2.56\cdot10^{-5}$
279.30	$4.49\cdot10^{-5}$	290.34	$1.36\cdot10^{-4}$	273.35	$2.60\cdot10^{-5}$
280.84	$5.76\cdot10^{-5}$	291.34	$1.48\cdot10^{-4}$	273.85	$2.72\cdot10^{-5}$
280.79	$5.76\cdot10^{-5}$	292.44	$1.61\cdot10^{-4}$	274.45	$2.92\cdot10^{-5}$
283.24	$7.17\cdot10^{-5}$	293.74	$1.79\cdot10^{-4}$	275.05	$3.03\cdot10^{-5}$
285.54	$9.01\cdot10^{-5}$	294.54	$1.91\cdot10^{-4}$	275.75	$3.44\cdot10^{-5}$
288.04	$1.13\cdot10^{-4}$	295.74	$2.08\cdot10^{-4}$	276.75	$3.76\cdot10^{-5}$
289.94	$1.32\cdot10^{-4}$	292.54	$1.61\cdot10^{-4}$	276.95	$3.88\cdot10^{-5}$
272.00	$2.31\cdot10^{-5}$	293.89	$1.80\cdot10^{-4}$	277.95	$4.29\cdot10^{-5}$

Data from McLeod [70]

T, K	p, kPa
293.14	0.000765

Data from Menzies [40, 94]

T, K	p, kPa	T, K	p, kPa	T, K	p, kPa
394.92	$1.1052 \cdot 10^{-1}$	602.72	$6.0942 \cdot 10^{1}$	645.54	$1.3366 \cdot 10^{2}$
423.10	$3.7357 \cdot 10^{-1}$	607.01	$6.6396 \cdot 10^{1}$	651.46	$1.4781 \cdot 10^{2}$
464.58	1.7359	611.05	$7.1667 \cdot 10^{1}$	656.74	$1.6140 \cdot 10^{2}$
526.92	$1.0943 \cdot 10^{1}$	615.66	$7.8228 \cdot 10^{1}$	659.45	$1.6873 \cdot 10^{2}$
533.29	$1.2911 \cdot 10^{1}$	619.97	$8.4660 \cdot 10^{1}$	662.35	$1.7680 \cdot 10^{2}$
537.10	$1.4201 \cdot 10^{1}$	620.57	$8.5622 \cdot 10^{1}$	666.82	$1.9012 \cdot 10^{2}$
540.92	$1.5604 \cdot 10^{1}$	624.95	$9.3023 \cdot 10^{1}$	677.05	$2.2335 \cdot 10^{2}$
544.75	$1.7141 \cdot 10^{1}$	625.06	$9.3022 \cdot 10^{1}$	679.94	$2.3255 \cdot 10^{2}$
548.61	$1.8805 \cdot 10^{1}$	627.66	$9.7609 \cdot 10^{1}$	683.43	$2.4629 \cdot 10^{2}$
556.53	$2.2641 \cdot 10^{1}$	628.79	$9.9700 \cdot 10^{1}$	689.93	$2.7159 \cdot 10^{2}$
565.97	$2.8103 \cdot 10^{1}$	630.13	$1.0205 \cdot 10^{2}$	692.87	$2.8342 \cdot 10^{2}$
571.23	$3.1592 \cdot 10^{1}$	630.54	$1.0256 \cdot 10^{2}$	699.29	$3.1121 \cdot 10^{2}$
577.63	$3.6429 \cdot 10^{1}$	633.86	$1.0892 \cdot 10^{2}$	706.78	$3.4653 \cdot 10^{2}$
583.62	$4.1294 \cdot 10^{1}$	635.24	$1.1151 \cdot 10^{2}$	707.47	$3.4988 \cdot 10^{2}$
587.20	$4.4652 \cdot 10^{1}$	638.43	$1.1809 \cdot 10^{2}$		
599.51	$5.7186 \cdot 10^{1}$	641.34	$1.2434 \cdot 10^{2}$		

Data from Millar [71]

T, K	p, kPa	T, K	p, kPa
468.30	1.960	575.33	$3.449 \cdot 10^{1}$
518.02	8.319	613.04	$7.475 \cdot 10^{1}$
571.93	$3.264 \cdot 10^{1}$	613.94	$7.605 \cdot 10^{1}$

Data from Morley [72]

T, K	p, kPa	T, K	p, kPa
289.14	$1.33 \cdot 10^{-4}$	323.13	$1.51 \cdot 10^{-3}$
303.13	$3.60 \cdot 10^{-4}$	333.12	$2.85 \cdot 10^{-3}$
313.13	$6.93 \cdot 10^{-4}$	343.12	$5.39 \cdot 10^{-3}$

Data from Murgulescu and Topor [73]

T, K	p, kPa	T, K	p, kPa
465.65	1.91	532.17	$1.27 \cdot 10^{1}$
476.15	2.57	546.58	$1.808 \cdot 10^{1}$
485.16	3.36	549.58	$1.933 \cdot 10^{1}$
494.16	4.44	559.18	$2.438 \cdot 10^{1}$
507.57	6.63		

Data from Neumann and Völker [74]

T, K	p, kPa	T, K	p, kPa
343.82	$6.881 \cdot 10^{-3}$	311.98	$7.32 \cdot 10^{-4}$
338.82	$5.005 \cdot 10^{-3}$	309.13	$6.03 \cdot 10^{-4}$
335.62	$3.956 \cdot 10^{-3}$	306.33	$4.91 \cdot 10^{-4}$
334.02	$3.557 \cdot 10^{-3}$	305.63	$4.57 \cdot 10^{-4}$
329.38	$2.597 \cdot 10^{-3}$	300.38	$2.99 \cdot 10^{-4}$
325.33	$1.964 \cdot 10^{-3}$	297.79	$2.56 \cdot 10^{-4}$
321.23	$1.448 \cdot 10^{-3}$	296.39	$1.96 \cdot 10^{-4}$
319.53	$1.31 \cdot 10^{-3}$	294.04	$1.79 \cdot 10^{-4}$
316.93	$1.09 \cdot 10^{-3}$	289.54	$1.20 \cdot 10^{-4}$
314.08	$8.84 \cdot 10^{-4}$		

Data from Pedder and Barratt [75]

T, K	p, kPa
556.68	22.49
557.18	22.61
573.18	33.13

Data from Pfaundler [76]

T, K	p, kPa
288.14	$1.080 \cdot 10^{-4}$
329.43	$2.401 \cdot 10^{-3}$
371.92	$3.507 \cdot 10^{-2}$

Data from Poindexter [77]

T, K	p, kPa	T, K	p, kPa
235.34	$1.84 \cdot 10^{-7}$	267.44	$1.34 \cdot 10^{-5}$
240.44	$3.63 \cdot 10^{-7}$	269.17	$1.65 \cdot 10^{-5}$
242.20	$4.95 \cdot 10^{-7}$	273.36	$2.52 \cdot 10^{-5}$
245.03	$7.60 \cdot 10^{-7}$	274.91	$2.92 \cdot 10^{-5}$
250.43	$1.56 \cdot 10^{-6}$	281.13	$5.76 \cdot 10^{-5}$
252.60	$2.34 \cdot 10^{-6}$	284.00	$7.71 \cdot 10^{-5}$
255.94	$3.28 \cdot 10^{-6}$	286.18	$9.61 \cdot 10^{-5}$
261.16	$6.95 \cdot 10^{-6}$	292.87	$1.61 \cdot 10^{-4}$
262.35	$7.86 \cdot 10^{-6}$		
193.58*	$4.00 \cdot 10^{-10}$	216.31*	$6.91 \cdot 10^{-9}$
203.25*	$8.00 \cdot 10^{-10}$	223.30*	$3.16 \cdot 10^{-8}$
206.30*	$5.33 \cdot 10^{-9}$	229.75*	$9.75 \cdot 10^{-8}$
209.47*	$1.69 \cdot 10^{-9}$	230.38*	$1.00 \cdot 10^{-7}$
215.43*	$6.47 \cdot 10^{-9}$	231.39*	$1.14 \cdot 10^{-7}$

* Point below triple point, not included in analysis.

Data from Ramsay and Young [36]

T, K	p, kPa	T, K	p, kPa	T, K	p, kPa
495.31	4.59	630.67	$1.0244 \cdot 10^{2}$	631.87	$1.0106 \cdot 10^{2}$
543.98	$1.6579 \cdot 10^{1}$	630.67	$1.0223 \cdot 10^{2}$	720.46	$3.8622 \cdot 10^{2}$
553.38	$2.0952 \cdot 10^{1}$	632.46	$1.0240 \cdot 10^{2}$	721.46	$3.8723 \cdot 10^{2}$
631.65	$1.0260 \cdot 10^{2}$	632.46	$1.0214 \cdot 10^{2}$		
631.65	$1.0269 \cdot 10^{2}$	631.87	$1.0181 \cdot 10^{2}$		

Data from Regnault [33]

T, K	p, kPa	T, K	p, kPa	T, K	p, kPa
296.71	$9.07 \cdot 10^{-3}$	473.65	2.934	627.79	$1.0109 \cdot 10^{2}$
311.14	$1.31 \cdot 10^{-2}$	631.66	$1.022 \cdot 10^{2}$	686.34	$2.0393 \cdot 10^{2}$
373.72	$7.40 \cdot 10^{-2}$	524.25	9.88	701.77	$3.5813 \cdot 10^{2}$
298.52	$4.53 \cdot 10^{-3}$	525.77	$1.04 \cdot 10^{1}$	717.51	$4.2405 \cdot 10^{2}$
322.28	$1.16 \cdot 10^{-2}$	528.62	$1.13 \cdot 10^{1}$	749.24	$6.1513 \cdot 10^{2}$
345.86	$2.44 \cdot 10^{-2}$	570.39	$3.1781 \cdot 10^{1}$	785.22	$9.7548 \cdot 10^{2}$
373.23	$5.43 \cdot 10^{-2}$	587.25	$4.6103 \cdot 10^{1}$	782.08	$9.3193 \cdot 10^{2}$
373.72	$7.47 \cdot 10^{-2}$	604.79	$6.4836 \cdot 10^{1}$	773.42	$7.9543 \cdot 10^{2}$
419.43	$4.61 \cdot 10^{-1}$	618.08	$8.3313 \cdot 10^{1}$	627.79	$1.0109 \cdot 10^{2}$
451.04	1.429	628.02	$1.0157 \cdot 10^{2}$		

Data from Rodebush and Dixon [79]

T, K	p, kPa	T, K	p, kPa
443.54	$8.39 \cdot 10^{-1}$	462.75	1.644
451.24	1.11	470.35	2.104
453.25	1.17	475.95	2.520
457.05	1.351		

Data from Roeder and Morawietz [80]

T, K	p, kPa	T, K	p, kPa
413.13	$2.433 \cdot 10^{-1}$	523.17	9.930
433.14	$5.466 \cdot 10^{-1}$	563.18	$2.646 \cdot 10^{1}$
453.15	1.187	613.19	$7.363 \cdot 10^{1}$
483.16	3.160		

Data from Ruff and Bergdahl [81]

T, K	p, kPa	T, K	p, kPa	T, K	p, kPa
478.15	1.6	573.18	$2.91 \cdot 10^{1}$	625.19	$1.01 \cdot 10^{2}$
508.17	4.3	583.18	$4.23 \cdot 10^{1}$	630.19	$1.01 \cdot 10^{2}$
513.17	4.7	597.19	$5.04 \cdot 10^{1}$		
533.17	$1.2 \cdot 10^{1}$	615.19	$6.87 \cdot 10^{1}$		
543.18	$1.3 \cdot 10^{1}$	628.19	$1.00 \cdot 10^{2}$		

Data from Schmahl, Barthel and Kaloff [82]

T, K	p, kPa	T, K	p, kPa	T, K	p, kPa
446.64	$9.3 \cdot 10^{-1}$	519.17	8.92	617.69	$8.121 \cdot 10^{1}$
449.64	1.0	529.17	$1.15 \cdot 10^{1}$	621.19	$8.765 \cdot 10^{1}$
478.15	2.72	531.67	$1.25 \cdot 10^{1}$	628.19	$9.806 \cdot 10^{1}$
479.66	2.84	540.68	$1.540 \cdot 10^{1}$	629.69	$1.010 \cdot 10^{2}$
482.16	3.04	549.68	$1.919 \cdot 10^{1}$	637.18	$1.148 \cdot 10^{2}$
487.66	3.60	551.68	$2.034 \cdot 10^{1}$	639.68	$1.211 \cdot 10^{2}$
492.66	4.23	562.68	$2.604 \cdot 10^{1}$	412.43	$2.37 \cdot 10^{-1}$
493.66	4.36	572.68	$3.260 \cdot 10^{1}$	415.33	$2.69 \cdot 10^{-1}$
498.66	4.99	574.18	$3.350 \cdot 10^{1}$	420.43	$3.32 \cdot 10^{-1}$
498.66	5.07	579.18	$3.746 \cdot 10^{1}$	425.64	$4.15 \cdot 10^{-1}$
499.16	5.13	582.68	$4.041 \cdot 10^{1}$	430.64	$5.03 \cdot 10^{-1}$
504.16	5.84	596.19	$5.313 \cdot 10^{1}$	435.54	$6.03 \cdot 10^{-1}$
507.17	6.36	606.19	$6.467 \cdot 10^{1}$	438.64	$6.81 \cdot 10^{-1}$
509.67	6.97	609.19	$6.819 \cdot 10^{1}$		
510.67	6.97	616.69	$7.923 \cdot 10^{1}$		

Data from Schneider and Schupp [83]

T, K	p, kPa	T, K	p, kPa	T, K	p, kPa
539.68	$1.484 \cdot 10^{1}$	500.16	5.31	550.18	$1.943 \cdot 10^{1}$
519.17	8.00	491.16	4.00	552.18	$2.038 \cdot 10^{1}$
519.17	7.93	484.16	2.95	553.18	$2.024 \cdot 10^{1}$
518.17	7.88	523.17	$1.01 \cdot 10^{1}$	554.18	$2.190 \cdot 10^{1}$
521.67	9.05	501.16	5.37	545.18	$1.727 \cdot 10^{1}$
519.17	8.81	502.16	5.21	563.18	$2.686 \cdot 10^{1}$
519.67	9.67	502.16	5.07	550.18	$1.933 \cdot 10^{1}$
575.18	$3.468 \cdot 10^{1}$	551.18	$1.993 \cdot 10^{1}$		

Data from Schönherr and Hensel [84]

T, K	p, kPa	T, K	p, kPa	T, K	p, kPa
1051.44	90	1581.99	991	1716.40	1490
1186.24	200	1632.52	1155	1726.05	1535
1322.14	382	1665.97	1275	1735.51	1575
1424.66	571	1686.68	1345		
1510.37	782	1704.76	1430		

Data from Scott [85]

T, K	p, kPa
293.14	$1.73 \cdot 10^{-4}$

Data from Shpil'rain and Nikanorov [86]

T, K	p, kPa	T, K	p, kPa	T, K	p, kPa
554.11	$2.152 \cdot 10^{1}$	635.61	$1.123 \cdot 10^{2}$	786.77	$9.6252 \cdot 10^{2}$
560.61	$2.505 \cdot 10^{1}$	639.81	$1.210 \cdot 10^{2}$	796.86	$1.0798 \cdot 10^{3}$
567.11	$2.893 \cdot 10^{1}$	642.11	$1.257 \cdot 10^{2}$	814.46	$1.3057 \cdot 10^{3}$
578.91	$3.740 \cdot 10^{1}$	643.81	$1.293 \cdot 10^{2}$	836.25	$1.63551 \cdot 10^{3}$
600.61	$5.854 \cdot 10^{1}$	664.30	$1.8254 \cdot 10^{2}$	803.66	$1.16117 \cdot 10^{3}$
604.11	$6.261 \cdot 10^{1}$	707.29	$3.4921 \cdot 10^{2}$	815.46	$1.31973 \cdot 10^{3}$
621.11	$8.635 \cdot 10^{1}$	742.78	$5.6147 \cdot 10^{2}$	822.45	$1.42302 \cdot 10^{3}$
622.21	$8.811 \cdot 10^{1}$	755.98	$6.6372 \cdot 10^{2}$	831.85	$1.56996 \cdot 10^{3}$
623.71	$9.038 \cdot 10^{1}$	774.67	$8.3905 \cdot 10^{2}$	845.39	$1.79551 \cdot 10^{3}$
626.81	$9.547 \cdot 10^{1}$	648.01	$1.3862 \cdot 10^{2}$	847.24	$1.82505 \cdot 10^{3}$
629.41	$1.002 \cdot 10^{2}$	677.30	$2.2531 \cdot 10^{2}$	854.54	$1.96728 \cdot 10^{3}$
635.21	$1.117 \cdot 10^{2}$	681.50	$2.3779 \cdot 10^{2}$	856.44	$1.99968 \cdot 10^{3}$
643.31	$1.279 \cdot 10^{2}$	694.70	$2.9070 \cdot 10^{2}$	866.64	$2.21186 \cdot 10^{3}$
619.71	$8.419 \cdot 10^{1}$	724.09	$4.4107 \cdot 10^{2}$	880.43	$2.51478 \cdot 10^{3}$
628.11	$9.815 \cdot 10^{1}$	732.39	$4.9111 \cdot 10^{2}$	882.13	$2.55352 \cdot 10^{3}$
628.31	$9.889 \cdot 10^{1}$	752.68	$6.3837 \cdot 10^{2}$	883.23	$2.57295 \cdot 10^{3}$
630.91	$1.034 \cdot 10^{2}$	774.57	$8.3449 \cdot 10^{2}$		

Data from Spedding and Dye [87]

T, K	p, kPa	T, K	p, kPa	T, K	p, kPa
533.825	$1.306 \cdot 10^{1}$	573.610	$3.3293 \cdot 10^{1}$	613.886	$7.5568 \cdot 10^{1}$
549.811	$1.9337 \cdot 10^{1}$	586.013	$4.3390 \cdot 10^{1}$	620.254	$8.5144 \cdot 10^{1}$
558.948	$2.3954 \cdot 10^{1}$	594.741	$5.1918 \cdot 10^{1}$	630.244	$1.0222 \cdot 10^{2}$
564.721	$2.7351 \cdot 10^{1}$	597.253	$5.4588 \cdot 10^{1}$		
565.743	$2.7964 \cdot 10^{1}$	604.288	$6.2792 \cdot 10^{1}$		

Data from Stock and Zimmermann [88]

T, K	p, kPa
283.14	$7.33 \cdot 10^{-5}$
273.15	$2.39 \cdot 10^{-5}$
253.17	$4.40 \cdot 10^{-6}$
213.19*	$6.53 \cdot 10^{-7}$

* Point below triple point, not included in analysis.

Data from Sugawara, Sato, and Minamiyama [9]

T, K	p, kPa	T, K	p, kPa	T, K	p, kPa
601.67	$6.0389 \cdot 10^{1}$	735.22	$5.2093 \cdot 10^{2}$	873.15	$2.3650 \cdot 10^{3}$
630.83	$1.0258 \cdot 10^{2}$	768.75	$7.9022 \cdot 10^{2}$	892.71	$2.8647 \cdot 10^{3}$
664.10	$1.8162 \cdot 10^{2}$	795.55	$1.0710 \cdot 10^{3}$	918.61	$3.5883 \cdot 10^{3}$
683.99	$2.4860 \cdot 10^{2}$	824.15	$1.4651 \cdot 10^{3}$	929.62	$3.8828 \cdot 10^{3}$
705.03	$3.3804 \cdot 10^{2}$	853.24	$1.9858 \cdot 10^{3}$		

Data from van der Plaats [89]

T, K	p, kPa	T, K	p, kPa	T, K	p, kPa
273.15	$6.27 \cdot 10^{-4}$	287.14	$1.32 \cdot 10^{-3}$	289.14	$1.53 \cdot 10^{-3}$
283.14	$1.07 \cdot 10^{-3}$	280.15	$9.47 \cdot 10^{-4}$	286.14	$1.33 \cdot 10^{-3}$
287.14	$1.33 \cdot 10^{-3}$	283.14	$1.06 \cdot 10^{-3}$	286.14	$1.25 \cdot 10^{-3}$
285.14	$1.35 \cdot 10^{-3}$	283.14	$1.12 \cdot 10^{-3}$	287.14	$1.35 \cdot 10^{-3}$
291.14	$1.77 \cdot 10^{-3}$	273.15	$6.40 \cdot 10^{-4}$		
273.15	$5.60 \cdot 10^{-4}$	292.14	$1.72 \cdot 10^{-3}$		
277.15	$7.73 \cdot 10^{-4}$	273.15	$5.87 \cdot 10^{-4}$		
282.14	$9.73 \cdot 10^{-4}$	284.14	$1.11 \cdot 10^{-3}$		
283.14	$1.03 \cdot 10^{-3}$	354.12	$1.49 \cdot 10^{-2}$		
273.15	$6.87 \cdot 10^{-4}$	358.12	$1.66 \cdot 10^{-2}$		
293.14	$1.77 \cdot 10^{-3}$	285.14	$7.73 \cdot 10^{-4}$		

Data from Villiers [90]

T, K	p, kPa	T, K	p, kPa	T, K	p, kPa
333.12	$3.47 \cdot 10^{-3}$	373.12	$4.00 \cdot 10^{-2}$	365.12	$2.55 \cdot 10^{-2}$
341.12	$5.73 \cdot 10^{-3}$	333.12	$3.67 \cdot 10^{-3}$	373.12	$4.01 \cdot 10^{-2}$
349.12	$1.01 \cdot 10^{-2}$	341.12	$5.87 \cdot 10^{-3}$		
357.12	$1.64 \cdot 10^{-2}$	349.12	$1.03 \cdot 10^{-2}$		
365.12	$2.57 \cdot 10^{-2}$	357.12	$1.64 \cdot 10^{-2}$		

Data from Volmer and Kirchhoff [91]

T, K	p, kPa	T, K	p, kPa
312.93	$8.293 \cdot 10^{-4}$	308.63	$5.934 \cdot 10^{-4}$
312.93	$8.175 \cdot 10^{-4}$	308.63	$5.990 \cdot 10^{-4}$
303.33	$4.048 \cdot 10^{-4}$	308.63	$6.000 \cdot 10^{-4}$
303.33	$3.957 \cdot 10^{-4}$	312.93	$8.257 \cdot 10^{-4}$
303.33	$3.960 \cdot 10^{-4}$	312.93	$8.211 \cdot 10^{-4}$

Data from von Halban [92]

T, K	p, kPa
255.16	$3.76 \cdot 10^{-6}$
219.79*	$3.31 \cdot 10^{-8}$

* Point below triple point, not included in analysis.

Data from Young [93]

T, K	p, kPa	T, K	p, kPa	T, K	p, kPa
456.95	1.33	495.31	4.59	629.95	$1.013 \cdot 10^{2}$
456.85	1.31	510.12	6.91	716.60	$3.862 \cdot 10^{2}$
510.07	6.913	543.48	$1.658 \cdot 10^{1}$	717.60	$3.872 \cdot 10^{2}$
456.90	1.32	553.38	$2.095 \cdot 10^{1}$		

Appendix B. Detailed Listing of Supplemental Experimental Data for the Heat Capacity of Mercury

All temperatures have been converted to ITS-90. Data are arranged alphabetically by first author.

Smoothed data from Amitin, Lebedeva and Paukov [123]

T, K	C_p, J/(mol·K)	T, K	C_p, J/(mol·K)
234.3375	28.543	289.9958	27.987
240.0066	28.473	298.1437	27.911
250.0049	28.359	299.9932	27.899
260.0029	28.255		
270.0007	28.162		
273.1500	28.134		
279.9984	28.076		

Smoothed data from Busey and Giauque [44]

T, K	C_p, J/(mol·K)	T, K	C_p, J/(mol·K)
234.3206	28.476	349.9729*	27.606
240.0264	28.430	399.9785	27.359
250.0185	28.351	449.9942	27.204
260.0103	28.275	500.0132	27.129
270.0024	28.196	550.028	27.117

		9	
279.9953	28.121	600.0361	27.146
289.9893	28.041	650.0326	27.217
298.1452	27.983	700.0199	27.338
299.9843	27.966	750.0049	27.514

* Note: Maximum temperature of their measurements was 330 K; values at higher temperatures are based on measurements in the literature.

Smoothed data from Douglas et al. [51]

T, K	C_p, J/(mol·K)	T, K	C_p, J/(mol·K)
234.3006	28.275	513.1679	27.158
253.166	28.147	533.1743	27.141
273.15	28.019	553.1796	27.132
293.1376	27.900	573.1835	27.130
298.1352	27.872	593.1858	27.137
313.1293	27.790	613.1863	27.150
333.1245	27.688	629.7653	27.167
353.1229	27.595	633.185	27.171
373.1238	27.511	653.182	27.198
393.127	27.435	673.1776	27.232
413.1319	27.368	693.172	27.274
433.1382	27.309	713.1658	27.321
453.1454	27.259	733.1596	27.374
473.153	27.217	753.1541	27.433
493.1607	27.183	773.1501	27.499

APPENDIX B

DATA SHEETS FOR ELEMENTAL MERCURY GENERATORS

DEVICE NAME Mercury Calibrator MC-3000

MANUFACTURER

Mercury Instruments GmbH
Liebigstrasse 11 b
85757 Karlsfeld / Germany
08131 / 505720
www.mercury-instruments.com

U.S. CEM Representative:
Ducon Technologies, Inc.
19 Engineers Lane
Farmingdale, NY 11735
631-694-1700
www.ducon.com

U.S. Instrument Representative:
ST2 Service Technologies
8550 West Ken Caryl Ave
Littleton, CO 80128
303-972-3740
www.st2-service.com

OUTPUT RANGE

Concentration	10 – 1,000 ug/m^3 (newly designed units will provide lower concentrations)
Flow Rate	1 – 9 L / min

EQUILBRATION CHAMBER GAS Air at 1-50 mL/min

DILUENT GAS Air at 0-10 L/min

PRINCIPAL OF OPERATON

Saturated elemental mercury in dry air is generated in a chamber containing 15 mL (200g) of elemental mercury at 40 ºC. This mercury in air mixture is then transferred to a cooler equilibrium chamber using air flow from a digital mass flow controller, to condense the excess mercury. Equilibration chamber temperature is controlled near ambient using a Peltier thermoelectric device. Temperature sensor accuracy is 0.1 ºC. The saturated air exiting the equilibrium chamber is diluted to the desired concentration with dry diluent air using a second mass flow controller.

FEATURES

The calibrator operates as a stand-alone unit, and it can be connected directly to a printer to document settings. Air can be provided by an available air compressor or tank. Wetted parts are borosilicate glass, perfluoroalkoxy polymer (PFA), polytetrafluoroethylene (PTFE), and Tygon R3603.

DEVICE NAME Model MGS-1 Elemental Mercury Calibration Unit

MANUFACTURER

Koji Tanida
Nippon Instruments Corporation
4-14-4, Sendagaya, Shibuya-ku
Tokyo, Japan 151-0051
+81-3-3479-6014

Dave Vojtko
Horiba Instruments, Inc.
1002 Harvest Court
Moon Township, PA 15108
724-457-2424
www.horiba.com

OUTPUT RANGE

Concentration	3 - 150 ug/m^3
Flow Rate	2-10 L / min

EQUILBRATION CHAMBER GAS Ultra pure nitrogen at 0.25 – 1 mL/min

DILUENT GAS Air at 2-10 L/min

PRINCIPAL OF OPERATON

Elemental mercury is in contact with air in an enclosed heated equilibration chamber at 50 - 60 ºC. Digital mass flow controllers are used to control the equilibrium chamber and diluent air flows. The air pressure to the equilibrium chamber mass flow controller is maintained at 0.05 MPa.

FEATURES

All wetted components are made of materials inert to mercury. The air is provided by an on-board air pump. The unit can be operated manually or in an automated mode, which allows automated multi-point calibration.

DEVICE NAME PSA Model 10.534 Mercury Calibration System - Cav Kit

MANUFACTURER

P S Analytical
1761 W. Hillsboro Blvd., Suite 318
Deerfield Beach, FL USA 33442
954-429-1577
www.psanalytical.com

Main Headquarters in UK:
P S Analytical
Arthur House
Crayfields Industrial Estate
Main Road, Orpington
Kent BR5 3HP England
+44 (0) 1689 891211

OUTPUT RANGE

Concentration	0.5 – 90,800 ug/m^3
Flow Rate	1 – 30 L / min

EQUILBRATION CHAMBER GAS Nitrogen or Air at 0 – 30 mL/min

DILUENT GAS Nitrogen or Air at 0 – 30 L/min

PRINCIPAL OF OPERATON

The equilibration chamber has 1 mL of mercury (13.5 g) immobilized on a proprietary sorbent bed of high surface area. The equilibration chamber temperature is controlled above ambient at 30 - 150 ºC using an oven. Flow of nitrogen or dry air through the chamber is controlled by a digital mass flow controller. The nitrogen or dry air exiting the chamber is saturated with mercury vapor, and this stream is diluted with nitrogen or dry air into the concentration range of interest. Output concentration is controlled by setting the flow rates.

FEATURES

The calibrator can be operated as a stand-alone unit. The unit also generates a mercury-free zero flow so that blank measurements can be performed. The digital mass flow controllers are certified at 20 ºC and 1 atm. Wetted components are perfluoroalkoxy polymer (PFA) and polytetrafluoroethylene (PTFE).

DEVICE NAME Model 3310 Elemental Mercury Calibration Unit

MANUFACTURER

Tekran Instrument Corporation
330 Nantucket Blvd.
Toronto, Canada M1P 2P4
1-888-383-5726 or 1-416-449-3084
A subsidiary of TSI, Inc., Shoreview, MN, USA
www.tekran.com

OUTPUT RANGE	Concentration	0.5 - 1,900 ug/m^3
	Flow Rate	2 - 30 L / min
EQUILBRATION CHAMBER GAS	Air at 3 – 50 sccm	
DILUENT GAS	Air at 2 – 30 slpm	

PRINCIPAL OF OPERATON

Elemental mercury is bound to a substrate that is enclosed in an equilibration chamber. The equilibrium chamber is temperature controlled from 5 - 45 ºC using a Peltier thermoelectric device. Chamber temperature is normally kept fixed as close to ambient as possible, and concentrations are mainly controlled by adjusting flow rates. Flow of dry air through the chamber is controlled by a precision mass flow controller. Absolute chamber pressure is continuously monitored, and the air flow is and continuously adjusted to provide a constant volumetric flow. The air exiting the chamber is saturated with mercury vapor to the chamber temperature. This stream is diluted with dry air in a heated environment to prevent condensation. The diluent air flow is provided using a digital mass flow controller. The flow from each mass flow controller is fed through a precision pressure regulator to eliminate flow fluctuation due to line pressure variations. The mass flow controllers are mounted on a heated, temperature controlled surface to eliminate thermal drift.

FEATURES

All wetted components are made of materials inert to mercury. The equilibrium chamber temperature sensor is calibrated using a NIST traceable temperature probe. The mass flow controllers are calibrated using NIST traceable flow standards at multiple points. Linear interpolation is used between calibration points. The pressure transducer is calibrated using a NIST traceable absolute pressure gauge. Output is calculated from first principles and shown in micrograms per standard cubic meter (0 ºC, 760 mm Hg). It may also be displayed under other conditions (e.g. 20 ºC, 760 mm Hg). Allowable ambient temperature is 5 – 40 ºC. Equilibrium chamber temperature accuracy is ±0.05 ºC. The init is fully remote controlled, allowing automated multi-point calibration or standard addition sequences.

DEVICE NAME Model 81i Hg Calibrator

MANUFACTURER

Thermo Electron Corporation
Environmental Instruments
27 Forge Parkway
Franklin, MA 02038
508-553-6939
www.thermo.com

OUTPUT RANGE	Concentration	3 - 50 ug/m^3
	Flow Rate	1 - 20 L/min
EQUILBRATION CHAMBER GAS	Air at 1-50 cc/min	
DILUENT GAS	Air at 1-20 L/min	

PRINCIPAL OF OPERATON

An equilibration chamber contains a bed of packed stationary phase with about 1g of immobilized mercury. The equilibration chamber temperature is controlled from 0-15 ºC using a Peltier thermoelectric device. Flow of dry air (with carbon prefilter) through the equilibration chamber is controlled by a digital mass flow controller. The air exiting the chamber is saturated with mercury vapor at the chamber temperature. Diluent dry air flow is provided using a digital mass flow controller.

FEATURES

The calibrator unit is based on the new Thermo i-Series gas analyzer platform. It also can be operated as a stand-alone unit. Wetted components are perfluoroalkoxy polymer (PFA) and polytetrafluoroethylene (PTFE).

APPENDIX C
WRI VISITIING SCIENTIST AT NIST REPORT

This is the Bill Dorko / Joe Rovani edited copy

Performance of Elemental Mercury Generators

[a]Joseph Rovani and [b]William Dorko
[a]Lead Scientist, WRI, Laramie, WY
EPRI-Sponsored Guest Researcher for the
Gas Metrology Group, NIST, Gaithersburg, MD
[b]Research Chemist, Gas Metrology Group, NIST

August 1 - September 22, 2006
EPRI Contract No. EP-P22203/C10861

Executive Summary

Elemental mercury (Hg°) vapor generators from five different manufacturers and one Hg° analyzer (detector) were evaluated at NIST, Gaithersburg, MD under EPRI sponsorship during August and September, 2006. The generators were examined for design features, and an assessment of their working characteristics was performed. The generators were then configured in a dedicated laboratory workstation to evaluate their Hg° vapor output. When comprehensive data sets revealed significant variability, the analyzer was examined and modified to provide more stable results. Experiments were performed to establish the ability to compare one generator with another over a generator output concentration range from 3 to 75 µg/m^3. The within-day and between-day variability in these measurements are described and discussed. The work described in this report is only a part of a larger comprehensive project underway at NIST. This report describes activities and results for only the units tested. This last statement is included to indicate that the data generated and described is for specific instruments; continual modifications to generators and analyzers are being made at factories to improve their performance. Some of the "improvements" are being driven because of feedback from NIST and EPA from work funded by EPA and EPRI. A comprehensive report including these activities is being prepared by NIST to provide EPA with the information needed for preparation of a Hg° traceability protocol.

1. Mercury Generators and Analyzer

Mercury generators from five manufacturers were examined for design, flow, and operational characteristics. Gas flow rates for the units were checked with a Bios DryCal ML-800 (serial # 107537) flow calibrator owned by NIST. For the initial assessments, the flow results of the ML-800 calibrator were volumetric, i.e., based on ambient laboratory temperature and atmospheric pressure.

A summary description of the assessment for each of the units is provided below.

Mercury Instruments MC-3000 Generator

The MC-3000 is manufactured in Germany. The specific unit examined is serial # 1005/006MC and is on loan from Mercury Instruments to WRI.

The design feature that makes this unit unique is that, in addition to the Hg saturation chamber maintained at 40°C, there is a subsequent Hg condensation chamber at near-ambient temperature. Both chambers are glass and contain a combined amount of 200 g liquid elemental Hg. The condensation chamber temperature, measured by a Pt-100 temperature sensor, is the temperature that is used for the Hg concentration calculation.

The flow characteristics of this unit are an air inlet operated at 15-30 psi, a mass flow controller #1 (MFC1) Hg flow operated at 0-50 ml/min, an MFC2 dilution flow operated at 0-10 l/min, and a fritted glass mixing chamber. Silicone and/or Tygon tubing is used in the unit, and many of the hose clamps associated with the multiple tubing transitions required additional tightening. The open/close valve arrangement located at the front of the unit exhibited pinched tubing. The leaks and restrictions identified were repaired without altering the design of the flow paths.

The routine operation of the unit is user-defined Hg vapor concentration input via keypad and digital display. The working range of the current unit at a Hg condensation temperature of 22°C is 9-78 μg/m³. Mercury Instruments plans to modify future units to achieve lower concentrations. The unit's output concentration is referenced to 21°C and 760 mm Hg (according to previous correspondence between NIST and the manufacturer). With the valve in the closed position, so that the entire flow could be measured at the vent at the rear of the instrument, the following flow checks were obtained:

[Hg vapor]	MFC1, ml/min	MFC2, l/min	ML-800, total l/min
9 μg/m³	5.1	9.0	9.264
45 μg/m³	25.7	9.0	9.280
78 μg/m³	44.8	9.0	9.301

For routine operation of the unit, only MFC1 flows are changed.

With the valve at the front of the unit in the open position, the gas flow is split between the Hg calibration gas port in the front, and the vent in the rear. The flows at both ports were measured in duplicate for the 9 μg/m³ experiment. The results are as follows:

[Hg vapor]	Hg Cal (front), l/min	Vent (back), l/min	Combined, l/min
9 μg/m³	2.803, 2.880	4.376, 4.144	7.179, 7.024

The ~25% discrepancy between the total flow in the closed position and the combined flow in the open position may indicate a leak or other undetermined flow mechanism in the open valve configuration. The output of this unit had previously been evaluated by NIST to be biased with regard to set point, i.e., the measured output was higher than was calculated from the set

points. The inability to match up total flow with the sum of individual flows might be the explanation for this bias.

Nippon MGS-1E Generator

The MGS-1E is manufactured in Japan. The specific unit examined has no serial number, and is on loan to WRI from Nippon/Horiba. A label was affixed to the outside rear of the unit identifying that it was "Evaluated At NIST" so that this specific unit can be referenced in future work. As received, the unit produced no mercury output regardless of setting.

The design feature of the MGS-1E that distinguishes it from the other units is the use of three MFCs. MFC1 delivers an ultrapure (99.999%) nitrogen flow of 1 ml/min from a cylinder or other pressurized source past an 80 µl droplet of elemental Hg in a glass tube heated to 50°C. After saturation, MFC3 augments the nitrogen flow with an additional 10 ml/min. Finally, MFC2 delivers 0-10 l/min of air, delivered via an external pump, to a mixing tee to dilute the Hg vapor to a final concentration. The unit is designed to deliver Hg vapor concentrations of 3 to 150 µg/m³. The unit is controlled using potentiometers with a digital display.

When the flow rates of the MFCs were measured, a problem in the flow path was observed. A check valve is engineered into the nitrogen flow between MFC1 and MFC3 that is intended to prevent backflow from the high flow region of the instrument into the Hg tube. However, the check valve is an inexpensive ball and spring device that frequently stuck open or closed. The overall effect is that Hg vapor was not generated in its intended and desired flow through the unit.

Other design versions incorporating flow path changes and valve arrangements have been provided by the manufacturer in schematic diagrams. After correspondence with the manufacturer, it was recommended that the check valve be removed and replaced with a piece of ¼" PTFE tubing. After making modifications and installing new parts received from the manufacturer the unit did work and data were generated for Section 2 of this report. The unit then stopped working again (see Section 3). A second unit was sent by the manufacturer to NIST and a representative from the company was scheduled to come to NIST to evaluate the situation, but had not yet arrived before the end of the project.

PSA 10.534 Generator

The 10.534 is manufactured in England. The specific unit examined is serial # 012, and is owned by NIST.

The design of this instrument is direct and straightforward. Air from a cylinder or other pressurized source is introduced into the instrument at a minimum of 10 psi. MFC1 delivers the air at 0-20 ml/min into a PTFE tube containing a Hg°-impregnated substrate heated to 40°C. MFC2 controls the dilution air at 0-20 l/min. The flows are varied manually via potentiometers with digital display. The unit's output concentration is referenced to 20°C and 760 mm Hg (according to previous correspondence between NIST and the manufacturer). The unit's flow check results are as follows:

MFC1 Pot Setting	Digital Readout, ml/min	ML-800, ml/min
0.98	2.00	1.978
5.01	10.00	10.407
10.00	19.92	21.226

MFC2 Pot Setting	Digital Readout, ml/min	ML-800, l/min
0.45	1.00	1.006
2.44	5.00	5.191
4.44	9.00	9.305

The agreement between the digital readout and the measured flow shows that there is no major problem with the flow.

The overall simplicity of design and ease of use are positive attributes of the PSA unit.

Tekran 3310 Generator

The 3310, serial # 3007, is manufactured in Canada and is on loan from the manufacturer to NIST.

A distinguishing feature of the 3310 is that it is controlled by software on an accompanying PC which displays instrument parameters with visual flow diagrams, and allows automated sequences of calibrations to be set up and run unattended. The 3310 has an MFC1 Hg source flow of 0-50 ml/min and an MFC2 dilution flow of 0-30 l/min from a compressed air source. The MFCs are located on a heated plate to eliminate thermal drift. The Hg source is heated/cooled from 5°C to 45°C using a Peltier unit, although a temperature closer to ambient is recommended for maximum stability. The source contains two solenoid valves that are located on the heated source block to minimize Hg condensation. The 3310 has a third temperature zone, for preheating the air supply. A total of five solenoid valves determine where the various flows of air and calibration gas are delivered. The instrument is designed to be powered up continuously for equilibrium, and it has 8 operating modes including a "safe" mode when the PC is shut off.

The unit's output concentration is referenced to 0°C and 760 mm Hg (according to previous correspondence between NIST and the manufacturer). The software allows flow rates to be calculated to reference both 0°C and 20° simultaneously. Entries of source temperature, MFC1 flow, MFC2 flow, and desired concentration are parameters that are all permitted using the software.

The MFCs on this unit were previously calibrated at NIST in December 2005. The flow check results at a source temperature of 15°C, heated plate temperature of 40°C, air pre-heater temperature of 85°C, and an internal case temperature of 40°C are as follows:

[Hg vapor]	MFC1, sccm	MFC2, slm @ 0°C	MFC2, lpm @ 20°C	ML-800, l/min
2.9	10	8.00	8.59	8.582
23.9	25	9.03	9.69	9.752
71.2	25	3.02	3.25	3.331
-----	40	-----	-----	42.709 ml/min

The agreement between the digital readout and the measured flow shows that there is no major problem with the flow.

The 3310 is a complex unit with many controllable features, all performed using software. The software does require a learning curve.

Thermo 81i Generator– (Thermo 01)

The 81i, no serial #, is manufactured in the U.S by Thermo Electron Corporation (Thermo) and is on loan to WRI from Thermo. A label was affixed to the outside rear of the unit identifying that it was "Evaluated At NIST" so that this specific unit can be referenced in future work. This unit had previously been evaluated at NIST to have a linear output that was well-correlated with the set points. Then work at a later date, but before August 1, showed that in fact it had a very non-linear output. Both sets of data were good, but the performance characteristics of the unit had changed.

The 81i is designed to be configured as a component of an integrated system of Thermo units. The operation of the unit is menu-driven via keypad digital display. Air from a cylinder or other pressurized source is introduced at 30-40 psi. MFC1 delivers 0-50 sccm through a PTFE tube Hg source maintained at known temperature and pressure. MFC2 delivers 0-20 slm of dilution air. The system uses an internal network of five solenoid valves and a pump to control flow within the unit and to deliver flow to other integrated components.

The Hg source can be heated or cooled, and a temperature as close as possible to ambient is recommended for optimum stability. Routine operation, however, sets the source to 15°C. The Hg calibration gas range of the instrument at this temperature is 3-50 μg/m³. The unit's output concentration is referenced to 20°C and 760 mm Hg (according to previous correspondence between NIST and the manufacturer). The calibration gas is generated by entering the desired concentration and allowing the internal control to vary both MFC flow rates. For example, an entered concentration of 3.00 μg/m³ yielded MFC flows of 6.800 sccm and 16.176 slm. A Hg concentration of 25.0 μg/m³ yielded 26.917 sccm and 9.229 slm. A concentration of 47.0 μg/m³ yielded 46.449 sccm and 8.487 slm.

Flow checks on MFC1 were not performed because it was not initially evident how to shut off the high flow rates of MFC2. Similarly, flow checks on MFC2 include the smaller flow contribution from MFC1, which are included in the following results:

MFC2 F.S. Setting, %	Volume, l/min	slpm	ML-800, l/min
5	1.000	1.092	1.021
20	4.000	4.366	4.275
35	7.000	7.641	7.470

The unit features menu-driven software which, for non-routine operation, requires consultation of the instrument manual to learn to navigate.

Thermo 81i Generator– (Thermo 02)

Because of the inability to get Thermo 01 to work properly, a second unit, serial # 0613917136, was loaned to WRI and sent directly to NIST from the manufacturer. This unit was tested as received and most of the data that is included in this report is from this unit (see Sections 5 and 6).

Thermo 80i Analyzer

The Hg vapor analyzer (detector), serial # 0613917104, is manufactured by Thermo in the U.S. and is owned by NIST. It operates on the principle of the ultraviolet (UV) 254 nm atomic fluorescence of mercury. The detector operates in an air matrix and has a detection limit of 2 ng/m^3. The detector samples elemental mercury through a critical orifice. It is a continuous analyzer that records into memory a digital reading every minute. The internal electronics collect data from the detector for one minute and the one-minute average is stored in memory. The analyzer has a front panel signal readout that can be set for displaying values averaged over varying times from 1 to 300 seconds. The front panel readout does not affect the one minute average value that is stored.

2. Initial Hg Vapor Generation

A dedicated work station was set up in Laboratory B119 of Building 227. The work station consisted of a side by side comparison of two generator units, using a consistent vapor delivery and venting system. The analyzer was set up adjacent to the generators. When a particular generator unit was not in the process of being evaluated, it was kept powered up in standby state on a nearby laboratory bench.

Hg vapor concentrations were generated with the five units, as is, without calibrating their MFCs. The analyzer was operated using conditions established for previous work at NIST, such as a critical orifice flow of 0.35 l/min, chamber settings of 45°C and 32 torr, and a PMT setting of 663 volts. The front panel readout was set to refresh every 30 seconds and display the averaged signal for that time period. Analyzer readings were found to stabilize within 5-10 minutes of switching the Hg vapor flow from one generator to another. The analyzer results for this phase of the project were not referenced or normalized to previous NIST work, and as such, do not represent accurate concentrations. The analyzer results, however, can be used to evaluate the unit outputs in a relative sense. This work was done to try to determine properties of the generators outputs before more rigorous tests were performed.

A series of Hg vapor concentrations were generated using the units in the following order: Tekran, PSA, Mercury Instruments, Nippon, Thermo, Tekran. The Tekran, PSA, and Nippon units yielded results (Hg concentration vs. analyzer result) that were fairly consistent for a broad range of Hg concentrations. The Thermo unit yielded results that were consistent with the Tekran, PSA, and Nippon units at concentrations <15 µg/m^3, but at higher concentrations, the Thermo-01 unit only generated about ½ of its indicated concentration. This unit was subsequently replaced by generator Thermo-02. The Mercury Instruments unit yielded results that were somewhat higher across all concentrations than the Tekran, PSA, and Nippon units.

The tests were performed within a 48 hour timeframe. The Hg vapor concentration sequence used for the Tekran at the beginning of the evaluation was repeated at the end of the evaluation, to assess the overall stability of the analyzer. The 48 hour drift was calculated as follows:

$$\frac{\text{Initial Concentration} - \text{48 Hour Concentration}}{\text{Initial Concentration}}$$

The analyzer drift was -3.65%, with an RSD of 9.40%. The drift value reported is the average of nine Hg vapor concentrations generated by the Tekran. The nine values for time 0 and 48 hours are graphed in Figure 1. This assumes that all of drift is due to the Thermo 80i analyzer, and not the Tekran 3310 generator. This is a reasonable assumption since this generator has been tested at NIST several times and found to have not drifted.

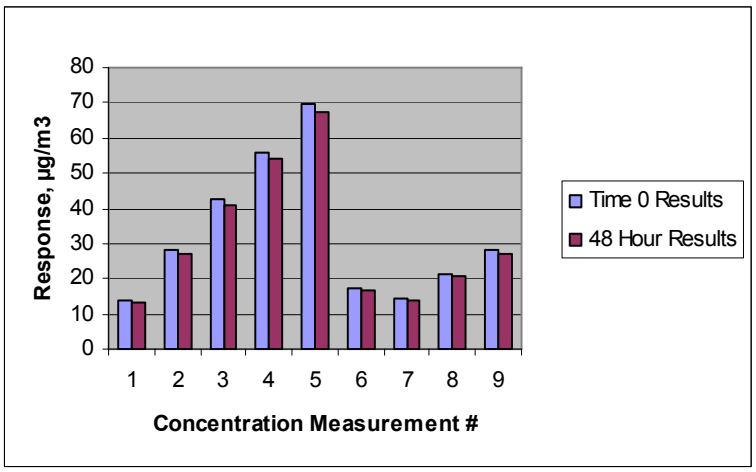

Figure 1. 48 Hour Analyzer Drift.

3. Comprehensive Hg Vapor Data

Before comprehensive data sets could be prepared, the analyzer needed to be "normalized" to NIST ICPMS data. This was performed for the Tekran and PSA generators using the precise calibration settings that were used for the ICPMS work, and comparing the 80i results to the ICPMS results. NIST has been working with these two particular units for several years, and the units have been optimized by the vendors during that time. The Tekran unit showed a -18.5% average relative difference between the analyzer and ICPMS results, as shown in Figure 2.

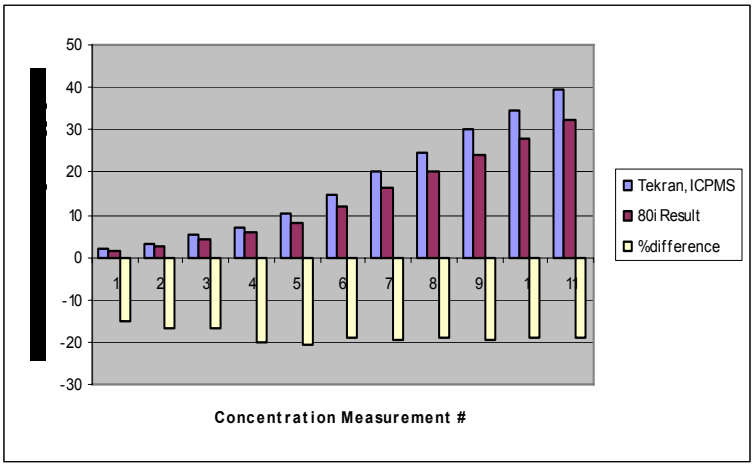

Figure 2. Difference Between Tekran and ICPMS Outputs.

The relative standard deviation for the 11 concentrations was 8.4% for concentrations that ranged from 2 - 40 μg/m^3.

The PSA unit also showed a negative offset for the analyzer, with a -16.8% average relative difference. However, the variation in the results was greater, with a relative standard deviation of 18.2%. A total of 9 concentrations from 3 to 36 μg/m^3 were used for the PSA unit. This work demonstrated that the analyzer had to be periodically calibrated with the generators. The generators are more stable in their outputs than the analyzer is in its readings.

After the normalization study, the lab bench was reorganized to accommodate four of the generators. In this configuration, the PSA and Tekran units were adjacent on the bench, the Mercury Instruments unit was placed on a small table above the PSA unit, and the Nippon unit was placed on a lab cart in front and below the PSA unit. Suitable space was allowed between the units for air circulation and cooling. The Thermo 81i (Thermo 01) was not included in the study until the new generator (Thermo 02) was received. The Tekran unit was initially excluded for the first few days, as an extended power failure at the NIST facility corrupted the communication link between the generator and its PC.

Comprehensive data set comparisons were obtained for the units using an experimental plan in which a common concentration set-point was entered for two or three of the units simultaneously. The analyzer values were recorded for each of the units serially as part of a sequence. One of the generators was chosen to bracket the beginning and end of a sequence so that "nesting" calculations could be performed. At first, the analyzer results were recorded every 5-10 minutes after the Hg output tube from a generator was switched to the analyzer delivery tee. It soon became apparent from the data that longer equilibration times, especially after changing generator settings, were required. When possible, results were obtained after an overnight equilibration.

The data collection began on August 28 with a direct comparison between the PSA and Nippon units. The Nippon unit was subsequently excluded from the study when it was found

once again, to be generating little to no Hg vapor. The unit was disassembled and the tubing, flow paths, connectors, MFCs, pump, and nitrogen source were checked. The source of the malfunction could not be identified and the service engineer was contacted. As instructed by the engineer, the Hg source inlet-side check valve was removed, but the unit still produced very little to no Hg vapor. MFC flow rates were rechecked using the NIST Bios flow calibrator, and the flows were found to be satisfactory. The unit remained un-operational for the remainder of this project, but it was subsequently replaced by the vendor at the end of September. Results with the new unit are not included in this report. It was later determined that 99.999% pure nitrogen is required for successful operation of the unit.

Closer examination of the downloaded data showed high variation for the PSA results, apparently confirming the higher %RSD value noted earlier. To help identify the source of the variation, the PSA unit was set to generate Hg vapor overnight. The data were downloaded in the morning and plotted (Figure 3).

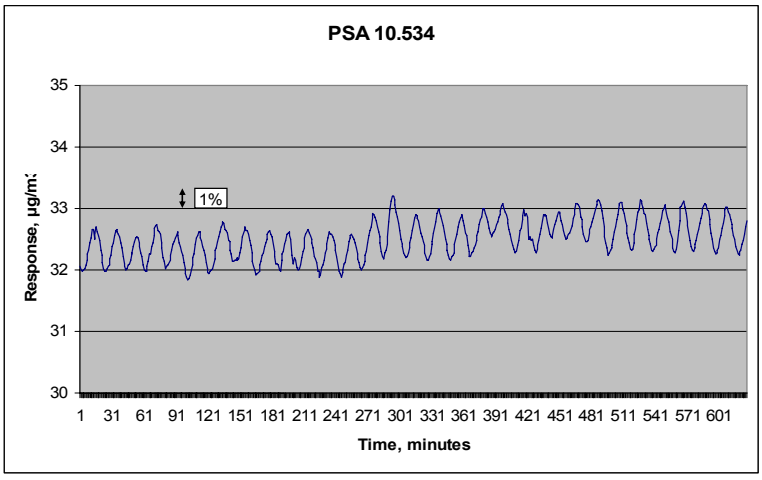

Figure 3. PSA Generator Output.

A sine-wave pattern is evident in the response profile, in which the top to bottom responses range from ~1 to 3% (note the 1% relative error bar for the y-axis response). Overnight data were then collected for the PSA unit with the source heater turned off, and with the heater set to 40°C. Although the sine-wave frequency changed, the overall effect could not be alleviated. It was determined that in order to statistically average PSA results, at least 20 minutes of data are required when using a Hg source temperature of 30°C. Since the analyzer needs 5-10 minutes to stabilize after switching the Hg exhaust tube, about 30 minutes total time is required for each individual reading for the PSA unit.

The Tekran unit was subsequently run unattended during a weekend, and the Mercury Instruments unit was run overnight. These data are plotted in Figure 4.

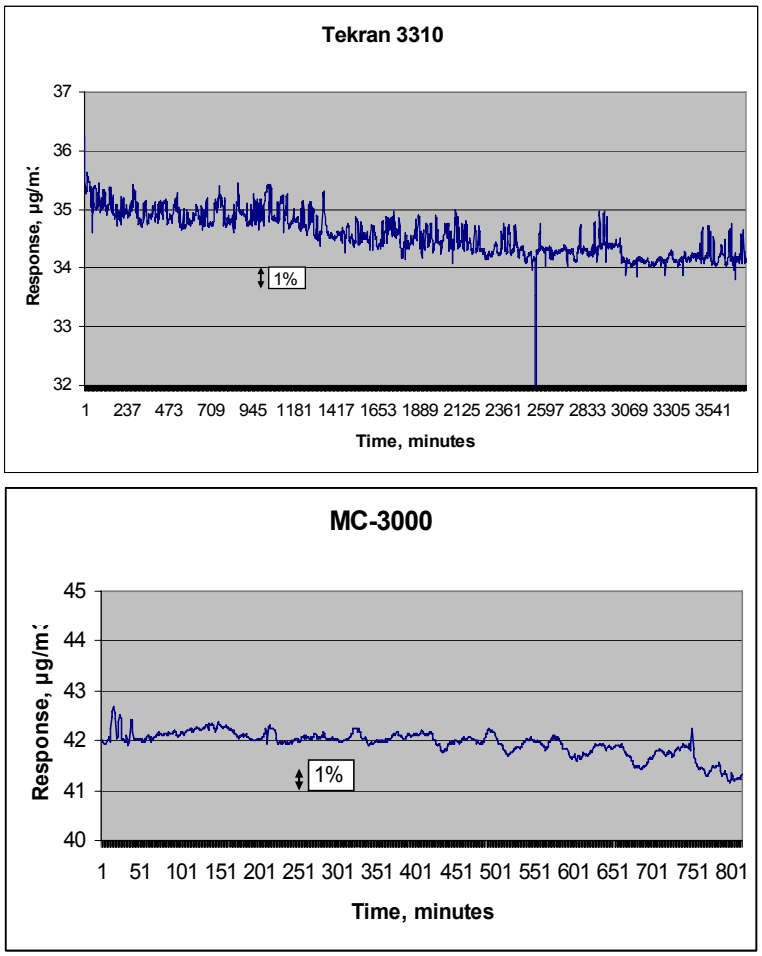

Figure 4. Tekran and Mercury Instruments Generator Outputs.

The units show unique profiles, but the variations still range from ~1 to 3%. There is a definite downward drift evident in both sets of data. The drift can be calculated many ways using 3600+ data points for the Tekran weekend run. One average calculation for the 60 hour timeframe yielded -2.8% drift. If this is assumed to be analyzer drift, it is less than the -3.65% value reported earlier. This is probably to be expected given the fact that the earlier drift calculation was for a broad range of concentrations utilizing a changing format of generator settings, while the latest calculation was for a single setting only.

4. Hg Analyzer Issues

At this point in the study, the operating characteristics of the 80i analyzer were investigated to determine how much noise and drift the detector was contributing to the data. First, the flow orifice was removed. This changed the flow in the detector from 0.35 l/min to 0.66 l/min, which increased the analyzer response. The response characteristics using the Tekran generator as the source of Hg vapor were compared with the orifice removed and with it reinstalled. The profiles are attached as the top two side by side plots in Figure 5. Both of the

plots show a variation of ~2%. Since there was no significant difference in the noise levels, the orifice was left in the instrument, as recommended by the instrument manual.

To determine whether the noise was an absolute function, or relative to the concentration of Hg vapor, a profile was obtained using the Tekran generator at a decreased concentration setting of 10 µg/m^3 Hg vapor. This profile is attached as the lower left plot in Figure 5. On a relative basis, the noise increased to ~4%.

Finally, to determine that the Tekran generator was not the source of the noise, the Thermo 01 81i unit was used as the Hg vapor source. This is attached as the lower right plot in Figure 5.

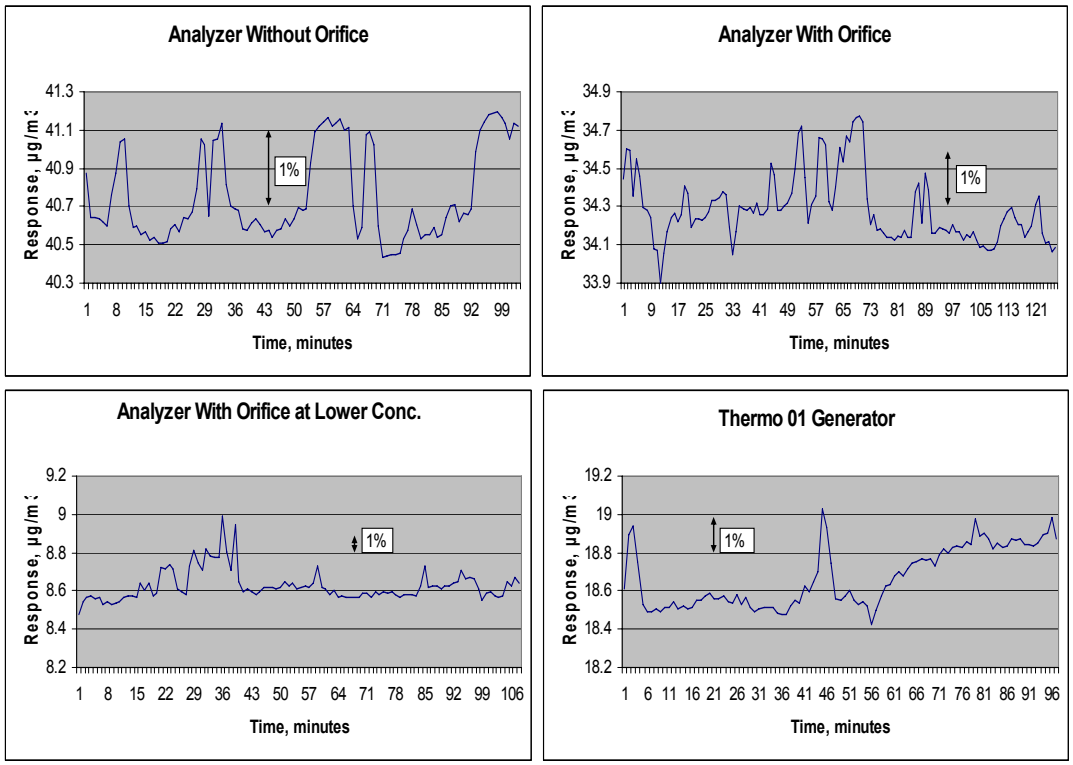

Figure 5. Variability Due To Analyzer.

The Thermo generator profile also demonstrates the variation in the signal, indicating that indeed, the analyzer must be the source of the noise. The analyzer's lamp intensity was subsequently plotted for the timeframe in which the above four plots were obtained. As shown in Figure 6, the lamp intensity shows a wide variation, not only evident as noise but as drift.

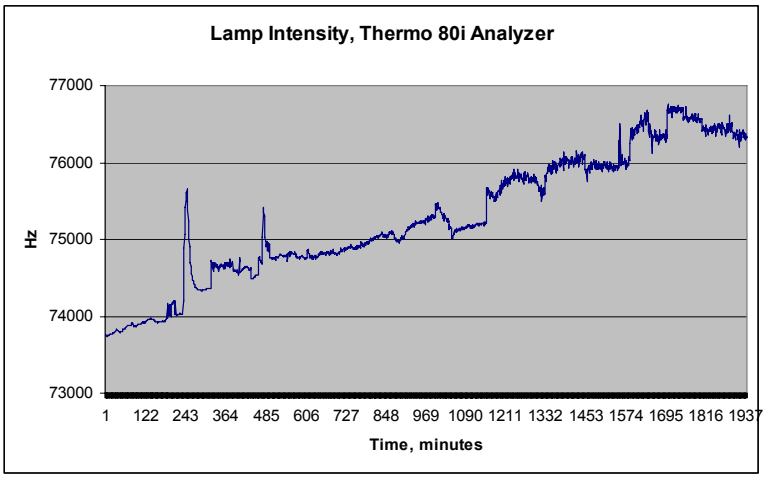

Figure 6. Old Lamp Intensity Profile.

As recommended by the Thermo service engineer, the old lamp was replaced with a new one, which was conditioned during a weekend. The analyzer was zeroed and spanned the following Monday (Sept. 18), and data were collected overnight. The lamp intensity data were downloaded and plotted (Figure 7) using the same scale intervals as above. The new lamp exhibits much less noise than the old one.

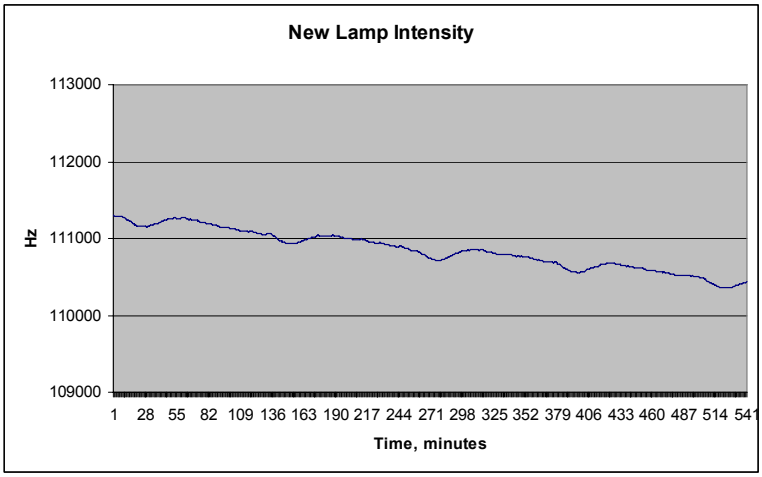

Figure 7. New Lamp Intensity Profile.

The new lamp does show drift, but the lamp compensation feature on the analyzer makes periodic adjustments to the lamp intensity to compensate for lamp intensity decay (until the lamp cannot function properly as in the case of the old lamp).

To investigate the source of the sine-wave pattern evident in the lamp intensity data, various analyzer parameters were examined. Ultimately, the cycling was traced to the ambient internal temperature inside the analyzer case. The internal temperature of the analyzer case influences the lamp intensity. Note how the negative dips in the intensity in Figure 7 correspond to the positive peaks in the internal case temperature shown in Figure 8.

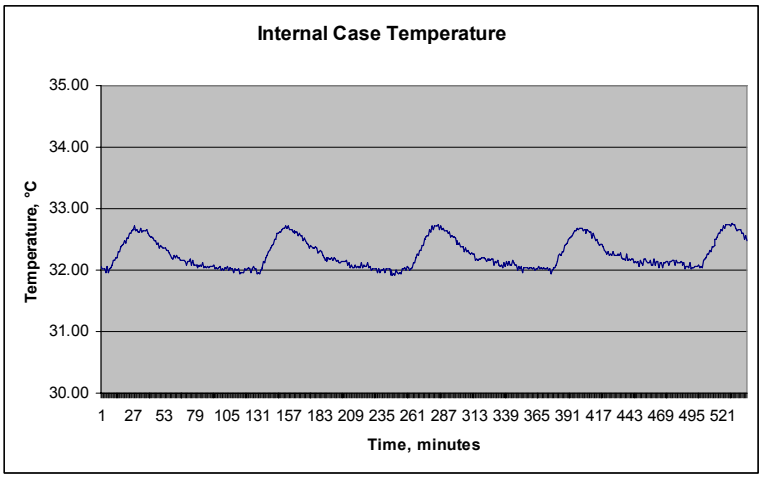

Figure 8. Analyzer Internal Case Temperature.

The overall effect on the concentration result is presented in Figure 9. The trendline and equation show a 0.4% negative drift in the concentration over the 9 hour timeframe. The variation in the data (top to bottom of the sine wave) is about 1.5% on a relative basis.

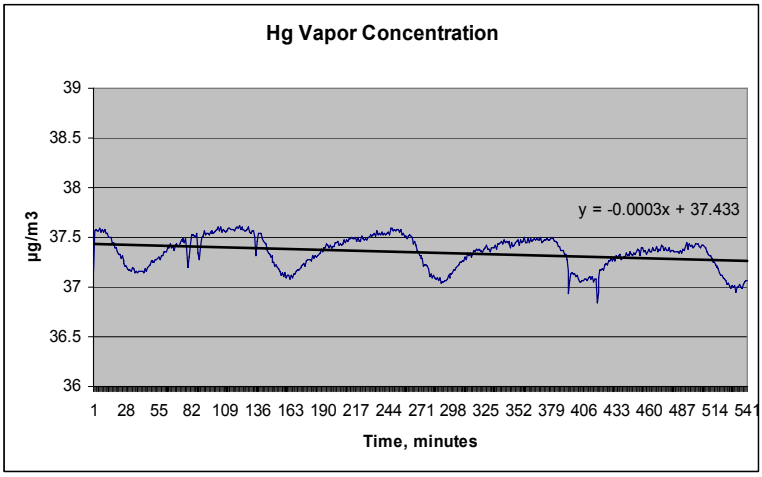

Figure 9. Overall Analyzer Drift and Fluctuation.

Overnight data were collected in similar fashion using the new Thermo 02 generator received at NIST on September 19. The results were similar to those shown above.

Finally, when the cooling fan inside of the 80i analyzer was disconnected, the lamp intensity did stabilize after the inside of the instrument case reached thermal equilibrium. With the analyzer noise and variation minimized, reliable data sets were achieved beginning the afternoon of September 20. Subsequent to this study, the vendor provided an upgrade kit for providing a constant lamp temperature to eliminate the effect of ambient temperature drift on lamp intensity.

Based on the issues encountered above, and how they were ultimately traced back to the analyzer, it is recommended that a periodic QA/QC check be written into the Hg calibration protocol. A periodic analysis of Hg calibration gas source (such as small volume cylinder) may be a viable option as a QA/QC check. For troubleshooting purposes, a calibration gas that is not dependent on the generator could be used to tell whether the generator or analyzer is at fault when data are out of control or suspect.

5. Summary of Generator Performance

The four plots in Figure10 show the variation in Hg output over 45 minutes for the four units that were functional on September 21. The units were set to generate a nominal Hg vapor concentration of 10 $\mu g/m^3$. After allowing time for equilibration, data were recorded for 45 minutes. The analyzer was not calibrated to give an accurate response because it was previously spanned with its cooling fan on, but the data can be compared on a relative basis.

The Mercury Instruments MC-3000 demonstrates high variation in its response profile. This variation was confirmed on several occasions including an overnight run. The variation may be caused by the design of the unit. Because this generator contains a condensation chamber, the unit is continuously adjusting its MFC1 flow based on the ambient (and uncontrolled) condensation temperature. As the condensation temperature changes based on the external and internal case temperatures, the MFC1 flow changes may give rise to the variation in Hg vapor concentration. The average response for the 45 minute timeframe is 7.4877 $\mu g/m^3$, and the standard deviation is 0.0412. This gives a relative standard deviation of 0.55%.

The PSA 10.534 also shows high variation in its response profile. However, the variation is cyclic, and an average value over a 20 minute timeframe yields a statistically consistent result. The average response for the 45 minute timeframe is 7.0196 $\mu g/m^3$. The standard deviation is 0.0406 which gives a relative standard deviation of 0.58%.

The Tekran 3310 shows lower variation in its response. The 45 minute average response of 6.9214 $\mu g/m^3$ is very close to the PSA 45 minute average response. The lower standard deviation value of 0.0167 provides a relative standard deviation of 0.24%.

The new Thermo 02 81i also demonstrates low variation. The average response for the 45 minute timeframe is 6.4179 $\mu g/m^3$. The standard deviation value of 0.0109 gives the lowest relative standard deviation of the four units, 0.17%.

The output for the Nippon generator could not be determined. However, Nippon/Horiba provided a new generator unit to NIST on September 22, which was the same day that Joe Rovani left NIST to return to WRI. It is currently being evaluated at NIST.

The results in Figure 10 were obtained in a short time frame with the particular units under evaluation at that time. Vendors have since modified and improved these devices. These results should not be used to compare relative merits of current devices from the vendors.

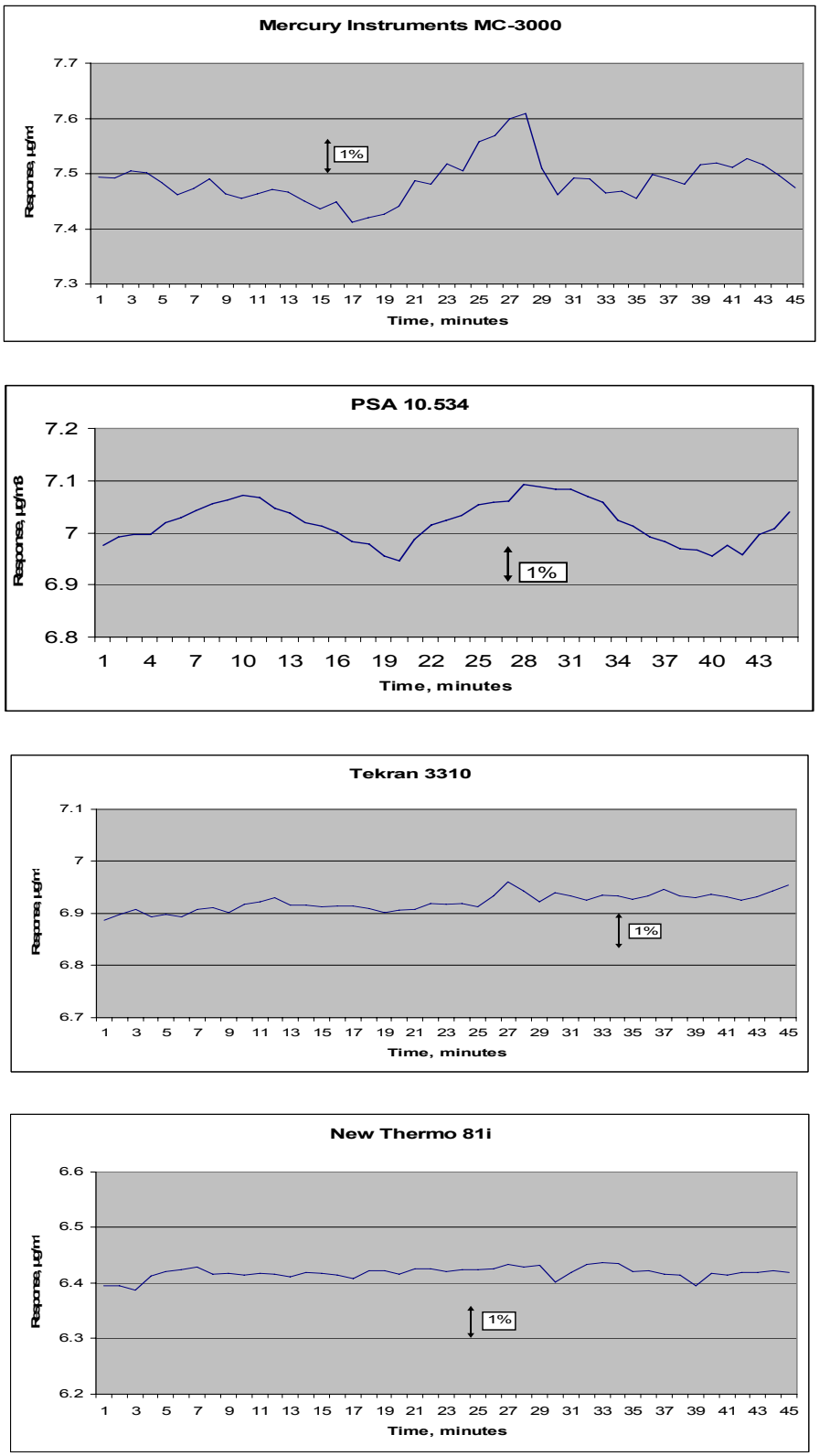

Figure 10. Generator Outputs For a 45 Minute Period.

The profiles in Figure 10 show that the responses for the four units are different. The signal variability for a short period of time, as well as the longer-term stability, are demonstrated and should be considered when further work is done on these units.

6. Generator Comparisons

The work presented in this section addresses the ability to compare the output of a Hg° generator to that of another Hg° generator set to similar concentration output. The current proposed protocol for attaining NIST traceability is for each generator manufacturer to compare the output of the generator units that they sell with that of the output of a NIST calibrated unit. The question that is to be answered is "how well can these comparisons be accomplished?" The previous sections of this report address the performance characteristics of individual generators and the detector. Using this information as a guide, an experimental design was established to try to attain comparisons with low variability. Some experimental conditions were adjusted as the work proceeded to incorporate new information that was observed regarding the performance of the various units.

The Thermo 80i continuous Hg° detector is used to compare the Hg° generator output signals. There are three terms used in this section of the report that differ from other terms that are in common usage. This is intentional and not accidental. They are used so that our experimental design and data processing concepts can more easily be understood. Two of the terms are "Hg° detector" instead of the more commonly used term "Hg° analyzer", and the term "Hg° generator" for the more commonly used term "Hg° calibrator". The third term is "comparison" instead of "analysis". We are using the Thermo detector as just that; a means to generate a signal from the flow of a gas sample into it containing Hg° vapor. The continuous flow Hg° generators are just that, a means to produce a flowing gas stream containing Hg° vapor. Using the term "calibrator" in connection with them implies implicitly that their "set" output is known to be correct. Part of our work, described elsewhere, is to establish the correlation of their output to the set point. The term "comparison" is used instead of "analysis" since that is all we are doing; we are comparing the signals from two different sources. The term analysis implies a much more involved operation and we do not want anyone to misconstrue the experiment.

The instrumentation that we had at our disposal is summarized below; a more complete description of each is given at the beginning of the report.

Detector/Analyzer

Thermo Model 80i

Hg° Generators/Calibrators

Tekran 3310
PSA 10.534
Thermo 81i (#02)
Mercury Instruments MC-3000

Nippon MGS 1E

During the time frame of the work, all of the generators did not function according to specification all of the time. The Nippon didn't work at all at the beginning. It was "fixed" after much discussion with the manufacturer and replacement parts being received from the manufacturer and installed on site. The Thermo #01 unit when originally received at NIST, about March 2006, worked well and a calibration curve was defined by the ICP/MS method. At some point after that work was performed and the current work started, August 1, 2006, the unit changed performance characteristics; it produced a very non linear output when plotting set concentration vs. response. Attempts to correct it did not work so a second unit was delivered from the manufacturer and tested.

Experimental Design

Any generator to be tested would have been turned on to reach operating conditions for at least 4 hours before the start of any experiment. The analyzer would also have been turned on and equilibrated in advance of use in data generation. In reality the generators and the analyzer were on most of the time. All work was performed under well controlled laboratory conditions. Air was used as the dilution gas through the generators. At each nominal concentration, each generator was set to the same settings each time it was tested. These were the settings that were characterized by the NIST ICP/MS work in the spring of 2006. The following notations will be used:

Generator 1 (G-1) is designated as the "reference". Generator (G-2) is the generator to be tested and in some instances two generators were tested, therefore, this third one would be G-3.

G-1 is the unit to which other units will be compared.
G-2 , G-3 etc will be the units being tested.
$G\text{-}1_a$, $G\text{-}1_b$, $G\text{-}1_c$ etc are the first, second and third signals recorded for G-1 during a nesting interval.
$G\text{-}2_a$, $G\text{-}2_b$, $G\text{-}2_c$ etc are the first, second and third signals recorded for G-2 during a nesting interval.
A nesting interval is a series of defined runs where it is started and ended with G-1 so that the signals from the other generators can be ratiod directly to the average of the signals from G-1 i.e., see below.

The detector (analyzer) was used as a comparative device. G-1 was run either every second or third time so that data was generated in a nesting form. A nesting interval is defined below: the reference and test generator(s) are set at the same nominal output and run sequentially till the data is collected. After this the set points are changed to achieve another nominal concentration and another nesting interval is started.

$G\text{-}1_a$, $G\text{-}2_a$, **$G\text{-}1_b$**, $G\text{-}2_b$, **$G\text{-}1_c$ …. n**
$G\text{-}1_a$, $G\text{-}2_a$, $G\text{-}3_a$, **$G\text{-}1_b$**, $G\text{-}2_b$, $G\text{-}3_b$, **$G\text{-}1_c$ ….**n

Where G-1_a is the 1st signal from G-1 and G-1_b is the 2nd signal from G-1 etc. The same notation is used for signals from G-2 and G-3. G-2_a was ratiod to the average of G-1a and G-1_b; G-2_b was ratiod to the average G-1_b and G-1_c etc., thus the term nesting. The experiment where two generators were being evaluated was handled in the same way. G-2_a and G-3_a were ratiod to the average of G-1_a and G-1_b. Note that the signals are being compared in real time not to an analyzer that had been "calibrated" sometime in the past. The simple ratioing technique is appropriate because the generators and the analyzers are fairly linear instruments and the signals being compared are very similar. This technique was also used to compensate for any drift or other variability in the performance of the generators and the detector.

No more than two generators were tested during any nesting interval. At the end of a nesting interval the generator settings would be changed to achieve another output concentration and there would be an equilibration period before data was taken for the next interval.

The signal from the detector was sent to an averaging circuit that was an integral part of the detector electronics. The detector sent an output value to data memory every minute. Data were collected continually in this manner. Most of the data were collected by letting each generator flow into the analyzer for 10 to 30 minutes and averaging the one minute averaged values after equilibrium was achieved. Some of the response values used in data processing were individual readings from the detector front panel after equilibrium was attained. Again, even though the generator outputs were flowing through the detector for up to 30 minutes, the generators were on continually and when the outputs weren't directed to the detector they were vented to either a hood or exhaust trunk.

During the experimental time frame some generators were out of service for varying amounts of time due to either malfunction or due to the fact that they were undergoing component evaluation. Because of this there isn't the same number of comparisons for each unit. Also, in order to generate data for "in service" units, two different generators had been used as G-1 at different times. This is actually good since this section of the report is to address the ability to compare one generator with another; it really doesn't matter which generator is designated as G-1 as long as it is identified.

Results and Discussion

The results of reproducibility of comparing generators within days are given in tables A1 thru A3 and the between day data are given in table A4. All values given for standard deviation (sd) and relative standard deviation (rsd) in this section of the report are for the data collected and do not address expanded total uncertainty; they are all 1 sigma. Within day reproducibility is the precision of the ratios for a generator within one nesting interval. Between day reproducibility is the precision of the averaged ratios for a generator within one nesting interval on day one with the average of the ratios in a similar interval on day 2.

Table A1 is the data for the comparison of the Nippon and the MC units with the PSA as the reference. In this case G-1 = PSA, G-2 = Nippon and G-3 = MC. At each nominal setting the PSA and the MC units were set at the same settings used for their calibration by ICP/MS; the

Nippon was set to produce a concentration near the output of the PSA and this same setting was used each time. No ICP/MS data was available for the Nippon unit since it was not functioning earlier in the year when the ICP/MS calibration work was done.

The data for the Nippon comparison on 08/28/06 shows a pattern that is to be expected; the variability at 10 $\mu g/m^3$ is greater than 15 $\mu g/m^3$ which is greater than 25 $\mu g/m^3$. The increase in variability with decreasing concentration is expected. The data for the Nippon on 08/29/06 is the opposite. The variability for 3 $\mu g/m^3$ is less than that for 15 $\mu g/m^3$ which is less than that for 40 $\mu g/m^3$. This is counterintuitive performance. The data for the MC unit on the same day, 08/29/06, shows that the variability at 10 $\mu g/m^3$ is greater than for the higher concentrations tested which were 15, 25 and 40 $\mu g/m^3$ but that there is not much difference in the variability at the three higher levels.

The important observation from Table A1 is the magnitude of the within day precisions, they range from 0.11% to 1.25% relative with the average value for all data in this table being about 0.7% relative.

Table A2 is the data for the comparisons of the PSA, MC and Thermo 02 to the Tekran unit. In this case G-1 = Tekran, G-2 = PSA, G-3 = MC and G-4 = Thermo-2. Note that "within day precision" is just the sd of the average of multiple values generated during one nesting period. If, during one day, more than one nesting was done at the same settings it is given as another data point for "within day precision" for that date (see PSA for 08/30/06 at 3 $\mu g/m^3$). We can spend paragraphs discussing the numbers in Table A2 but, exhaustive statistical analyses would not be appropriate. Some of these numbers were generated under different conditions of equilibration times, instrument reset times, and data handling. It is best to submit this table as data that was collected and consider Table A3.

Table A3 reduces the within day precisions that were given in Tables A1 and A2 to nominal concentration, reference generator and test generator. The last column then reduces the data further to just nominal concentration and averaged precisions.

There are two observations regarding this last column. The first is that the data seem to be intuitive; the variability decreases with increasing concentration. The second observation is that these precisions are much lower than we had anticipated; the highest being 0.8% relative at 3 $\mu g/m^3$ and the lowest being 0.4% relative at 60 $\mu g/m^3$.

Table A4 is the data for the output concentrations for the generators for each day during one nesting interval. If two same setting nesting intervals were run on one day then two numbers are given for that day. It is counterproductive to apply rigorous statistics to this data because all the numbers were not generated in the same manner. There were different time intervals between data taking and some different equilibration times between changes in generator settings. Some readings used were averages of the one minute stored averages after the data was sent to and processed in Excel. Some readings were manually recorded from the front panel display after signal equilibrium was attained.

However, there are two important observations to make; 1) the % day to day differences and 2) the rsd of the average output for given settings for each generator.

On the left side of the table are the dates and the concentrations for given generator settings. To the right of this information there are a series of columns labeled "% Relative Difference Day to Day". The number in column one of this "% Relative Difference" heading would be the relative difference between day 1 and day 2; the second column between day 2 and day 3; the third column the difference between day 3 and day 4 etc. This is important in a practical sense since it gives a guide as to what you might expect when testing a generator over several days. For example, should you expect 10% variation or 0.1% variation?

The reality of our data sets show that day to day relative differences can vary from 0.03% to 2.03%.

To the right of the "% Difference" series of columns is the avg, sd and rsd for all the concentration values for a given setting on each generator. The important column is the last one, "rsd", which is a measure of the precision of pooled averaged day to day results for a given generator. Again, these values should only be used as a guide and too much time can't be spent analyzing why there is no real trend in the magnitude of the rsd vs. nominal concentration. Observe that some of the statistics are for two data points whereas other statistics are for six data points.

The average value for this rsd column is about 0.7% which is almost the same as the average for the pooled rsd for the within day data.

These results are closer to a worst case scenario than they are to a best case scenario. If an Hg° generator manufacturer is to set up a similar system, where there is a detector and a NIST calibrated unit (G-1), then all of the generators can be adjusted to the proper settings and sufficient data can be collected to provide better statistical evaluation. The behavior of the generators and the detector can more readily be taken into account and the experimental design modified to account for the drift and spikes that have been described in other parts of this report. Again, it is expected that more precise comparisons should be achieved when units that are similar to each other are compared under well defined conditions and more data at each point are taken. This is the situation that will exist when a manufacturer compares its G-1 to other units that are being sold.

Uncertainty

The work performed was to establish the ability to compare the output of one generator with another. There are many variables involved in the performance of the three instruments (generators 1 and 2 plus the detector) involved in the measurement system. The performance of the generators and the detector are addressed in other portions of this report and therefore will not be repeated here. The true measure of the ability to compare two units comes out of the statistics on the data generated which have already been presented.

Section 6 Conclusions

This part of the work was supposed to establish some guidelines as to the ability of an Hg° generator manufacturer to compare one unit to other sister units. The suggested NIST traceability protocol is for a manufacturer to use one of its NIST calibrated units to compare other units that are manufactured and sold. The overall relative standard deviation of the within day pooled data (1 sigma) over the concentration range tested is 0.7 %. The overall relative standard deviation of the between day pooled data over the concentration range tested is 0.7 %. All data was used for these determinations. Data at some concentration ranges for certain generators is limited while data for others is more extensive. Experimental conditions evolved in the course of the experiments to take into account observed behavior of generators and the detector. Data generated under all of the experimental conditions were used. In future comparisons, the variability should be less since the desired experimental conditions have been established and better statistics can be achieved since more data can be generated at each setting.

Table A1: Within Day Precision (% rsd) of Multiple Comparisons of Two Generators to PSA Unit

C_{nom}	Nippon 08/28/06	Nippon 08/29/06	MC 08/29/06
3		0.11	
3			
10	0.96		1.25
15	0.87	0.21	0.56
25	0.53		0.74
40		0.35	0.61
60			

Table A2: Within Day Precision (% rsd) of Multiple Comparisons of Three Generators to Tekran Unit

C_{Nom}	PSA 8/30	PSA 8/31	MC 8/31	PSA 9/11	MC 9/11	PSA 9/12	MC 9/12	PSA 9/19	Thermo-2 9/19	PSA 9/20	Thermo-2 9/20	PSA 9/21	Thermo-2 9/21	MC 9/21
3	0.79					3.25		0.00				0.28	2.54	
3	0.26							0.57	0.26					
10	0.51	0.55	0.80	0.88	1.07	0.34	0.53	1.10	0.99	0.14	0.08			
15														
25	0.57	0.34	0.87							0.31	0.05		0.11	0.06
40	0.10	0.84		1.03	0.06									
60						0.02	0.73							

Table A3: Within Day Precision (% rsd) of Multiple Comparisons of Generators

	Compare with PSA		Compare with Tekran			
C_{Nom}	Nippon	MC	PSA	MC	Thermo-2	average
3	0.11		0.86		1.40	0.79
10	0.96	1.25	0.59	0.80	0.53	0.83
15	0.54	0.56				0.55
25	0.53	0.74	0.41	0.46	0.08	0.44
40	0.35	0.61	0.65	0.06		0.42
60			0.02	0.73		0.38

Table A4. Average nested concentrations (µg/m^3) for generators day to day output and relative % differences

Compare to PSA

Nippon 8/28	Nippon 8/29	% Relative Difference Day to Day	avg	sd	rsd
17.91	18.08	0.95	18.00	0.12	**0.67**

Compare to Tekran

PSA 8/30	PSA 8/30	PSA 8/31	PSA 9/11	PSA 9/12	PSA 9/12	PSA 9/19	PSA 9/19	PSA 9/20	PSA 9/21	% Relative Difference Day to Day					avg	sd	rsd
2.496	2.498			2.511		2.460	2.490		2.495	-0.08	-0.52	2.03	-1.22	-0.20	2.49	0.02	**0.68**
10.26		10.20	10.35	10.31		10.25	10.31			0.58	-1.47	0.39	0.58	-0.59	10.28	0.05	**0.52**
23.35		23.04								1.33					23.20	0.22	**0.95**
36.19		36.46	35.92					36.49		-0.75	1.48	-1.59			36.27	0.27	**0.74**
				58.19	59.11					-1.58					58.65	0.65	**1.11**

Compare to Tekran

MC 8/31	MC 9/11	MC 9/12	MC 9/12	% Relative Difference Day to Day				avg	sd	rsd
10.67	10.77	10.76		-0.94	0.09			10.73	0.06	**0.51**
		75.66	75.69	-0.04				75.68	0.02	**0.03**

Compare to Tekran

Thermo-2 9/19	Thermo-2 9/20	Thermo-2 9/21	% Relative Difference Day to Day	avg	sd	rsd
2.76		2.79	-1.09	2.78	0.02	**0.76**
9.275	9.365		-0.97	9.32	0.06	**0.68**
	36.00	36.01	-0.03	36.01	0.01	**0.02**

7. Conclusions

The mercury generators from five different manufacturers were tested to characterize their Hg° output performance. During the test period, three of the units worked all of the time as designed while two of the units did not. Plots are included to demonstrate the short and long term variability of the Hg° concentration output of the generators tested. A plot is also included to demonstrate the performance of the Hg° detector that was used during the experiments. A series of experiments was performed to measure the ability to compare the output of one generator to that of another under similar concentration output conditions. The within day and between day variability were about the same and were determined to have a relative standard deviation of 0.7%.

APPENDIX D

NIST EVALUATION OF ELEMENTAL MERCUEY GENERATORS USING ISOTOPE DILUTION INDUCTIVELY COUPLED PLASMA / MASS SPECTROMETRY

Final Report for "Evaluation of Mercury Vapor Pressure Calibrators" Western Research Institute

Stephen E. Long and Gerald D. Mitchell
Analytical Chemistry Division
Chemical Science and Technology Laboratory
National Institute of Standards and Technology

Executive Summary

Calibrations measurements have been made on five commercially available Hg^0 generators by both isotope dilution cold-vapor inductively coupled plasma mass spectrometry and gold-trap atomic absorption spectrometry. The agreement between the two measurement systems was very good, and demonstrates the viability of this measurement approach for delivering CAMR calibration services on a commercial basis. The data show that, for the most part, the delivered output Hg^0 concentrations are highly linear over the test range 2-40 $\mu g/m^3$. In the future, this work needs to be substantiated with additional ICP-MS experimental data using a new improved, more efficient gas-liquid separator device for introduction of the isotopic spike, and further measurements on some of the generators when they have been developed beyond a prototype stage, and are more reliable.

This Report is provided as completion documentation for Statement of Work submitted by Western Research Institute, entitled "Evaluation of Mercury Vapor Pressure Calibrators." The work was performed under Purchase Order #063002, John Schabron, Technical Contact.

Final Report for "Evaluation of Mercury Vapor Pressure Calibrators" Western Research Institute

Stephen E. Long and Gerald D. Mitchell
Analytical Chemistry Division
Chemical Science and Technology Laboratory
National Institute of Standards and Technology

1. Introduction

Growing concerns about the effects of anthropogenic mercury pollution on the environment, and potential transfer to the human food chain, particularly through the consumption of seafood, have led to an increasing focus on industrial sources of mercury and attempted reduction of these emissions through federal and state regulation. The largest single source of mercury to the atmosphere in the United States is the operation of coal-fired electric power utilities (approximately 40 % contribution). These utilities account for about 50 % of the total electric power generated in the United States, a share which is expected to increase to 57 % by 2030. Although the mercury content of coal is relatively low (typically 100 μg/kg), the large mass of coal burned annually by electric utilities results in an estimated 48 tons (1999 estimate) of mercury being released to the atmosphere. The emitted mercury is present in three forms which consist of elemental mercury, oxidized mercury and particulate bound mercury. The oxidized mercury, being water soluble, is susceptible to removal from the atmosphere through rainfall, ending up in local watersheds. The elemental mercury has a longer atmospheric half-life and enters the global mercury cycle.

With the objective of reducing these emissions, the U.S. Environmental Protection Agency (U.S. EPA) recently promulgated the Clean Air Mercury Rule (CAMR) [1] which establishes performance standards for both new and existing coal-fired plants, and also creates a market driven cap-and-trade program designed to reduce emissions on a nationwide basis. The cap and trade program will be implemented in two phases, which are designed to reduce emissions to 18 tons annually by 2018. In order to support the new rule, which will require accurate stack measurements of both total and speciated mercury, there is a need to establish a traceable measurement system based on certified reference standards. Measurement systems which have been proposed include continuous emission monitoring systems (CEMS) and sorbent trap technologies. These systems have to be calibrated using NIST traceable devices, which will include some combination of traceable mercury gas cylinders and mercury generators (both Hg^0 and speciated Hg), which can be used to generate known mercury concentrations in nitrogen or air. The analytical and physical performance of these mercury generators needs to be fully evaluated.

In this work, calibration measurements are provided for five commercial Hg^0 generator devices currently on the market. Three of these devices (Thermo-Scientific, Nippon Instruments and Mercury Instruments) were loaned by Western Research Institute (WRI). Additional data are also provided for two other devices (Tekran and PS Analytical) which are based at NIST.

Disclaimer: *Certain commercial equipment, instruments or materials are identified in this work to specify adequately the experimental procedure. Such identification does not imply recommendation or endorsement by the National Institute of Standards and Technology, nor does it imply that the materials or equipment identified are necessarily the best available for this purpose*

2. Background and Scope

The purpose of this work, as described in the SOW, was to evaluate and provide calibration data for several commercial Hg^0 generator systems. The initial SOW requested measurements for four generators, but the SOW was subsequently amended in May 2006 to provide additional data on one more unit (Nippon Instruments) which had been recently developed. Specifically this work involved the accurate measurement of output concentrations of Hg^0 and comparing these measurements with the output concentrations predicted by the manufacturer of the device. The mercury generators are all designed around a common concept, where a low flow of gas provided by a mass flow controller (MFC1) passes over a mercury reservoir or mercury impregnated support and is mixed with a larger dilution gas flow provided by another mass flow controller (MFC2) before exiting the device. The output concentration of Hg^0 is varied by a combination of the settings of the mass flow controllers and the temperature (T) of the mercury source. This scenario can allow for an almost infinite number of settings that can be adopted to obtain a desired output concentration. The design concept is based on predictions of the mercury output based on the Hg^0 vapor pressure curve as a function of the temperature of the mercury source. The established vapor pressure curve used by the industry sector for some considerable time is based on data in the 1928 International Critical Tables [2]. Recently a new correlation for the vapor pressure of mercury, valid from the triple point to the critical point [3] has been proposed by the NIST Physical and Chemical Properties Division in Boulder, CO. This equation, which is based on a Wagner-type form, has estimated expanded uncertainties of about 1 % in the temperature region of interest.

The purpose of this work was not to make a direct assessment of the validity of any vapor pressure equations, but to make calibration measurements on the generator devices as provided by the manufacturer. Such an assessment is beyond the scope of this work, and requires a more sophisticated experimental procedure, specifically designed to address this issue. In the implementation phase of the CAMR, calibrations of mercury generators will be made by NIST Gaithersburg as part of the official EPA traceability protocol. The output of the generators produced for electric utility measurements will then be based on the actual traceable calibrated output and not on any thermodynamic relationship.

The measurements were made using an isotope dilution method employing cold-vapor mercury generation inductively coupled plasma mass spectrometry (ID-CV-ICP-MS). This methodology has been developed into a protocol which is attached to this report. The accuracy of this methodology for the determination of mercury in liquid and solid matrices has been well established [4-6], however, application to the measurement of mercury in gas streams is not as straightforward, and the methodology is still undergoing refinement. The use of isotope dilution mass spectrometry should give high-accuracy measurements, but it relies on the conversion of an aqueous isotopic spike to Hg^0 prior to mixing with the sampled gas stream. This is achieved by the use of chemical reduction in a gas-liquid separator device. The efficiency of this device must be well established in order to maintain critical accuracy of the measurement data.

Additional measurements were made on some of the devices using a gold-trap atomic absorption spectrometer system. These data are also provided as part of this report, and a comparison of the data sets is made.

The generators examined in this study were tested as supplied by the manufacturer via WRI. Some of the devices exhibited operational problems during the study, which significantly delayed some of the testing. Some of the devices (Nippon Instruments and Thermo-Scientific) were eventually replaced with new ones by the manufacturer. Only one device from each manufacturer was tested by ID-CV-ICP-MS and these data are reported here. The operational characteristics and any associated problems with the device are documented in the Equipment Section. Although only one device was tested for the purposes of this

report, the intention is to eventually test all of the available devices when their operational reliability has been established.

A comprehensive examination of the repeatability of the devices for Hg^0 concentration was beyond the scope of the funded work. This is an important metric, however, and this is the focus of current research work at NIST.

3. Equipment

Hg^0 Generators

Three Hg^0 generators (Thermo-Scientific 81i, Mercury Instruments MC-3000 and Nippon MGS-1) were provided by WRI to NIST for evaluation during this study. Two additional generators already located at NIST (Tekran Model 3310 and PSA 10.534 Cavkit) were also evaluated. All of the generators were evaluated on an as-received basis. No additional calibrations of the mass flow controllers and/or temperature sensors were attempted. Specific notes concerning the condition of each generator are provided in each summary.

Tekran Instruments Corporation, Model 3310 Mercury Generation System

The Tekran generator system (Serial number 3007) was manufactured in Toronto, Canada. This unit is based at NIST and is the only device having a computer controlled interface running on a Windows platform. All instrument functions and performance logs are controlled through this interface. This allows the user to automate a sequence of measurement calibrations which can then be run unattended. The unit can also be run in a manual step mode, which was employed for these measurements. The unit appeared to be extremely well engineered and did not require any maintenance or repair during the course of the measurements. The MFCs on this particular unit were calibrated at NIST in December 2005. The generator was equipped with a heater/cooler facility on the mercury source, so the temperature of the mercury source could be adjusted as needed to produce a desired output concentration. Gas was sampled from the rear of the device through the auxiliary (quarter inch) port.

Tekran 3310 Front-View

Tekran 3310 Rear-View

PS Analytical Generator, Model 10.534 Mercury Generation System (Cavkit)

The PSA 10.534 Cavkit generator (Serial number 012) was manufactured in the UK. The company has been in business in the mercury measurements sector for several decades and has considerable experience. This unit is based at NIST. The basic design of the generator is very simple, employing a mercury impregnated substrate contained in a PTFE tube. Gas is directed over the source by one low-flow mass flow controller (MFC1) and is subsequently diluted by a high-flow controller (MFC2). These controllers are adjusted by means of two manual potentiometers located on the front of the device, with a digital display of each flow rate. There was some hysteresis associated with these potentiometers, so adjustments were always made from the same rotational direction. There was some noise associated with the first mass flow controller, MFC1, as evidenced by a fluctuating digital display, which could be minimized by not having an excessive MFC2 to MFC1 flow ratio. The manufacturer is aware of this characteristic and it is not considered to unduly affect the accuracy of the device. The mercury source was not equipped with a cooling facility, so only temperatures above ambient laboratory temperature could be selected. This limited the lowest output concentration that could be achieved on this unit.

PSA Cavkit Front-View

Thermo-Scientific, Model 81i Mercury Generation System

The 81i generator is manufactured in the U.S. The specific unit examined did not have a specific serial number and was provided by WRI. This generator is usually operated by means of keypad entry combined with a digital display located on the front of the device. The unit is usually paired with a sister device, the Model 80i, which is an atomic fluorescence measurement system. The various sub-menus of the 81i were sometimes confusing to navigate, and it was fairly easy to change a setting without realizing the implications. The device was equipped with a heater/cooler facility for the mercury source, although the default temperature of the source was 15 ºC for routine operation. To operate this device, the user inputs a target output concentration and the device programs the mass flow controllers as necessary to achieve the output, which is predicted from a pre-programmed vapor pressure equation. The user can select which equation is used. The device worked fairly well during the course of the measurements by ID-CV-ICP-MS, but subsequently developed a problem with severe non-linear output at elevated output concentrations. The unit was eventually replaced by Thermo with a new unit.

Thermo 81i Front-View

Mercury Instruments, Model MC3000 Mercury Generation System

This device was manufactured in Germany with a serial number of 1005/006MC, and was provided by WRI. The design of this unit was slightly different to the others in that there are two chambers consisting of a saturation chamber maintained at 40°C, and a paired condensation chamber which is operated at near-ambient temperature. These chambers contain a substantial amount of liquid mercury, so the unit cannot be tipped or inverted during shipping. Several problems were encountered with this device during use, which included a badly designed manual flow switch on the front of the unit, which did not always work when turned in the indicated direction. The design arrangement did not allow the selection of output concentrations below 9 µg/m³. The operation of the device was similar to the Thermo device having user keypad entry and a digital display. It was suspected that there might be a slight leak in this device as it was sometimes difficult to maintain the desired output flow into the ICP-MS instrument.

MC3000 Front-View

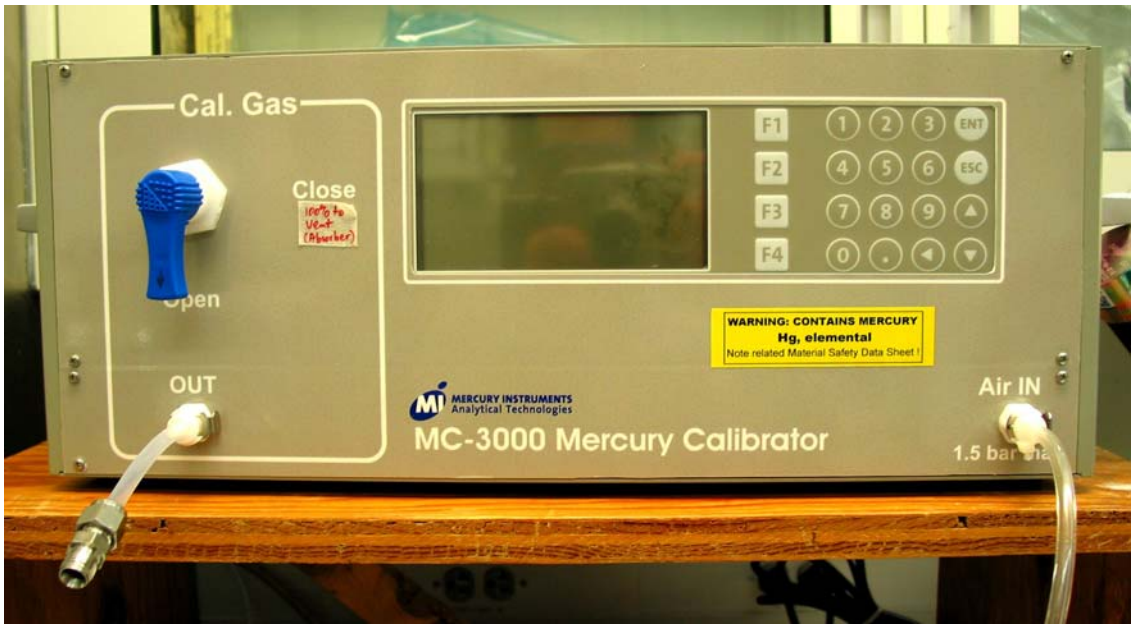

Nippon Instrument Corporation, Model MGS-1 Mercury Generation System

This device was manufactured in Japan and did not have a serial number. The unit was incorporated into the SOW study when it became available in the summer of 2006. The unit was provided by WRI. This unit incorporates two mass flow controllers. The first delivers a flow of nitrogen at approximately 1 mL/min over an 80 µL droplet of liquid mercury in a glass saturation cell. This flow is then diluted with air supplied in this case from an external pump. This configuration can supply mercury output concentrations in the range 3-150 µg/m³. The mercury source is heated to 50 ºC, which is substantially higher than the other devices. The unit is similar to the PSA device in that the output concentration is selected using two manual potentiometers on the front panel and a digital display. The output concentrations are calculated from the set points and a calculation algorithm supplied by the manufacturer.

Unfortunately this device exhibited many problems. Initially the device would not output any mercury concentrations because of a design problem with a check valve inserted into the flow path. This problem was eventually diagnosed and solved by removing the flow check valve. After this it was found that the device would work erratically, where it would work one day and not the next. This problem was suspected to be a result of contamination of the mercury droplet, significantly decreasing the vapor pressure. Replacement of the droplet would temporarily improve the performance, but it would decrease again a few days later. The use of ultra high-purity nitrogen was recommended by the manufacturer but this did not solve the problem. It is evident that there are still some design considerations that need to be resolved on this unit before it can be used routinely. The unit was eventually replaced by another more updated unit, which was the one tested. Measurements on this unit were made immediately after inserting fresh triple-distilled mercury into the source. It was also found that it was sometimes

difficult to maintain the desired output flow into the ICP-MS instrument. Following this work, it was found that the output for a given set-point was drifting downwards over the course of several hours.

Nippon MGS-1 Front-View

Nippon MGS-1 Rear-View

Thermo X7 Inductively Coupled Plasma Mass Spectrometer

Measurements of Hg^0 concentrations were made using a quadrupole ICP-MS instrument manufactured by Thermo Electron. This instrument was fitted with a collision cell system pressurized with a 7 % v/v H_2/He gas mixture, but this feature was not used for these measurements owing to the lack of any spectral interferences on the mercury isotopes measured. The instrument is normally supplied with a glass concentric nebulizer and spray chamber assembly for liquid sample introduction. For these measurements this assembly was removed and replaced with a ball joint and tubing through which the flow from the mercury generation system was directed. A mixing tee allowed simultaneous introduction of a make-up gas stream to provide the optimal flow of gas into the sample injector of the plasma torch. The isotopic spike was added to the sampled gas stream from the generator by means of a commercial gas-liquid separator device (CETAC).

Nippon Instrument Corporation Model MA-2000 Mercury Analyzer (MA-2)

Supporting measurements of the Hg^0 generators were made using a double gold-trap Nippon mercury analyzer equipped with an atomic absorption (AA) detector.

Nippon Mercury Analyzer

4. Reference Standards and Calibration

For the ICP-MS measurements, two SRMs were used for calibrations. The primary calibration standard used was SRM 3133 (Mercury Standard Solution), having a certified concentration of 10.00 ± 0.02 mg/g. This SRM was prepared from triple-distilled mercury dissolved in 10 % (volume fraction) nitric acid. This standard was used to accurately calibrate the ^{201}Hg working spike solutions. This was achieved by preparing two calibration stock solutions by serial dilution of SRM 3133 and then preparing four spike calibration mixtures, two mixtures for each of the stock solutions, by gravimetrically mixing an aliquot of the stock solution with an aliquot of the working spike solution. These mixtures were then analyzed by ID-CV-ICP-MS using the same operating conditions as for the Hg^0 generator gas stream measurements. Secondary maintenance calibrations were also made with SRM 1641d (Mercury in Water), having a certified concentration of 1.590 ± 0.018 μg/g.

For the CVAA Instrument Calibrations, serially diluted stock solutions of SRM 3133 were prepared gravimetrically in 2 % (volume fraction). A known aliquot of standard was pipetted into the ceramic sample boat of the analyzer and vaporized onto the gold trap system. The gold trap was then heated and measurements were made as for the gas stream samples.

5. Experimental

Operation of Generators

The Hg^0 generators were operated as recommended by the individual manufacturers. Nominal target set points spanning the range 2-40 μg/m^3 Hg^0 were chosen for calibrations. These set points were 2, 3, 5, 7, 10, 15, 20, 25, 30, 35 and 40 μg/m^3. This was considered a sufficient number of points to define the output correlation for each device. Measurements higher than 40 μg/m^3 were not made because the ICP-MS pulse counting detection system was not linear above this point. Additionally some of the generators were not capable of operating as low as 2 μg/m^3, so the calibrations were made only down to their lower limit. These are noted in the text. All generators (with the exception of the Nippon generator which was 4 hours) were equilibrated for a minimum of 24 hours in the laboratory environment before calibration measurements were made.

Only part of the flow from each Hg^0 generator was sampled into the ICP-MS instrument. This had two principal advantages, one being that there was not excessive flow of air or nitrogen into the inductively coupled plasma, which would have resulted in major instability, and also that each generator could then be sampled with no back pressure on the output port, as the majority of the output flow was directed to an open vent. This was important, because many of the generators were not designed to function with any back-pressure on the output, and this could cause biases in the concentrations output by the generator. Notably, the Tekran 3310 is apparently designed to compensate for back-pressure variations, but other systems, such as the PSA Cavkit, are not.

For each Hg^0 generator, a set of operating conditions (source temperature, MFC1 and MFC2 flow rates) were employed which resulted in a close approximation to the desired output concentration point. To ensure consistency, the same or similar gas flow and temperature operating conditions were used for both the ID-CV-ICP-MS measurements and the gold-trap AAS measurements. All of the ID-CV-ICP-MS measurements were made using pressure-regulated high-purity nitrogen as the transport medium, except for the Nippon unit which used air supplied from a supplied pump system.

ICP-MS Measurements

ID-CV-ICP-MS measurements on the generator devices were made using the procedures specified in the Method Protocol (attached). Typical ICP-MS operating conditions employed for these measurements are compiled in Table 1.

Table 1: ICP-MS Typical Instrument Operating Conditions

Extraction	-431 V
Lens 1	-5.9 V
Focus	22.7 V
D1	-29.8 V
Pole bias	4.5 V
Hexapole bias	-3.0 V
L2	-20.4 V
L3	-87.1 V
D2	-146 V
Differential aperture	-80.0 V
Plasma forward power	1420 W
Plasma coolant flow	13.0 L/min
Plasma auxiliary flow	0.90 L/min
Ar make-up flow	0.88 L/min
Sampled gas flow	40 mL/min
^{201}Hg spike uptake rate	0.6 g/min
Detector voltage	-3180 V
Dead-time correction	37 ns

Gold Trap AAS Measurements

To verify the ICP-MS measurements, additional measurements were made using a double gold trap collection system followed by atomic absorption analysis. The analyzer system was cleaned several times by purging the system at 600 °C. To assure a low Hg background, the gold tube and sample holders were cleaned before each run. The analyzer was calibrated by using aliquots of a gravimetrically prepared calibration standard, traceable to SRM 3133, to cover the calibration range of interest. After each calibration and at the start of each day a standard check was run using the calibration standard. Each gold tube was placed in a manifold where it collected Hg^0 from a gas stream from the generator. The output of the Hg^0 Generator was attached to one port of a tee with one of the other ports going to vent. An on/off valve was attached to the third port of the tee. The output of the valve went to a fitting into which the input of a gold amalgam trap was placed. The output of the gold amalgam trap was then connected to the input of a MFC (Figure 1). To obtain a sample of Hg on the gold amalgam trap, the following procedure was used:

1. The valve attached to the tee was turned off so that no flow would go through the sampling section of the manifold.
2. A cleaned gold amalgam trap was fixed into the fittings.
3. A flow measuring device was placed onto the vent line to assure that excess Hg^0 mixture flow was attained.
4. After flushing the connecting lines the valve was opened and a timer started.
5. The valve remained opened for the predetermined time, after which the valve was shut and the timer stopped.

Figure 1. Manifold for Sampling Hg^0 Vapor

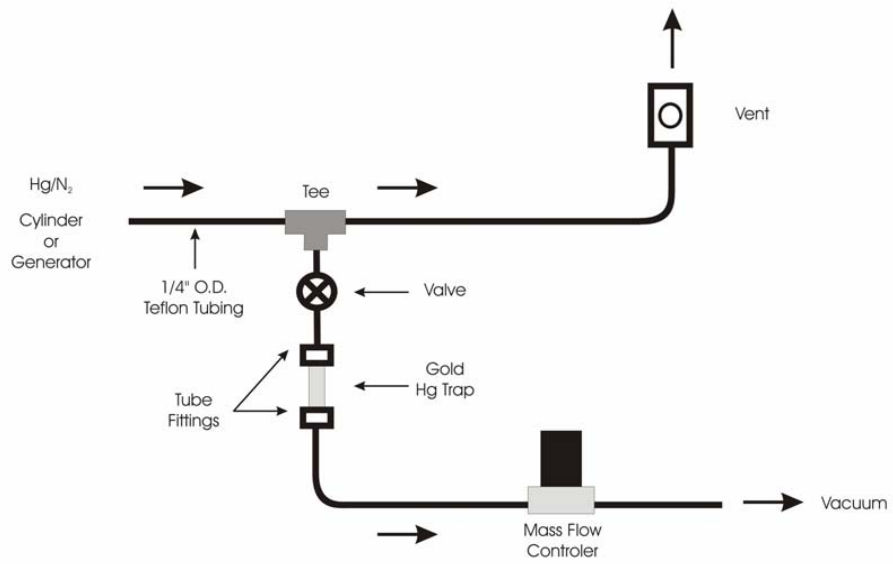

The gas sample was collected for 60 s at a flow rate of 0.75 L/min. After sample collection, the gold tube was placed in a sample boat inside the analyzer and heated to 800 °C. The Hg^0 released was collected on a second gold tube that was heated to 600 °C before measurement by AAS.

Data Calculations and Reporting

For the ID-CV-ICP-MS measurements, the measured $^{201}Hg/^{202}Hg$ isotope ratios were corrected for ICP-MS instrument mass discrimination and detector dead-time and downloaded to a Microsoft Excel spreadsheet from which Hg^0 concentrations in the sampled gas streams were calculated.

For consistency, **all of the measured concentrations were normalized to standard conditions of temperature and pressure (STP), at 0 ºC and 760 mm Hg**. There was some variation in the terminology of the output concentrations used by the manufacturers of the generator devices, with some being calculated at conditions of STP and some being calculated at laboratory conditions. For comparative purposes, the predicted Hg^0 output concentrations of the various devices were all converted to STP. To accomplish this, laboratory temperature and barometric pressure measurements, using a NIST traceable instrument, were recorded at the same time as the generator measurements.

Measurement Uncertainty

A discussion of the expanded uncertainty calculations and uncertainty components associated with the measurements by ID-CV-ICP-MS can be found in the Method Protocol (attached). The uncertainty components were combined according to ISO guidelines [7]. The total expanded uncertainty was of the order of 0.95 % relative for output mercury concentrations in the middle of the test range (20 $\mu g/m^3$).

6. Hg^0 Generator Measurements and Discussion

Data for the five Hg^0 generators tested are provided in the following sections. For the ID-CV-ICP-MS measurements, the data represent a mean concentration calculated for a five minute (300 s), or in some cases, a ten minute (600s) data acquisition (sampling) period. It was found that the output of the generator systems equilibrated in less than a minute. Sampling was not commenced until equilibration was established. For each generator (with the exception of the Nippon generator) a data set is provided for both ID-CV-ICP-MS and gold-trap AAS measurements.

It is emphasized that these data represent a snapshot of a given generator output. The data are not necessarily representative of other devices from the same manufacturer, and it is to be expected that there will be some variation in the performance of similarly manufactured devices. It would be advantageous to test several devices from each manufacturer to assess the device-to-device variability.

Tekran 3310 Generator

ID-CV-ICP-MS Measurements

Calibration data were obtained by ID-CV-ICP-MS for the range 2-40 µg/m^3. These data are summarized in Table 2a. The Table contains the operating parameters for the measurements, the measured data with associated expanded uncertainty and a calculation of the deviation of the measured concentration values from those predicted. The data points for the entire measurement range are plotted graphically in Figure 2a, with the measured concentration values plotted along the ordinate and the predicted calculated values along the abscissa.

Table 2a: ID-CV-ICP-MS Measurement Data for Tekran 3310
Run Date: February 2006

Nominal µg/m^3	Reservoir T °C	MFC1 mL/min	MFC2 L/min	Predicted µg/m^3	Measured µg/m^3	Uncertainty µg/m^3	Deviation Predicted, %
0	5.00	0.00	6.00	0.000	0.000	--	--
2	5.00	5.00	8.70	2.023	2.029	0.019	0.31
3	5.00	5.13	6.00	3.009	3.033	0.029	0.80
5	5.00	8.57	6.00	5.027	5.070	0.048	0.86
7	15.00	4.90	6.00	7.038	7.006	0.067	-0.47
10	15.00	7.00	6.00	10.055	10.052	0.096	-0.03
15	15.00	10.50	6.00	15.082	14.957	0.142	-0.83
20	15.00	13.93	6.00	20.008	20.054	0.191	0.23
25	15.00	17.42	6.00	25.023	24.849	0.236	-0.69
30	15.00	20.90	6.00	30.021	29.885	0.284	-0.45
35	15.00	24.40	6.00	35.049	34.786	0.331	-0.75
40	15.00	27.85	6.00	40.004	39.609	0.376	-0.99
						Mean	**-0.18**

Figure 2a: ID-CV-ICP-MS Calibration Correlation for Tekran 3310 Generator

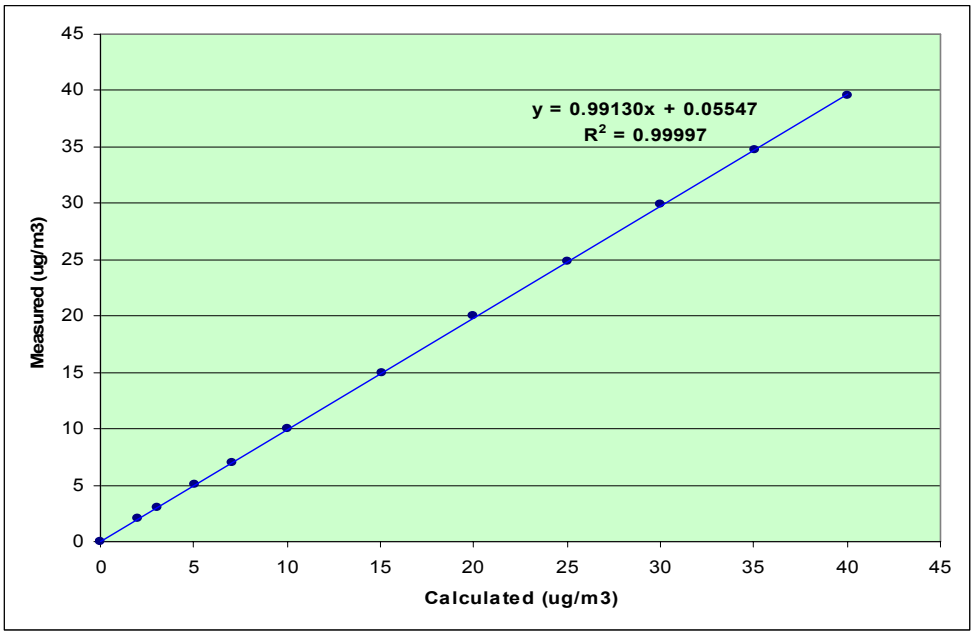

Tekran 3310 Generator

Gold-Trap AAS Measurements

Calibration data obtained by gold-trap AAS using the same generator operating conditions as the ID-CV-ICP-MS measurements are summarized in Table 2b. The correlation data are plotted graphically in Figure 2b.

Table 2b: Au Trap AAS Measurement Data for Tekran 3310

Run Date: August 2006

Calculated Setting µg/m^3	MA-2000 Mean Value µg/m^3	Deviation Predicted, %
2.023	1.948	-3.71
3.460	2.858	-17.40
5.027	5.062	0.70
7.038	6.709	-4.67
7.038	6.793	-3.48
10.055	10.009	-0.46
10.055	9.773	-2.80
20.008	19.778	-1.15
25.023	24.467	-2.22
30.021	29.697	-1.08
30.021	29.317	-2.35
35.049	34.513	-1.53
40.004	39.542	-1.15

Figure 2b: Au Trap Calibration Correlation Data for Tekran 3310 Generator

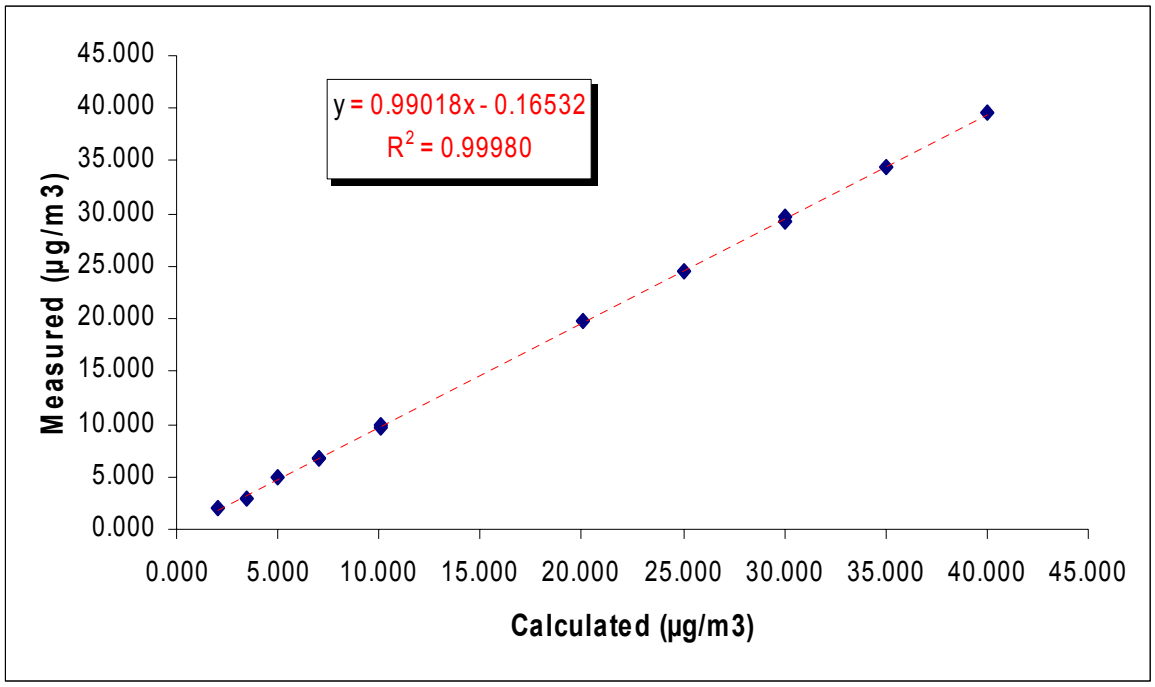
y = 0.99018x - 0.16532
R2 = 0.99980
Measured (µg/m3)
Calculated (µg/m3)
45.000
40.000
35.000
30.000
25.000
20.000
15.000
10.000
5.000
0.000
0.000
5.000
10.000
15.000
20.000
25.000
30.000
35.000
40.000
45.000

PSA Cavkit Generator

ID-CV-ICP-MS Measurements

Calibration data were obtained by ID-CV-ICP-MS for the range 3-40 µg/m^3. These data are summarized in Table 3a. The Table contains the operating parameters for the measurements, the measured data with associated expanded uncertainty and a calculation of the deviation of the measured concentration values from those predicted. The data points for the entire measurement range are plotted graphically in Figure 3a, with the measured concentration values plotted along the ordinate and the predicted calculated values along the abscissa.

Table 3a: ID-CV-ICP-MS Measurement Data for PSA Cavkit

Run Date: February 2006

Nominal µg/m^3	Reservoir T ºC	MFC1 mL/min	MFC2 L/min	Predicted µg/m^3	Measured µg/m^3	Uncertainty µg/m^3	Deviation Predicted, %
0	30.00	0.00	14.00	0.000	0.000	--	--
2							
3	30.00	1.30	14.00	2.740	2.717	0.026	-0.84
5	30.00	2.10	10.40	4.426	4.290	0.041	-3.06
7	30.00	2.20	10.00	6.241	6.084	0.058	-2.52
10	30.00	3.40	10.00	10.031	9.659	0.092	-3.71
15	30.00	4.60	10.00	13.572	13.027	0.124	-4.01
20	30.00	6.10	10.00	17.997	18.174	0.173	0.98
25	30.00	7.71	10.00	22.747	23.035	0.219	1.27
30	30.00	9.20	10.00	27.143	26.937	0.256	-0.76
35	30.00	10.71	10.00	31.598	31.569	0.300	-0.09
40	30.00	12.21	10.00	36.024	36.038	0.342	0.04
						Mean	**-1.27**

Figure 3a: ID-CV-ICP-MS Calibration Correlation for PSA Cavkit Generator

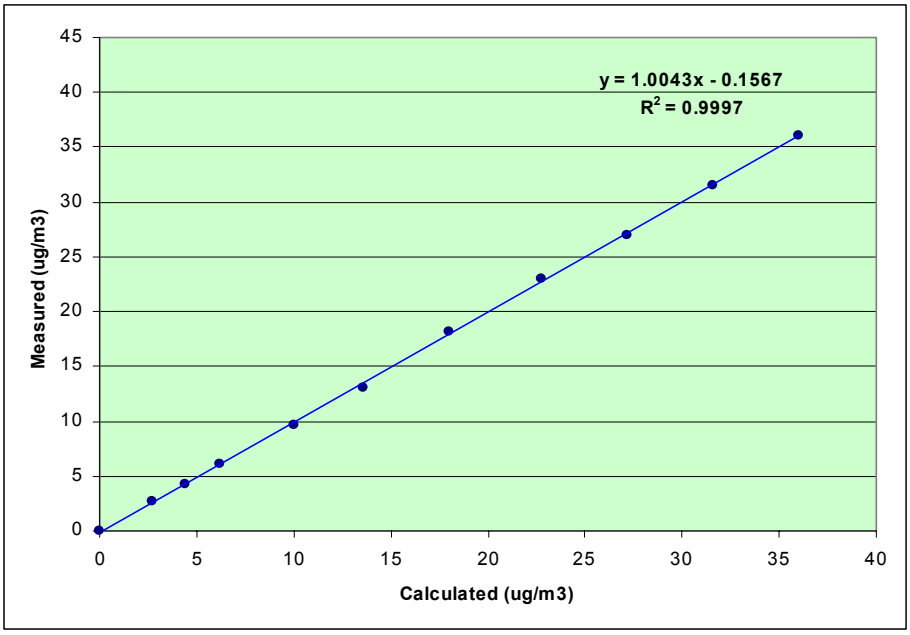

PSA Cavkit Generator

Gold-Trap AAS Measurements

Calibration data obtained by gold-trap AAS using the same generator operating conditions as the ID-CV-ICP-MS measurements are summarized in Table 3b. The correlation data are plotted graphically in Figure 3b.

Table 3b: Au Trap AAS Measurement Data for PSA Cavkit
Run Date: August 2006

Calculated Setting µg/m^3	MA-2000 Mean Value µg/m^3	Deviation Predicted. %
2.023	1.434	-29.12
3.460	2.547	-26.39
5.027	4.468	-11.12
10.055	8.846	-12.02
15.082	14.860	-1.47
20.008	19.727	-1.40
25.023	24.917	-0.42
30.021	29.506	-1.72
35.049	34.512	-1.53
40.004	39.709	-0.74

Figure 3b: Au Trap Calibration Correlation Data for PSA Cavkit Generator

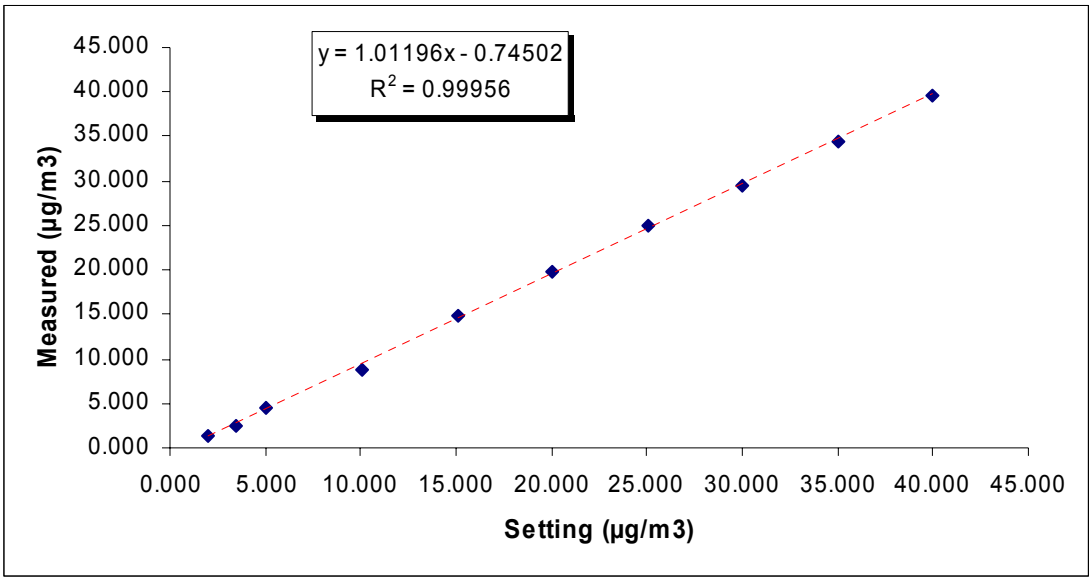

Thermo 81i Generator

ID-CV-ICP-MS Measurements

Calibration data were obtained by ID-CV-ICP-MS for the range 3-40 µg/m^3. These data are summarized in Table 4a. The Table contains the operating parameters for the measurements, the measured data with associated expanded uncertainty and a calculation of the deviation of the measured concentration values from those predicted. The data points for the entire measurement range are plotted graphically in Figure 4a, with the measured concentration values plotted along the ordinate and the predicted calculated values along the abscissa.

Table 4a: ID-CV-ICP-MS Measurement Data for Thermo 81i

Run Date: February 2006

Nominal µg/m^3	Reservoir T °C	MFC1 mL/min	MFC2 L/min	Predicted µg/m^3	Measured µg/m^3	Uncertainty µg/m^3	Deviation Predicted, %
0							
2							
3	14.95	6.751	14.485	4.000	3.516	0.033	-12.09
5	14.95	8.424	11.886	6.082	5.825	0.055	-4.23
7	14.95	10.147	10.635	8.188	8.002	0.076	-2.27
10	14.95	12.626	9.624	11.278	11.377	0.108	0.88
15	14.95	16.853	8.785	16.462	16.875	0.160	2.51
20	14.95	21.087	8.352	21.666	22.171	0.177	2.33
25	14.95	25.281	8.083	26.840	27.937	0.265	4.09
30	14.95	29.495	7.903	32.027	33.012	0.314	3.08
35	14.95	33.697	7.771	37.211	36.899	0.370	4.54
40	14.95	37.911	7.669	42.421	44.453	0.422	4.79
						Mean	**0.36**

Figure 4a: ID-CV-ICP-MS Calibration Correlation for Thermo 81i Generator

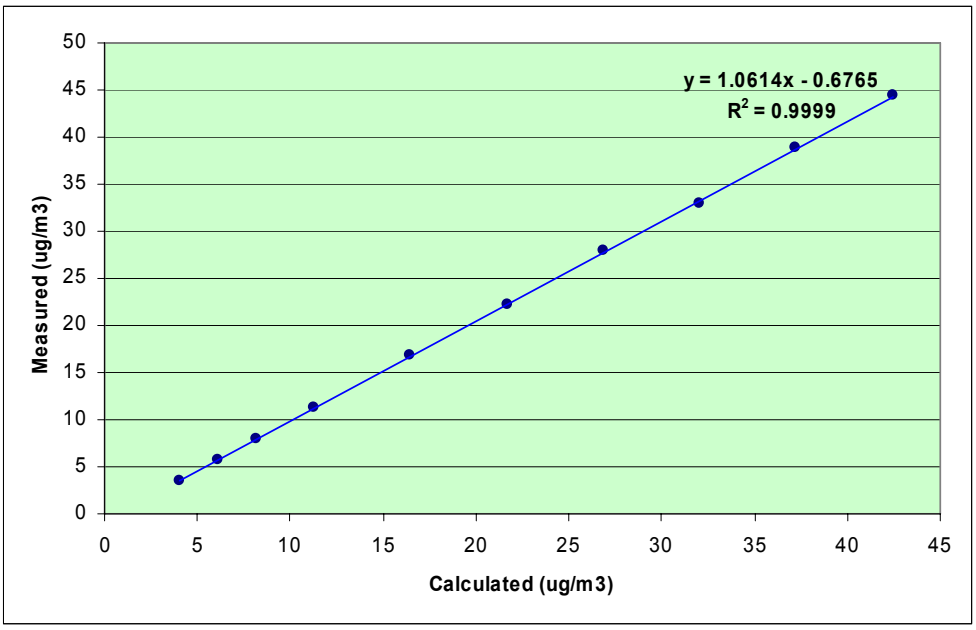

Thermo 81i Generator

Gold-Trap AAS Measurements

Calibration data obtained by gold-trap AAS using the same generator operating conditions as the ID-CV-ICP-MS measurements are summarized in Table 4b. The correlation data are plotted graphically in Figure 4b.

Table 4b: Au Trap AAS Measurement Data for Thermo 81i

Run Date: August 2006

Calculated Setting µg/m^3	MA-2000 Mean Value µg/m^3	Deviation Predicted, %
3.460	5.017	45.00
5.027	6.237	24.07
10.055	11.023	9.63
10.055	11.513	14.50
15.082	16.251	7.75
20.008	20.725	3.58
30.021	28.542	-4.93
40.004	36.098	-9.76

Figure 4b: Au Trap Calibration Correlation Data for Thermo 81i Generator

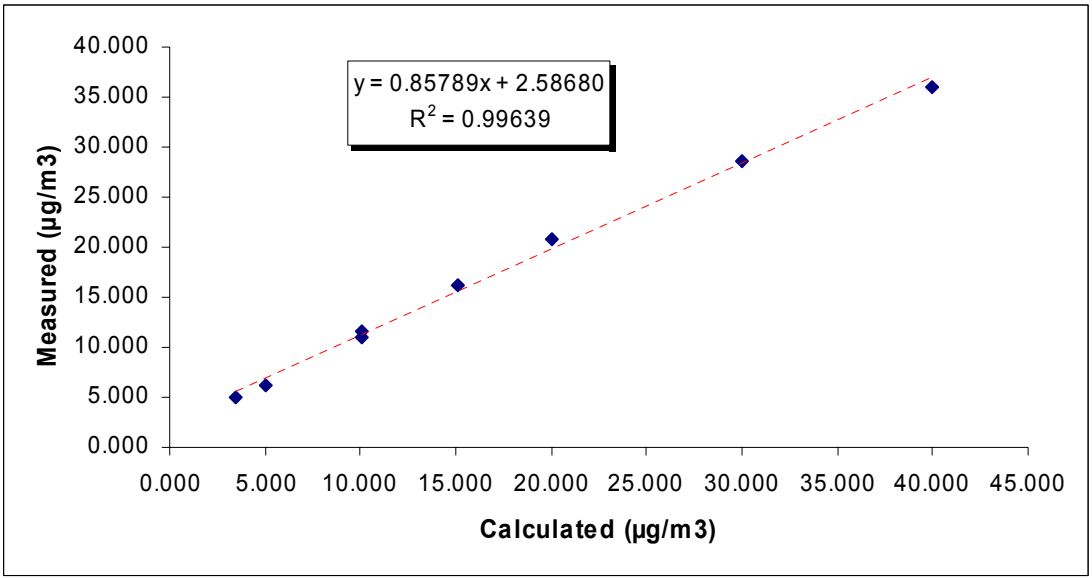

Mercury Instruments MC3000 Generator

ID-CV-ICP-MS Measurements

Calibration data were obtained by ID-CV-ICP-MS for the range 10-40 µg/m^3. These data are summarized in Table 5a. The Table contains the operating parameters for the measurements, the measured data with associated expanded uncertainty and a calculation of the deviation of the measured concentration values from those predicted. The data points for the entire measurement range are plotted graphically in Figure 5a, with the measured concentration values plotted along the ordinate and the predicted calculated values along the abscissa.

Table 5a: ID-CV-ICP-MS Measurement Data for MC3000
Run Date: February 2006

Nominal µg/m^3	Reservoir T °C	MFC1 mL/min	MFC2 L/min	Predicted µg/m^3	Measured µg/m^3	Uncertainty µg/m^3	Deviation Predicted, %
0							
2							
3							
5							
7							
10	21.3	6.1	9.0	10.031	11.848	0.113	18.11
15	21.3	9.2	9.0	15.129	18.183	0.173	20.19
20	21.3	12.4	9.0	20.057	24.283	0.231	21.07
25	21.3	15.4	9.0	25.116	31.422	0.299	25.11
30	21.3	18.5	9.0	30.172	37.921	0.360	25.68
35	21.3	21.6	9.0	35.227	44.086	0.419	25.15
40	21.3	24.9	9.0	40.275	50.141	0.476	24.50
						Mean	**22.83**

Figure 5a: ID-CV-ICP-MS Calibration Correlation for MC3000 Generator

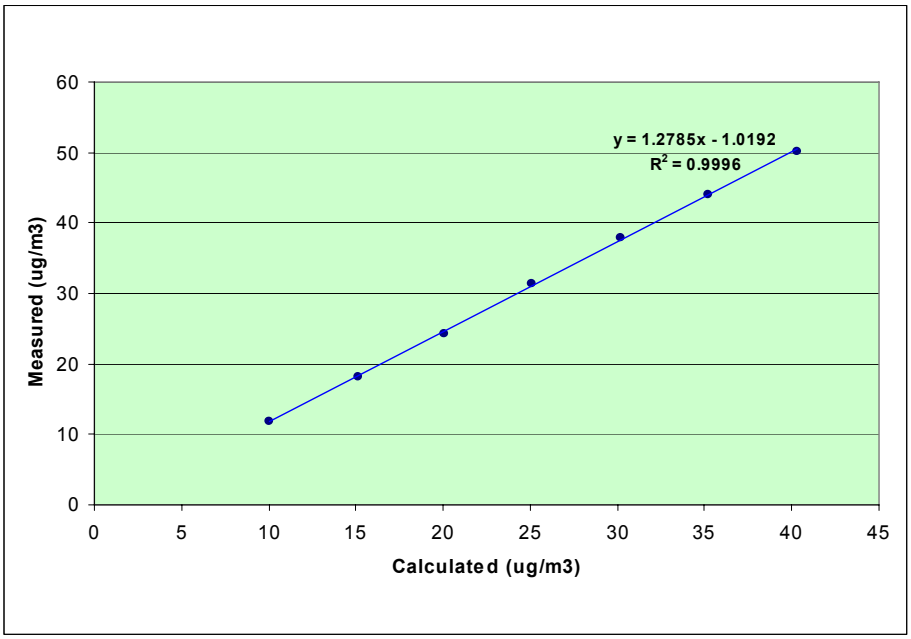

Mercury Instruments MC3000 Generator

Gold-Trap AAS Measurements

Calibration data obtained by gold-trap AAS using the same generator operating conditions as the ID-CV-ICP-MS measurements are summarized in Table 5b. The correlation data are plotted graphically in Figure 5b.

Table 5b: Au Trap AAS Measurement Data for MC3000

Run Date: August 2006

Calculated Setting µg/m^3	MA-2000 Mean Value µg/m^3	Deviation Predicted, %
10.055	12.077	20.11
15.082	18.774	24.48
20.008	23.981	19.86
30.021	38.827	29.33
30.021	37.588	25.21
40.004	51.415	28.52
40.004	50.886	27.20

Figure 5b: Au Trap Calibration Correlation Data for MC3000 Generator

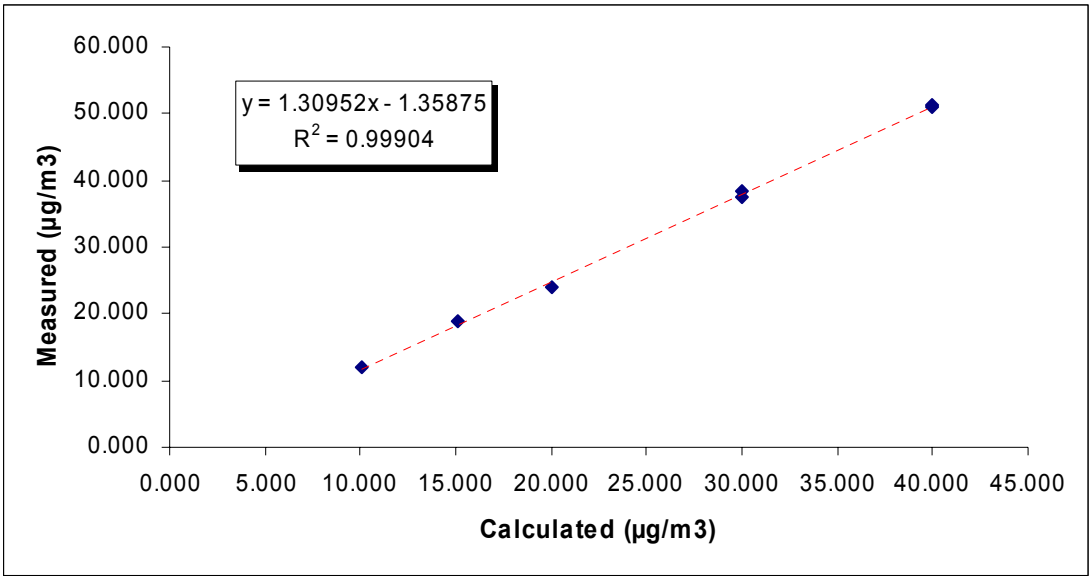

Nippon MGS-1 Generator

ID-CV-ICP-MS Measurements

Calibration data were obtained by ID-CV-ICP-MS for the range 2-40 µg/m^3. These data are summarized in Table 6a. The Table contains the operating parameters for the measurements, the measured data with associated expanded uncertainty and a calculation of the deviation of the measured concentration values from those predicted. The data points for the entire measurement range are plotted graphically in Figure 6a, with the measured concentration values plotted along the ordinate and the predicted calculated values along the abscissa.

Table 6a: ID-CV-ICP-MS Measurement Data for Nippon MGS-1
Run Date: Dec 2006

Nominal µg/m^3	Reservoir T °C	MFC1 mL/min	MFC2 L/min	Predicted µg/m^3	Measured µg/m^3	Uncertainty µg/m^3	Deviation Predicted, %
0	50.00	0.00	10.0	0.000	0.000	--	--
2	50.00	0.13	10.0	1.940	1.728	0.016	-10.93
3	50.00	0.20	10.0	2.984	2.567	0.024	-13.99
5	50.00	0.34	10.0	5.073	4.249	0.040	-16.24
7	50.00	0.47	10.0	7.013	6.194	0.059	-11.68
10	50.00	0.67	10.0	9.997	8.622	0.082	-13.76
15	50.00	1.00	9.90	15.071	13.103	0.125	-13.06
20	50.00	1.00	7.50	19.893	17.689	0.168	-11.08
25	50.00	1.00	6.00	24.866	22.044	0.370	-11.35
30	50.00	1.00	5.00	29.838	26.262	0.441	-11.98
35	50.00	1.00	4.30	34.694	30.358	0.509	-12.50
40	50.00	1.00	3.70	40.319	35.057	0.588	-13.05
						Mean	**-12.69**

Figure 6a: ID-CV-ICP-MS Calibration Correlation for Nippon MGS-1 Generator

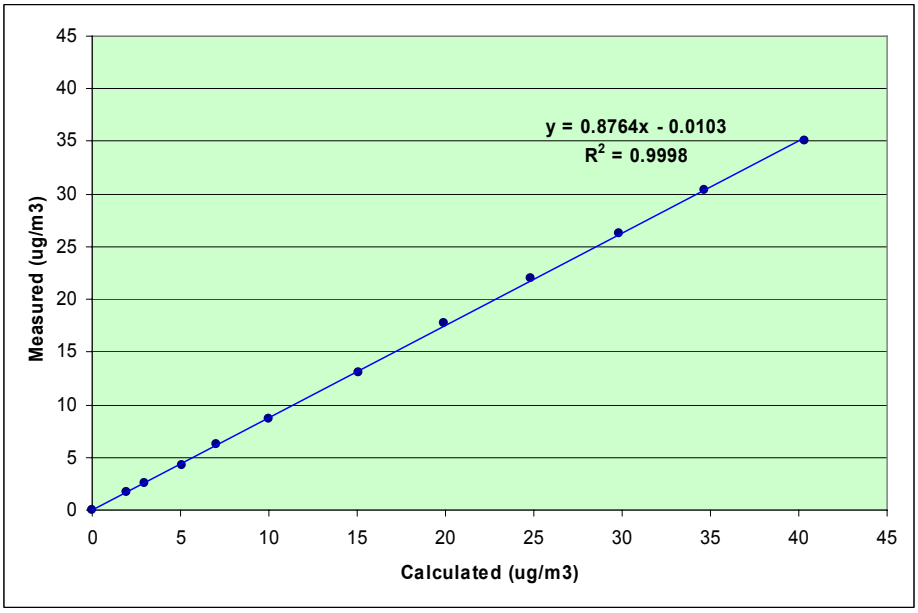

Composite Data

For convenience, graphical overlays, on the same basis, of all of the generators tested, are shown in Figures 7a and 7b respectively for the ID-CV-ICP-MS measurements and the Au Trap AAS measurements.

Figure 7a: ID-CV-ICP-MS Calibration Overlays

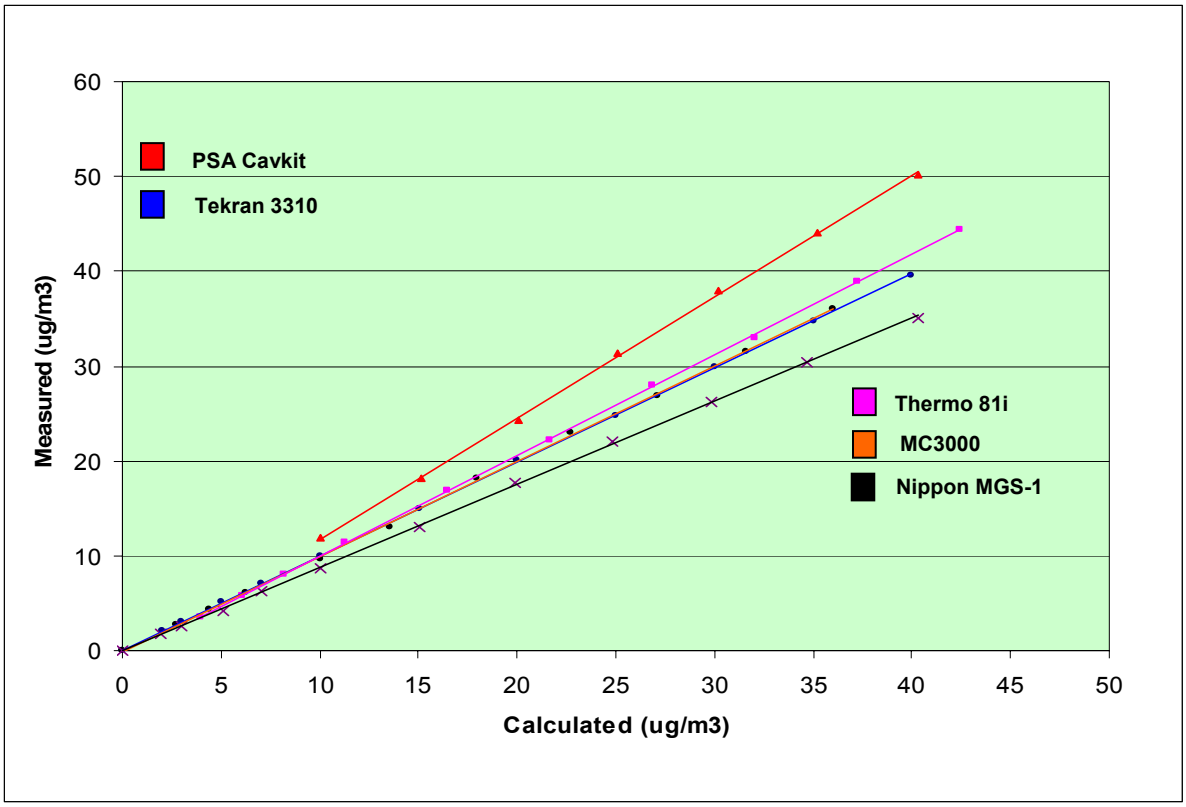

Figure 7b: Au Trap AAS Calibration Overlays

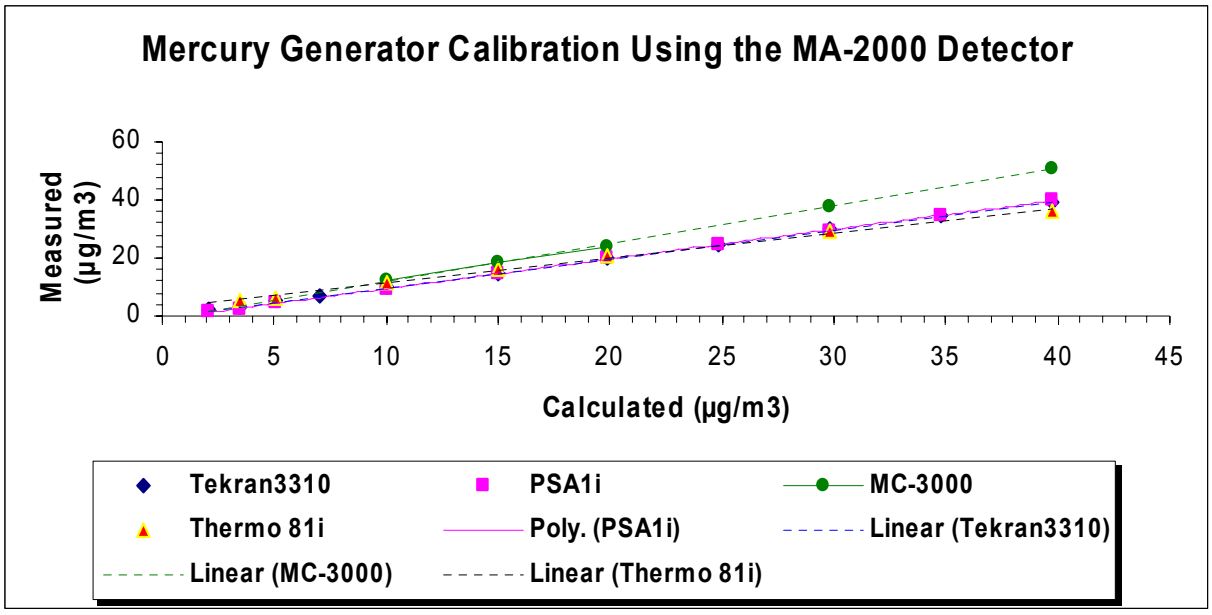

Additional Measurements at Low Hg^0 Concentrations

The calibration range tested in this work was 2-40 µg/m^3 Hg^0. However, there is also specific interest in the performance of such generator systems for lower concentrations, in the range 0-2 µg/m^3 Hg^0. Although this was not part of this contract, the performance of the generators in this range was examined. With the existing designs, the output of such low concentrations is problematic because it requires the use of a combination of very low MFC1 gas flow, very high MFC2 gas flow and relatively low mercury source equilibrium temperatures. The measurement of these low concentrations was not a problem by ID-CV-ICP-MS because the method has a detection limit of the order of 0.02 µg/m^3. However, only one generator is currently capable of reaching these low concentrations, which is the Tekran 3310. Calibration points at 0, 0.5, 1 and 2 µg/m^3 were measured. This required a source temperature of 2 ºC, which was not easy to maintain in the ambient laboratory environment. Enhanced capability in this range will require the development of generators with additional MFC dilution channels. Data for the Tekran 3310 system is summarized in Table 7 and graphically in Figure 8.

Table 7: ID-CV-ICP-MS Measurement Data for Tekran 3310 (Low Range)
Run Date: March 2006

Nominal µg/m^3	Reservoir T ºC	MFC1 mL/min	MFC2 L/min	Predicted µg/m^3	Measured µg/m^3	Uncertainty µg/m^3	Deviation Predicted %
0	5.00	0.00	6.00	0.000	0.000	--	--
0.5	2.00	3.00	14.00	0.569	0.582	0.013	2.26
1	2.00	5.50	14.00	1.043	1.032	0.022	-1.04
2	5.00	5.00	8.70	2.023	2.029	0.019	0.31

Figure 8: ID-CV-ICP-MS Calibration Correlation for Tekran 3310 (Low Range)

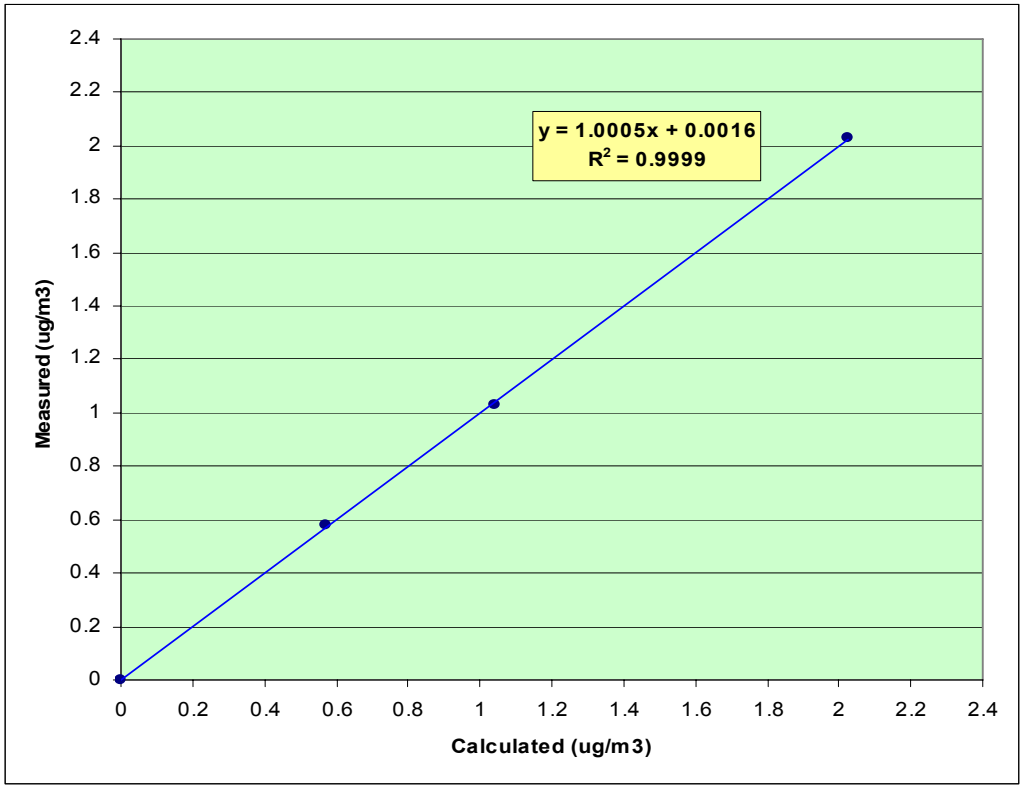

Cold-Vapor Reduction Cell Design

The efficiency of the cold-vapor reduction cell for conversion of $^{201}Hg^{2+}$ to $^{201}Hg^{0}$ is a crucial aspect of the accuracy of the ICP-MS measurement approach. This has to be well defined in order for the data to be valid. The cell used for these measurements was a commercial device sold by CETAC (Omaha, NE) for use with their CV-AAS systems. As such it is a compromise between compactness and efficiency. For the intended application in CVAAS measurements, the efficiency is immaterial because the standards used in the measurements are run under the same conditions as the samples.

In this work it was clear that the efficiency of the device was not 100 %. The efficiency was measured in two ways: 1. Connecting two such devices together by connecting the waste outlet of the cell of interest to the inlet of a second cell and performing an isotope dilution calibration on any mercury remaining in the liquid waste stream (i.e. not converted to $^{201}Hg^{0}$) and 2. Capturing the $^{201}Hg^{0}$ leaving the reduction cell in an EPA Method 101A type impinger experiment and performing an isotope dilution measurement on the impinger solutions. These experiments yielded an overall conversion efficiency of 89.5 %, which was used in the calculation of the data in this work.

Such a system is not ideal, because it raises the issue of the stability of this efficiency factor as a function of time. This has not been rigorously evaluated so far. However, a new improved reduction cell has been designed at NIST with the objective of increasing the conversion efficiency to 100 %. This would be the ideal situation, because it would comprise a more robust measurement system. The newly designed device is currently being evaluated at NIST.

7. Traceability

It is important that the analytical measurements of the Hg^0 generators are traceable to the International System of Units (SI). This is achieved by the use of a primary method based on isotope dilution mass spectrometry and standardization using a high-quality reference material (SRM 3133). All measuring instruments were calibrated and made directly traceable to NIST reference standards.

8. Recommendations

This work is part of a continuing effort to provide a NIST traceable calibration system for both elemental mercury and speciated mercury generation devices. This is necessarily an evolutionary process. The generators measured in this work appear to have a highly linear output, but these measurements need to be repeated on some of the generators which did not function very well during the tests, and were replaced, or have been re-designed. Further measurements on the repeatability of the generator outputs over a defined time-frame, is also needed.

All of the generators were tested using a high-purity nitrogen transport gas source. Additional measurements using air as the transport medium are warranted where this is specified by the manufacturer as there may be slight differences in the Hg^0 output as result of slight differences in the MFC calibrations.

9. References

[1] *Standards of Performance for New and Existing Stationary Sources: Electric Utility Steam Generating Units; Final Rule,* May 18, 2005, Part II, *Federal Register 40 CFR Parts 60, 72 and 75.*

[2] *International Critical Tables of Numerical Data,Physics, Chemsitry and Technology, Volume III,* E.W. Washburn, McGraw-Hill, New York, 1928.

[3] *Correlation for the Vapor Pressure of Mercury,* M.L. Huber, A. Laesecke and D.G. Friend, *Indust. Engineer. Chem. Res.* 2006, 45, 7351-7361.

[4] *Development of High Accuracy Vapor Generation Inductively Coupled Plasma Mass Spectrometry and its Application to the Certification of Mercury in Standard Reference Materials,* S.J. Christopher, S.E. Long, M.S. Rearick and J.D. Fassett, *Anal. Chem*. 2001, 73, 2190-2199.

[5] *Accurate Determination of Mercury in Coal by Isotope Dilution Cold-Vapor Generation Inductively Coupled Plasma Mass Spectrometry***,** S.E. Long and W.R. Kelly, *Anal. Chem*. 2002, 74, 1477-1483.

[6] *Determination of Mercury in SRM Crude Oils and Refined Products by Isotope Dilution Cold Vapor ICP-MS Using Closed-System Combustion*, W.R. Kelly, S.E. Long and J.L. Mann, *Anal. Bioanal. Chem*. 2003, 376, 753-758.

[7] *Guide to the Expression of Uncertainty in Measurement*, ISBN 92-67-10188-9, 1st Ed. ISO, Switzerland, 1993.

Acknowledgements

The authors would like to acknowledge Joe Rovani, Lead Scientist, WRI who helped to troubleshoot some of the generator systems and provided some valuable insight into their technical operation while a guest researcher in the Gas Metrology Group at NIST.

METHOD PROTOCOL FOR CALIBRATION OF ELEMENTAL MERCURY GAS GENERATION DEVICES USING ISOTOPE DILUTION COLD-VAPOR GENERATION INDUCTIVELY COUPLED PLASMA – MASS SPECTROMETRY

Prepared by
Stephen Long, PhD.
Isotopic Methods Team
Inorganic Chemical Metrology Group
Analytical Chemistry Division
Chemical Science and Technology Laboratory
National Institute of Standards and Technology

Version 2.0

Disclaimer: *Certain commercial equipment, instruments or materials are identified in this work to specify adequately the experimental procedure. Such identification does not imply recommendation or endorsement by the National Institute of Standards and Technology, nor does it imply that the materials or equipment identified are necessarily the best available for this purpose.*

Glossary of Symbols Used in This Document

A	is the natural abundance of the reference isotope
A_S	is the abundance of the reference isotope (202) in the spike
B	is the natural abundance of the spike isotope
B_S	is the abundance of the spike isotope (201) in the spike
C_{LTP}	is the concentration of Hg at LTP in the sampled gas stream (μg/m^3)
C_{SPK}	is the concentration of ^{201}Hg in the spike (ng/g)
C_{STP}	is the concentration of Hg at STP in the sampled gas stream (μg/m^3)
E_{GLS}	is the efficiency of the gas-liquid separator (% rel.)
F_{AVG}	is the mean sampled gas flow (mL/min.)
G_F	is the mass flow rate of Hg in the sampled gas stream (pg/s)
K	is the natural to spike atomic weight ratio
M_S	is the mass of ^{201}Hg spike aliquot added to the mix (g)
M_{STD}	is the absolute mass of Hg primary standard added to the spike mix (ng)
P_{LAB}	is the measured barometric pressure in the laboratory (Pa)
R_S	is the corrected ^{201}Hg/^{202}Hg ratio for the sampled gas stream
R_{SC}	is the corrected ^{201}Hg/^{202}Hg ratio in the spike mix
S_F	is the mass flow rate of the spike into the sampled gas stream (pg/s)
S_U	is the liquid flow rate of the spike into the separator (g/s)
T_{LAB}	is the measured temperature in the laboratory (K)

Revision History

Date	***Version***	***Revision***	***Modified by***
17th April 2006	1.0	Original technical draft	Stephen E. Long
14th July 2006	2.0	Updated Appendix	Stephen E. Long

METHOD PROTOCOL FOR CALIBRATION OF ELEMENTAL MERCURY GAS GENERATION DEVICES USING ISOTOPE DILUTION COLD-VAPOR GENERATION INDUCTIVELY COUPLED PLASMA –MASS SPECTROMETRY

1. Background, Scope and Applicability

The method protocol is applicable to the calibration of reference gas generation devices. These devices are used in turn to calibrate secondary devices which will be used to support measurement of elemental mercury in coal fired utility emissions streams. Such gas generation systems include commercial compressed gas cylinders containing gaseous mercury in a balance gas and calibration of commercial mercury dynamic generator devices intended for the calibration of analytical continuous emission monitoring (CEM) instrumentation. The method is applicable to the determination of gaseous elemental mercury in the concentration range from the detection limit **0.02 µg/m^3 to 40 µg/m^3**.

The method is applicable to matrix balance gases consisting of argon or nitrogen.

2. Principle of Measurement

The method is based on isotope dilution cold-vapor generation inductively coupled plasma mass spectrometry (ICP-MS) [1,2]. A stable isotopic spike of $^{201}Hg^{2+}$ is converted to mercury vapor by reduction with tin (II) chloride in a gas-liquid separator cell, and mixed quantitatively with an accurately known flowing stream of gas from the sample source. The ^{201}Hg / ^{202}Hg isotope ratio is measured using optimized plasma conditions. Figure 2-1 shows a schematic of the measurement system arrangement. The output from the gas generation device is split into two streams, one passing to waste, the other passing through the gas-liquid separator where it is mixed dynamically with the ^{201}Hg spike. The mass flow of the liquid spike is determined by mass loss on a balance. The flow rate of the gas stream is measured using a calibrated mass flow meter.
The method is extremely sensitive, accurate and selective for mercury. The use of isotope dilution mass spectrometry is the fundamental basis for measurement traceability.

3. Measurement Strategy and Experimental Design

The determination of mercury by isotope dilution ICP-MS is straightforward in that there are no significant spectral interferences and no variability in the natural isotopic composition resolvable on a traditional quadrupole ICP-MS. The detection limit of the method is also low enough to measure mercury in gases at levels of current interest. The amount of spike mixed with the sample gas stream must be optimized to comply with calculated error propagation

FIGURE 2-1: Schematic of Measurement System for Mercury in Gas Streams by Isotope Dilution Cold Vapor Generation ICP- MS

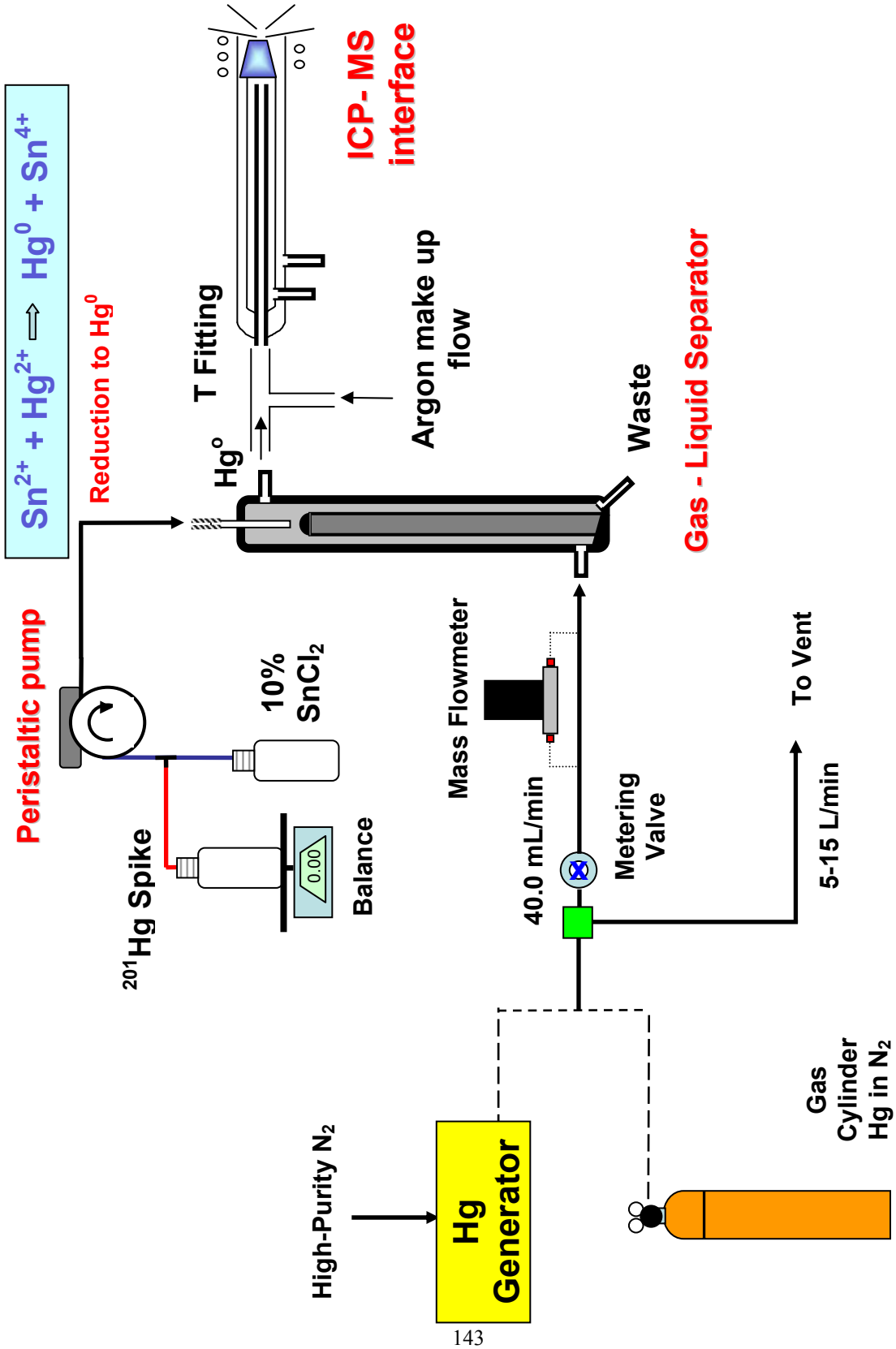

limits. The error propagation using a ^{201}Hg spike has been calculated and plotted in Figure 3-1 for a typical measurement system using a ^{201}Hg spike of 98 % isotopic purity. The calculated error magnification factor (EM) is at a minimum (EM = 1.16) for a ^{201}Hg / ^{202}Hg ratio of 6.01. However, although this is the ideal ratio, it is better to slightly underspike the system to yield an isotope ratio between 1 and 2. Under these conditions, the effects of detector dead time and pulse counting statistics, which are important aspects of ICP-MS measurement systems, are minimized. As is evident from Figure 3-1, **a ratio lower than unity should not be used as the EM factor increases rapidly**. The mixtures used for the spike calibration should be matched as closely as possible to those used for the sample such that detector dead-time effects and mass discrimination cancel out. This approach requires some assessment of the concentration of mercury in the sample prior to analysis.

FIGURE 3-1: Typical Error Propagation Curve for ^{201}Hg – ^{202}Hg System

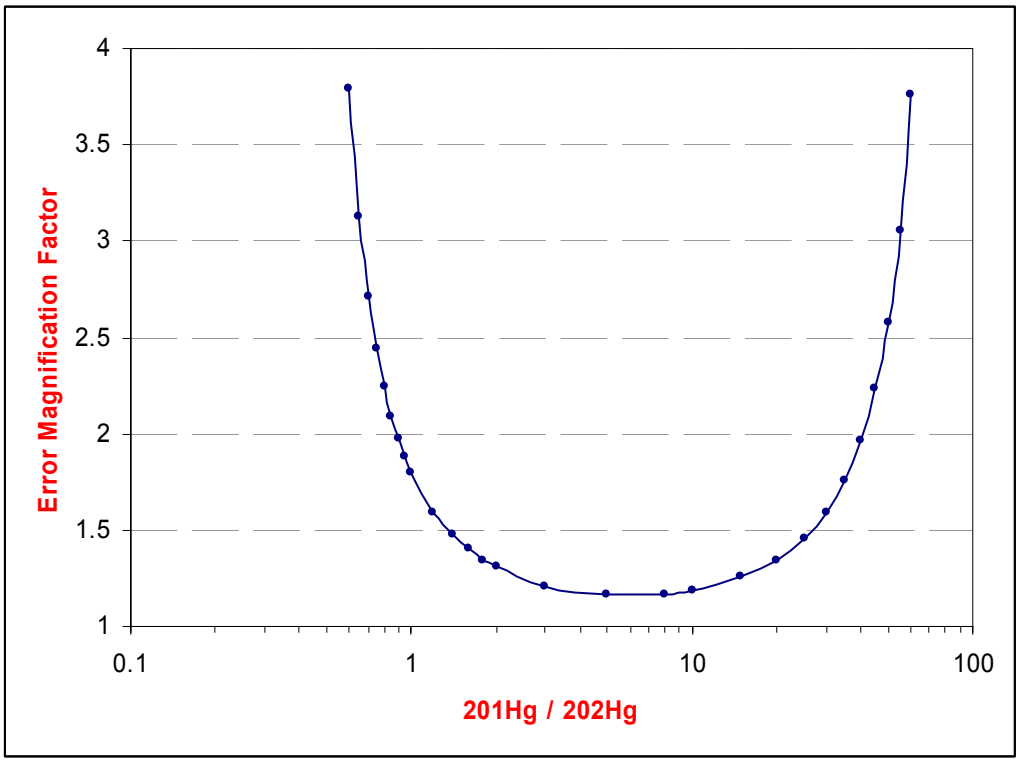

4. Safety

Exposure to certain mercury compounds and vapor is hazardous. The appropriate gloves and a fume hood **MUST** be used when handling inorganic mercury compounds. Gas generation devices must not be vented into the general laboratory space and must be ducted out of the laboratory through operational exhaust hoods or extraction systems. Appropriate handling procedures should be observed for high-pressure gas cylinders and connection of fittings intended for direction of gas flow

under high-pressure. Where mercury traps are fitted to commercial gas generation systems, these must be checked and maintained according to the manufacturers schedule to prevent inadvertent release of mercury into the laboratory space.

5. Required Reagents

5.1 *$^{201}Hg^{2+}$ Isotopic Spike*

A spike having an isotopic purity ≥ 95 %, can be obtained through Oak Ridge National Laboratory (ORNL) or other stable isotope supplier in a form such as ^{201}HgO. A stock solution can be prepared by dissolving a small amount of the ^{201}HgO in 1.1 mol/L (5 % v/v) high-purity nitric acid to yield a concentration of about 100 µg/g (0.5 µmol/g) and storing in a cleaned polyethylene bottle. The stock solution should be stable for at least five years.

NOTE: The stock solution MUST be stored in a hermetically sealed container or aluminized bag at 4 ºC to prevent the infiltration of laboratory air containing natural mercury. If this is not done, the isotopic abundance of the spike will change as a function of time and the composition will have to be re-measured.

The stock solution should be further diluted as needed in 1.1 mol/L nitric acid (5 % v/v) to the concentration level appropriate for measurement of Hg gas phase concentrations. Typical working concentrations are in the range 0.1 – 0.5 ng/g ^{201}Hg. It may be necessary to prepare more than one working spike solution to cover the full range of output concentrations from the generation device. Diluted stock solutions should be stored at 4 ºC in clean polyethylene containers, and a sufficient amount of potassium dichromate stock solution (1 % w/w) added to produce a concentration of 0.01% by weight (pale yellow color) in the solution. The spike solutions are stable for up to three months at a concentration of 0.1 ng/g or higher. These stock solutions must be stored in a hermetically sealed system if they are to be stored for longer than one week (see **NOTE** above).

5.2 *Primary Calibrants*

Two primary calibrants may be used to calibrate the $^{201}Hg^{2+}$ spike using reverse isotope dilution. SRM 3133 is generally the preferred calibrant because the expanded uncertainty of the certified concentration value is smaller.

5.2.1 ***SRM 1641d, Mercury in Water:*** Material supplied in sealed glass ampoules. Open according to instructions and dilute to desired concentration level. The concentration is certified at 1.590 mg/kg ± 0.018 mg/kg (1.1 % relative). Note that the relative uncertainty on this material is higher than SRM 3133, but the concentration is much lower making it less of a contamination hazard for the handling of samples for ultra-trace mercury measurements.

5.2.2 ***SRM 3133, Mercury Standard Solution:*** Material supplied in sealed glass ampoules. Open according to instructions and dilute gravimetrically in a sequential process to obtain desired concentration level. The concentration is certified at 10.00 mg/g ± 0.02 mg/g (0.2 % relative).

5.3 ***High-Purity Nitric Acid***

High-purity acid is essential to minimize the extent of mercury contamination from reagent sources. High-purity acid may be obtained from a number of commercial suppliers such as Seastar and J.T. Baker.

NOTE: *Nitric acid should be stored at all times in a hermetically sealed system to prevent the infiltration of mercury from the laboratory atmosphere. Failure to do this will result in an increase in the mercury contamination level. Use the reagent within one year of purchase.*

5.4 ***Hydrochloric Acid***

Hydrochloric acid is used for dissolution of tin chloride reagent. Analytical grade hydrochloric acid can be obtained from a number of commercial suppliers. High-purity acid is not essential as any mercury will be lost during the preparation of the tin chloride reduction reagent.

5.5 ***Tin (II) Chloride Reagent***

Analytical grade tin (II) chloride dihydrate ($SnCl_2$. $2H_2O$) can be obtained from a number of commercial suppliers. Prepare a 10.0 % (w/w) solution in 7 % (v/v) hydrochloric acid by dissolving 100.0 g of the reagent in 83 g of concentrated hydrochloric acid and diluting with 930 g high-purity water in a 1000 mL cleaned polyethylene container. Purge the solution with a stream of nitrogen for one hour to remove any mercury contamination and store in a refrigerator at 4 ºC. Tin chloride is easily oxidized by oxygen from the atmosphere and should be stored under nitrogen headspace at all times to prevent degradation. This is applicable also to the dry reagent, which should be sealed tightly in a nitrogen atmosphere and stored in a refrigerator at 4 ºC. These procedures will greatly increase the shelf-life of the reagent.

5.6 ***Potassium Dichromate Reagent***

Analytical grade reagent, available from a number of commercial suppliers. Prepare a 1 % w/w solution by dissolving 0.5 g in 100 g of high-purity water.

5.7 ***High-purity Water***

De-ionized or quartz-distilled water, which has been tested and is low in mercury contamination is used for sample dilution. At a minimum, the water should meet or exceed the specifications of ASTM Type I [3].

6. Equipment

6.1 ***ICP-MS System***

The method utilizes a standard ICP-MS system employing a quadrupole mass spectrometer. The instrument should be capable of operating in pulse counting, time-resolved detection mode, with a sample introduction system set up for the direct introduction of gaseous species into the plasma (see Figure 2-1). This normally involves removing the nebulizer/spray chamber assembly.

6.2 ***Analytical Balance (3-place) with Optional Data Transfer Software***

A three-place top-pan balance should be used for measuring the mass uptake per unit time of the isotopic spike. This is monitored either by recording the mass of the spike solution placed on the balance at the start of the run and again at the end of the run and timing the run interval, or by downloading time segmented balance data directly through an RS232 data interface to a computer spreadsheet.

6.3 ***Peristaltic Pump***

Digital peristaltic pump with associated tubing for dispensing $SnCl_2$ reagent and $^{201}Hg^{2+}$ spike into the gas-liquid separator.

6.4 ***Timing Device***

NIST traceable digital stopwatch using quartz timing system.

6.5 ***Gas-Liquid Separator***

Suitable device for continuous generation of $^{201}Hg^{0}$ vapor from the spike solution and separation from the waste liquid stream prior to transfer to the ICP-MS measurement system. The efficiency of this device for converting the liquid $^{201}Hg^{2+}$ to $^{201}Hg^{0}$ should be accurately known. If the efficiency is not 100 %, it must be measured using the procedure in Appendix A.

6.6 ***Gas Transfer System***

Sections of Teflon PFA tubing and Teflon PFA connectors to transfer the gas stream from the mercury gas generation system to the gas inlet of the gas-liquid separator and to the ICP-MS instrument.

6.7 ***Flow Control Valve***

Micrometer needle valve for controlling the flow of gas from the mercury generation device into the measurement system. The valve should not sequester mercury and should therefore be constructed either of Teflon PFA or stainless steel passivated with a coating such as RESTEK *Siltek*®.

6.8 ***Mass Flow Meter***

Traceable calibrated gas flow rate measurement device appropriate to the flow rate range and gas type entering the ICP-MS measurement system, and having negligible back-pressure on the gas flow passing through it.

6.9 ***Environmental Measurement Device***

Traceable digital measurement device for determination of laboratory temperature and barometric pressure.

6.10 ***Sample Bottles***

Clean polyethylene (Nalgene) sample bottles of different sizes for reagent and spike storage.

6.11 ***Micro-Pipette***

Automatic or manual micropipette for dispensing spike and standard aliquots for sequential dilutions. A capped plastic syringe fitted with a PTFE or PFA uptake tube may also be used for this purpose, depending on the weighing method employed.

6.12 ***Analytical Balance (5 place)***

Five place analytical balance for weighing and dilution of spike and standard aliquots. The balance should be calibrated and verified to be functioning correctly prior to weighing measurements.

7. Analytical Measurement Procedure

7.1 ***Measurement Configuration***

Set up gas–phase measurement configuration similar to that shown in Figure 2-1.

7.2 ***Hg Gas Generation Device***

Prepare and equilibrate the gas generation device as recommended by the supplier or manufacturer if appropriate.

7.3 ***Instrument Preparation***

Prior to analytical measurements, the ICP-MS system should be equilibrated for at least 30 minutes. The sample introduction system should be cleaned if necessary prior to use, including the sampler and skimmer cones, plasma torch and gas liquid separator. These procedures are designed to mitigate the background from mercury as much as possible.

7.4 ***Instrument Optimization***

The instrument should be optimized for maximum ion transmission at m/z 201using the standard spike solution of ^{201}Hg and adjusting ion lens voltages, plasma gas flows, torch position (relative to the sample cones) and rf forward power. It should be noted that for nitrogen as the matrix gas, the maximum tolerated flow rate into the ICP-MS may only be 50 mL/min or so before serious degradation of sensitivity and plasma instability results. This will depend on the type of ICP-MS instrument being used and its associated tolerance to nitrogen. Note the flow rate to be used for the measurements.

7.5 ***Dead-time Correction***

If not already known, measure the appropriate dead-time correction for the ICP-MS detector system.

7.6 ***$^{201}Hg^{2+}$ Spike Calibration***

Using not less than three spike calibration mixtures, calibrate the $^{201}Hg^{2+}$ spike using a primary standard and a conventional reverse isotope dilution approach. The same optimized conditions to be used for the analyses should also be used for the spike calibration.

7.7 ***Instrument Mass Discrimination Measurement***

Measure the instrument mass discrimination prior to analytical measurements on gas phase samples. However, it should be noted that the mass discrimination at m/z 200 is typically very small. This can be conveniently achieved by measurement of a gas stream from the generation device without adding the ^{201}Hg spike. The naturally occurring $^{201}Hg/^{202}Hg$ isotope ratio is 0.4414 ± 0.0049.

7.8 ***Instrument Background***

Prior to measurements on gas-phase samples, record the instrumental background at m/z 201 and m/z 202.

7.9 ***Generation of $^{201}Hg^{0}$ from Stock Solution***

Place the container with the $^{201}Hg^{2+}$ spike on a 3-place balance protected from laboratory air currents by means of a protective cover or shroud. Start the flow of $SnCl_2$ reagent and $^{201}Hg^{2+}$ spike solution to the gas-liquid separator using the same liquid flow rate as that used to determine the efficiency of the separator system. Use of a much different flow rate may change the efficiency of the separator.

7.10 ***Gas Sampling***

Select desired output setting of Hg^0 generation device and connect the mass flow meter in–line with the transfer line to the gas-liquid separator. The balance gas from the device output should pass to an open vent to minimize back pressure on the device. Adjust the micrometer valve to obtain the flow rate used for the instrument optimization and record the exact flow rate passing to the gas-liquid separator. Disconnect the mass flow meter from the line as it will sequester mercury. Once the measurement has been completed, reconnect the mass flow meter in-line to check the gas flow rate. Record the final flow rate of the gas stream, and calculate the mean flow rate F_{avg}.

7.11 ***Laboratory Environmental Conditions***

Record the laboratory temperature T_{Lab} in the vicinity of the measurement system.

Record the laboratory barometric pressure. P_{Lab}.

7.12 *Isotope Ratio Acquisition of Spiked Gas Stream*

Once equilibration of the ^{201}Hg spike flow rate and the output of the mercury generation device has been obtained, zero the balance and start the timing device. The isotope intensities (cps) at m/z ^{201}Hg and ^{202}Hg should be acquired in peak jumping, time-resolved analysis mode. A typical acquisition scheme would be a run time of ten minutes using a dwell time of 250 ms per isotope. At the end of the run, stop the timing device and simultaneously note the mass loss recorded on the balance. Record the mass loss M_{spk} and the time period T_{spk}. The isotope data should be both dead-time and background corrected and downloaded to a spreadsheet program such as Excel. A typical isotope intensity - time trace is shown in Figure 7-1.

FIGURE 7-1: Typical Isotope Intensity – Time Trace

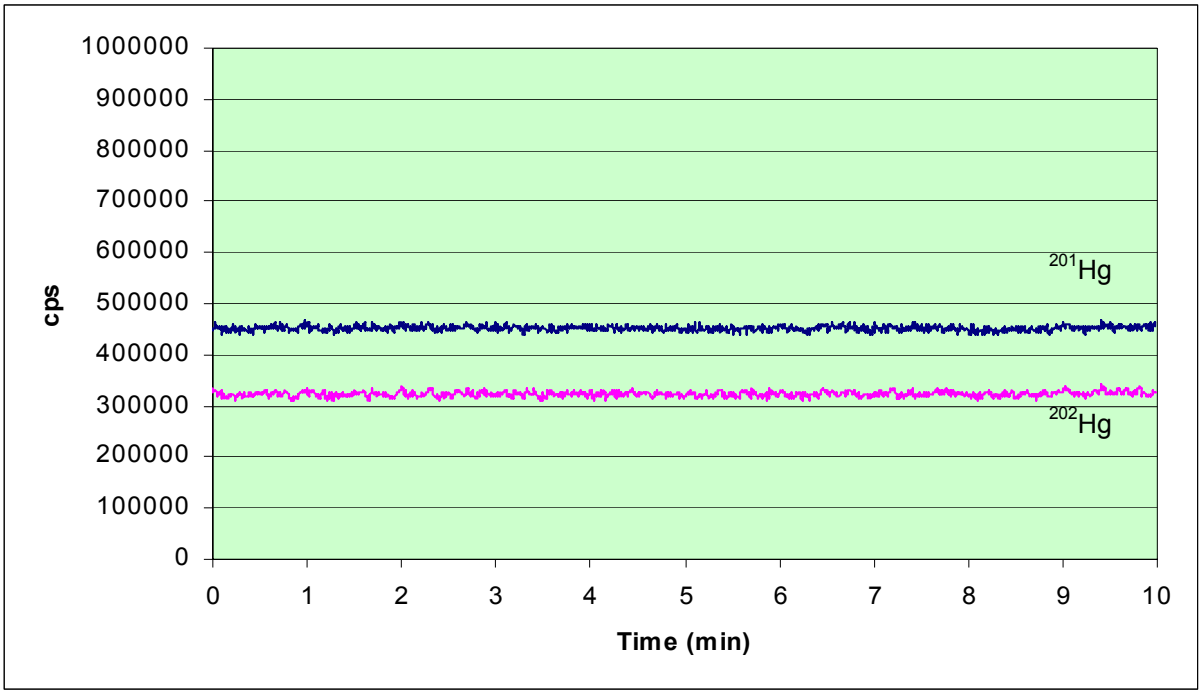

From the isotope intensities at m/z 201 and m/z 202 calculate the resulting ^{201}Hg / ^{202}Hg isotope ratios as a function of time, and then calculating the mean isotope ratio R_S and its associated standard deviation and relative standard deviation. The mean isotope ratio can be obtained using the whole time profile or a section of the time profile if there is confidence that it represents the true measured ratio.

8. Data Reduction

8.1 *Mass Discrimination Corrections*

Convert the experimentally measured ^{201}Hg/^{202}Hg isotope ratios to absolute ratios using the following equation:

$$\left[\frac{^{201}Hg}{^{202}Hg}\right]_{CORR} = \frac{\left[\frac{^{201}Hg}{^{202}Hg}\right]_{TRUE}}{\left[\frac{^{201}Hg}{^{202}Hg}\right]_{MEAS}} \quad (1)$$

Where, $\left[\frac{^{201}Hg}{^{202}Hg}\right]_{CORR}$ is the discrimination corrected sample ratio

$\left[\frac{^{201}Hg}{^{202}Hg}\right]_{TRUE}$ is the true ratio for the isotopic standard

$\left[\frac{^{201}Hg}{^{202}Hg}\right]_{MEAS}$ is the measured ratio for the isotopic standard

8.2 ***Spike Calibration***

Calculate the concentration C_{spk} of the $^{201}Hg^{2+}$ spike using the following equation:

$$C_{SPK} = \left[\frac{M_{STD}\,(BR_{SC} - A)}{M_s\,K(\,A_s - B_s R_{SC}\,)}\right] \quad (2)$$

Where, C_{SPK} is the concentration of $^{201}Hg^{2+}$ in the spike (ng/g)

M_{STD} is the absolute mass of Hg primary standard added to the spike mix (ng)

B is the natural abundance of the spike isotope (201)

R_{SC} is the corrected $^{201}Hg/^{202}Hg$ ratio in the spike mix

A is the natural abundance of the reference isotope (202)

M_S is the mass of ^{201}Hg spike aliquot added to the mix (g)

K is the natural to spike atomic weight ratio

A_S is the abundance of the reference isotope (202) in the spike

B_S is the abundance of the spike isotope (201) in the spike

Calculate the mean and standard deviation of the spike calibration mixtures.

8.3 ***Calculation of $^{201}Hg^0$ Mass Flow Rate***

Calculate the $^{201}Hg^0$ mass flow rate using the following equation:

$$S_F = \left[C_{SPK} \cdot S_U \cdot 1000 \cdot E_{GLS}\right] \quad (3)$$

Where, S_F is the mass flow rate of the spike into the sampled gas stream (pg/s)

C_{SPK} is the concentration of $^{201}Hg^{2+}$ in the spike (ng/g)

S_U is the liquid flow rate of the spike into the separator (g/s)

E_{GLS} is the efficiency of the gas-liquid separator (% rel.)

8.4 ***Calculation of Elemental Mercury Gas Phase Concentrations***

Calculate the Hg^0 mass flow rate (pg/s) and concentration (µg/m^3) in the sample at the laboratory temperature and pressure (LTP) using the following equations:

$$G_F = \left[\frac{S_F \cdot K \cdot (B_s - B_s \cdot A_S)}{(A \cdot R_S - B)} \right] \qquad (4)$$

Where, G_F is the mass flow rate of Hg in the sampled gas stream (pg/s)

S_F is the mass flow rate of the spike into the sampled gas stream (pg/s)

K is the natural to spike atomic weight ratio

A_s is the abundance of the reference isotope in the spike

B_s is the abundance of the spike isotope in the spike

R_S is the corrected $^{201}Hg/^{202}Hg$ ratio for the sampled gas stream

B is the natural abundance of the spike isotope

A is the natural abundance of the reference isotope

$$C_{LTP} = \left[\frac{G_F \cdot 60}{F_{AVG}} \right] \qquad (5)$$

Where, C_{LTP} is the concentration of Hg at LTP in the sampled gas stream (µg/m^3)

G_F is the mass flow rate of Hg in the sampled gas stream (pg/s)

F_{AVG} is the mean sampled gas flow (mL/min.)

8.5 ***Correction to Standard Temperature and Pressure***

The data obtained using the ambient laboratory conditions **should be corrected to Standard Temperature and Pressure (STP)** to provide a standard basis for comparisons of the data with other calibrations. Use the following equation to correct the data:

$$C_{STP} = \left[C_{LTP} \cdot \left(\frac{T_{LAB}}{273.15} \right) \cdot \left(\frac{101325}{P_{LAB}} \right) \right] \qquad (6)$$

Where, C_{STP} is the concentration of Hg at STP in the sampled gas stream (µg/m^3)

C_{LTP} is the concentration of Hg at LTP in the sampled gas stream (µg/m^3)

T_{LAB} is the measured temperature in the laboratory (K)

P_{LAB} is the measured barometric pressure in the laboratory (Pa)

9. Uncertainty Components and Expanded Uncertainty Calculation

The expanded uncertainty for the set of samples should be calculated according to ISO guidelines [4] by combining both Type A and Type B uncertainties. Typical Type A and Type B uncertainty components for this application are shown in Table 9-1.

Table 9-1: Typical Uncertainty Components for Hg in Gas Streams

Source	Basis	Type	Degrees of Freedom
Sample measurement repeatability	Repeatability of sample measurement based on 6 replicate measurements.	**A**	**5**
Calibration of isotopic spike	Repeatability of calibration of the spike using 4 independently prepared calibration mixes.	**A**	**3**
Spike flow rate	Estimated uncertainty of the measurement of liquid flow rate of the ^{201}Hg spike solution into the gas-liquid separator.	**B**	infinite
Gas flow rate	Estimated uncertainty of the measurement of gas flow rate of sampled gas stream into the gas-liquid separator.	**B**	infinite
Primary calibrant	Uncertainty of concentration of primary calibrant used for the calibration of the ^{201}Hg spike.	**B**	infinite
ICP-MS instrument discrimination correction	Uncertainty in evaluation and temporal drift of mass discrimination and validity of correction.	**B**	infinite
ICP-MS instrument dead-time correction	Uncertainty in evaluation and temporal drift of dead-time and validity of correction.	**B**	infinite
ICP-MS instrument background correction	Estimated uncertainty of instrument background subtraction from analytical signals.	**B**	infinite
Weighing measurements	Estimated uncertainty in accuracy, drift (temporal and electrostatic) and relative impact on weighing measurements for spike preparation and calibration.	**B**	infinite
Gas-liquid separator Efficiency	Estimated uncertainty in the measurement of the gas-liquid separator conversion efficiency.	**B**	infinite
Lab temperature	Uncertainty of temperature conversion of gas phase concentrations from LTP to STP.	**B**	infinite
Lab barometric pressure	Uncertainty in pressure conversion of gas-phase concentrations from LTP to STP.	**B**	infinite

Combine the Type A and Type B components and calculate the total expanded uncertainty using the following equation:

$$U = k\,[s_1^2/df_1 + \ldots + s_n^2/df_n + B_1^2 + \ldots + B_n^2]^{1/2}$$

Where, ***U*** is the expanded uncertainty

k is the coverage factor

s is the observed standard deviation of (n) Type A components

df is the degrees of freedom associated with each component
B is the Type B component (n components having infinite degrees of freedom).

10. Calibration of Generation Devices

For gas cylinders report the measured gas-phase concentration of elemental mercury and the associated expanded measurement uncertainty in units of **µg/m^3**, together with all of the recorded conditions used to obtain the concentration data.

For dynamic gas generation devices calibrate the device at various standardized settings as defined in the NIST/EPA mercury traceability protocol and report the calibration system in the form of a regression equation describing the output of the device as a function of the defined concentration range (See Figure 12-1).

11. Traceability Statement

This method is considered to be a primary method for the determination of elemental mercury (Hg^0) in gas streams. Fundamental traceability to the mole is obtained through the calibration of the ^{201}Hg spike using a NIST primary SRM calibrant material.

12. Performance Statement

12.1 Measurement Repeatability

The measurement repeatability of this method is affected by short term drift occurring in the flow of spike to the gas-liquid separator, short-term drift in the sampled flow rate of the gas stream and drift or noise in the ICP-MS measurement system. Typical measurement repeatability on a quadrupole ICP-MS system for this application is approximately 0.5 %.

12.2 *Detection Limit*

The instrument detection limit is primarily influenced by the instrument background, but may also be affected by the sensitivity of the instrument to the matrix gas being sampled. A typical instrument detection limit for a well-optimized quadrupole ICP-MS instrument is 0.02 µg/m^3. This is considerably lower than the mercury concentration levels of interest in gas-phase calibration applications.

12.3 Instrument Background

The ICP-MS instrument background tends to be very low for this application. A typical background count rate is approximately 200 cps for ^{201}Hg and 500 cps for ^{202}Hg. The background originates mostly from residual mercury contamination in the gas stream entering the ICP-MS instrument.

12.4 Dynamic Range

The dynamic measurement range of this method is primarily ICP-MS instrument limited, and ranges from the detection limit up to approximately 40 µg/m^3 Hg^0. At higher concentrations the instrument pulse-counting detection system will start to become increasingly non-linear. Although the instrument could be de-tuned to extend the linear range or to switch the detector mode to analog instead of pulse-counting, this is not recommended. Concentration measurements higher than 40 µg/m^3 Hg^0 must be made by dynamic dilution of the output gas stream with an auxiliary zero Hg gas stream.

12.5 *Performance Summary*

A summary of the typical performance parameters associated with use of this method is provided in Table 12-1. A typical calibration curve for a gas generation device showing calibration points at 0, 2, 3, 5, 7, 10, 15, 20, 25, 30, 35 and 40 µg/m^3 is shown in Figure 12-1.

Table 12-1: Method Performance Summary

Parameter	Typical Value or Range
Sample measurement repeatability	0.5 % relative
Instrument detection limit	0.02 µg/m^3
Typical measurement uncertainty	0.95 % relative
Applicable concentration range	0.02 – 40 µg/m^3
Sample throughput (measurement)	4 samples per hour

FIGURE 12-1: Typical Calibration Data for an Elemental Mercury Gas Generator Device

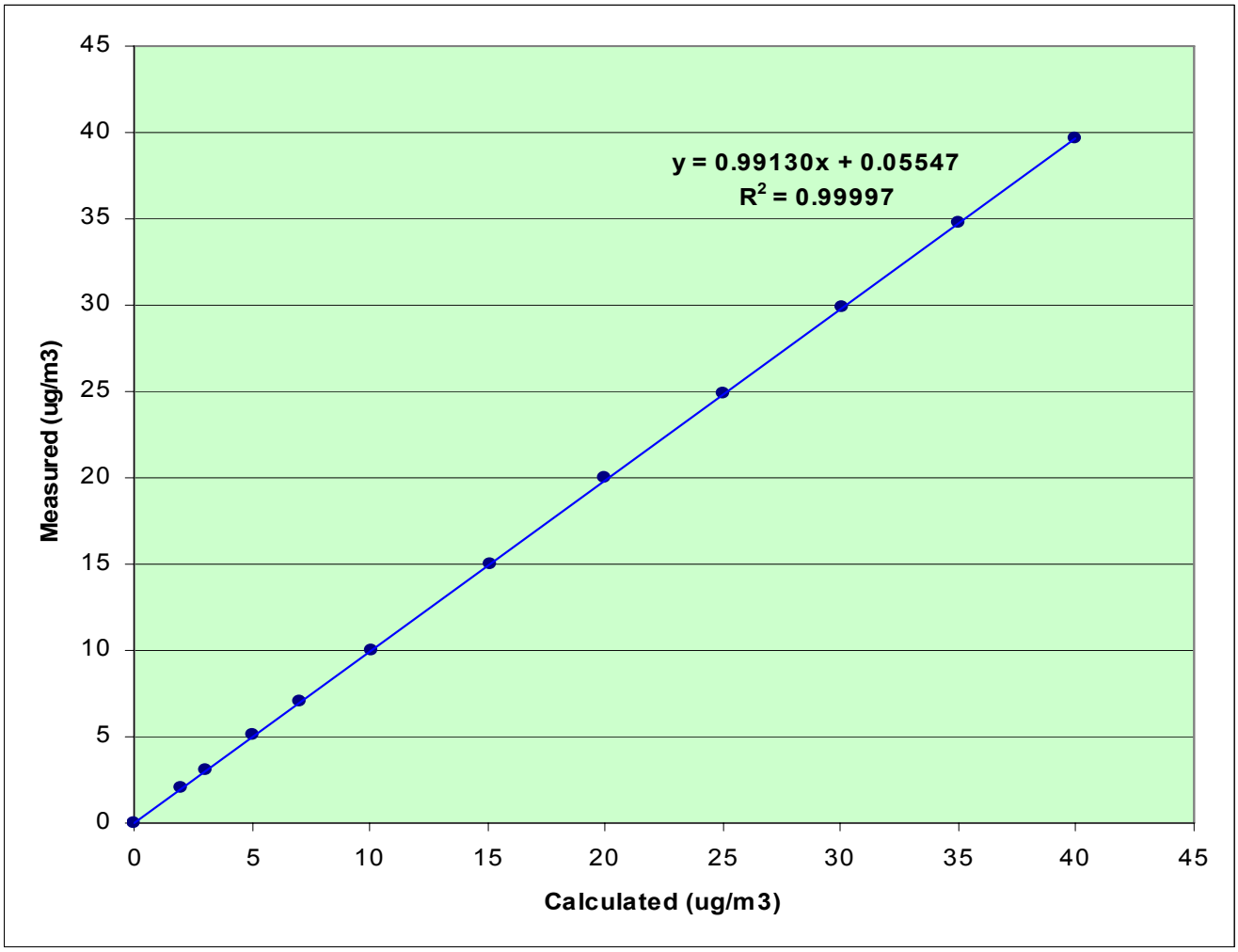

13. Reference Citations

1. Christopher S.J., Long S.E., Rearick M.S. and Fassett J.D., "*Development of Isotope Dilution Cold Vapor Inductively Coupled Plasma Mass Spectrometry and its Application to the Certification of Mercury in NIST Standard Reference Materials.*"
   Anal. Chem. **73** (10), 2190-2199 (2001).

2. Long S.E. and Kelly W.R., *"Determination of Mercury in Coal by Isotope Dilution Cold-Vapor Generation Inductively Coupled Plasma Mass Spectrometry."*
   Anal. Chem. **276** (52), 49371-49377 (2002).

3. *ASTM D1193-99e1: Standard Specification for Reagent Water,* ASTM International, West Conshohoken, PA 19428, USA (1999).

4. *Guide to the Expression of Uncertainty in Measurement*, ISBN 92-67-10188-9, 1st Ed. ISO, Switzerland, 1993.

APPENDIX A

Total Elemental Mercury Using Impinger Trapping and Isotope Dilution Inductively Coupled Plasma – Mass Spectrometry

1. Background

1.1 This procedure may be used to measure total elemental mercury in gas streams using a trapping technique based on an impinger train assembly containing acidified potassium permanganate. The procedure is based loosely on EPA Method 101A (Determination of Particle-Bound and Gaseous Mercury Emissions, from Sewage Sludge Incinerators), except that the impingers also contain an accurately known aliquot of ^{201}Hg spike.

1.2 At the completion of the sampling process the impinger contents are analyzed using isotope dilution ICP-MS following reduction of the Hg^{2+} to Hg^0 with tin (II) chloride. Quantitative recovery of the contents of the impingers is not necessary because the isotope ratio is fixed by the amount of added spike and the absolute mass of mercury trapped in each impinger. Similarly, matrix induced reduction interferences caused by the impinger reagents do not affect the accuracy of the measurements.

2. Significance and Use

2.1 This procedure may be used to measure the efficiency of the gas-liquid separator used for generation of $^{201}Hg^0$ gas as well as a control system for testing the accuracy of measurements using the on-line isotope dilution ICP-MS measurement protocol.

3. Interferences

3.1 There are no known matrix or spectral interferences.

4. Reagents and Materials

4.1 ***Potassium Permanganate/ Sulfuric Acid Absorbing Solution (0.4 % w/v $KMnO_4$ / 10 % v/v H_2SO_4).***

Mix carefully, with stirring, 0.8 g $KMnO_4$ and 180 mL high-purity water. Slowly add 20 mL of concentrated H_2SO_4. **CAUTION:** Follow standard safety procedures for diluting concentrated acids. Sulfuric acid mixtures evolve copious amount of heat. Exercise care during the mixing process.

4.2 ***^{201}Hg Spike***

Calibrated solution of ^{201}Hg stable isotopic spike (See section 5.1).

4.3 ***Tin (II) Chloride ($SnCl_2$).***

Reducing reagent (See Section 5.5).

4.4 ***High-purity Water***

See Section 5.7

4.5 ***Hydroxylamine Hydrochloride (10 % w/v NH_2OH. HCl)***

Add 50 g of Hydroxylamine hydrochloride to 500 mL High-Purity water and agitate to dissolve.

4.6 ***Dilute Nitric Acid (5 % v/v HNO_3)***

Mix 10 mL high-purity concentrated HNO_3 with 190 mL high-purity water. **CAUTION:** Follow standard safety procedures for diluting concentrated acids. Nitric acid mixtures evolve heat. Exercise care during the mixing process.

5. Equipment

5.1 ***Sampling Train***

Consists of two mini-impingers maintained at room temperature and connected in series using non mercury adsorbing tubing (such as PFA, coated stainless steel etc.). The impingers must contain leak-free ground-glass fittings or other material (Do not use grease or other sealants). The two impingers each contain 20 mL of 0.4 % w/v potassium permanganate in 10 % v/v sulfuric acid together with ^{201}Hg isotopic spike. The assembly is illustrated in Figure 1.

5.2 ***Flow Control Valve and Mass Flow Meter***

If a sub-sample of the output gas stream is to be measured the following components are required.

4.2.1 *Micrometer needle valve* for controlling the flow of gas from the mercury generation device. The valve should not sequester mercury and should therefore be constructed either of Teflon PFA or stainless steel passivated with a coating such as RESTEK *Siltek*®.

4.2.2 *Traceable calibrated gas flow meter* appropriate to the flow rate range and gas type entering the ICP-MS measurement system, and having negligible back-pressure on the gas flow passing through it.

5.3 ***Dessicant Tube***

Dryer tube containing a small amount of magnesium perchlorate for removing water vapor from gas stream exiting the sampling train.

5.4 ***Timing Device***

NIST traceable digital stopwatch using quartz timing system.

5.5 ***ICP-MS Measurement Equipment***

See Method Protocol.

6. Procedure

6.1 *Impinger Preparation*

Fill each impinger with approximately 20 mL of the $KMnO_4$ / H_2SO_4 absorbing solution. NOTE: Rigorously clean all impingers and connecting tubing prior to use. Add accurately, a known mass of a calibrated ^{201}Hg isotopic spike using a five-place analytical balance and record the mass. The mass of spike added will depend on the concentration of the spike and the amount of natural mercury that is expected to be collected during the sampling process.

6.2 *Equipment Assembly*

Set up impinger train and components as illustrated in Figure 1. Connect impinger train to gas stream containing mercury source. Prepare an impinger blank by filling a spare impinger with the absorbing solution and allow to sit for the same time duration as for the gas sampling.

6.3 *Sampling*

Start the mercury gas stream flow through the impinger train and measure the gas flow through the train using the mass flow-meter. Collect for a prescribed period of time and measure this time period accurately using a stop-watch.

6.4 *Impinger Solution Processing*

At the completion of the sampling period, disconnect the mercury gas stream source. Wash the impinger connecting tubes and impinger nozzles with 5 % (v/v) nitric acid followed by sufficient 10 % (w/v) hydroxylamine solution to remove any brown deposits of reduced $KMnO_4$ from the top of the impingers and nozzles. Dilute the contents of the impingers with high-purity water to a concentration level suitable for measurement by ICP-MS.

6.5 *Impinger Solution Analysis*

Determine the absolute mass of mercury collected in each impinger solution and in the impinger blank using standard isotope dilution ICP-MS measurement protocols.

6.6 *Calculations*

Calculate the concentration of mercury in the source gas stream as follows:

$$C_{Hg} = [(M_{Hg}^{Imp1} - M_{Hg}^{Blk}) + (M_{Hg}^{Imp2} - M_{Hg}^{Blk})] / (t_{flow} \cdot F)$$

Where,
- C_{Hg} = Concentration of Hg in the gas stream µg/m^3
- M_{Hg}^{Imp1} = Mass of mercury collected in impinger 1 (µg)
- M_{Hg}^{Blk} = Mass of mercury associated with blank impinger measurement (µg)
- M_{Hg}^{Imp2} = Mass of mercury collected in impinger 1 (µg)
- t_{flow} = Time of flow through impinger train (s)
- F = Volume flow rate through impinger train (m^3/s)

6.7 ***Gas-Liquid Separator Efficiency Measurements***

The measurements obtained using the impinger approach can be used to accurately determine the generation efficiency of the gas-liquid separator used in the on-line calibration protocol. The relative efficiency of the device (E_{GLS}) employed can be calculated by measuring the output of mercury from the separator device and dividing by the amount of mercury entering the device.

FIGURE 1: Impinger Train Sampling Assembly